

# **Mining Machines**

**(2023) VOLUME 41  
ISSUE 2**

**QUARTERLY OF SCIENCE AND TECHNOLOGY**

**e-ISSN 2719-3306**

# Mining Machines

(2023) Vol. 41 Issue 2



Research Institute

Quarterly of Science and Technology

July 2023

**Pages 85-92**

Andrzej CHMIELA, Janusz SMOLIŁO

**The method for preliminary estimation of expenditures and time necessary for liquidation of a mining plant**

**Pages 93-106**

Kinga MOCEK, Piotr MOCEK

**Proper control of working conditions as a stimulator for reducing the incidence of pneumoconiosis in the coal mining industry**

**Pages 107-118**

Jozef MASCENIK, Tomas CORANIC, Juraj RUZBARSKY, Tibor KRENICKY

**Monitoring of belt floating under controlled belt transmission load**

**Pages 119-131**

Mateusz WÓJCICKI, Andrzej N. WIECZOREK, Krzysztof NIEŚPIAŁOWSKI

**Identification of dynamic forces in the chain during the steady operation of a rescue scraper conveyor**

**Pages 132-142**

Leonid SHYRIN, Andrii HERASYMENKO, Ivan INYUTKIN

**Modelling the suspended monorail route stresses and deflections during the transport of heavy loads with use of diesel locomotives**

**Pages 143-157**

Paweł FRIEBE

**Development of a prototype shredder for WEEE equipped with NdFeB magnets**

**KOMAG Institute of Mining Technology**

Pszczyńska 37, 44-101 Gliwice, POLAND

[miningmachines@komag.eu](mailto:miningmachines@komag.eu)



e-ISSN 2719-3306

<https://doi.org/10.32056/KOMAG2023.2.1>

## The method for preliminary estimation of expenditures and time necessary for liquidation of a mining plant

Received: 07.04.2023

Accepted: 02.06.2023

Published online: 31.07.2023

Author's affiliations and addresses:

Andrzej CHMIELA <sup>1\*</sup>, Janusz SMOLIŁO <sup>1</sup>

<sup>1</sup> SRK S.A.  
ul. Strzelców Bytomskich 207,  
41-914 Bytom, Poland

\* Correspondence:

e-mail: achmiela@srk.com.pl  
tel.: +48 505 685 118

Abstract:

A comprehensive scientific approach will facilitate rationalization processes and minimization of mine liquidation costs. The study, based on a statistical analysis of liquidation processes in 19 mining plants from 2015 to 2023, proposes a method for preliminary estimation of costs and time of potential liquidation of hard coal mines.

The method can be used for preliminary estimation of mine liquidation costs and as a cost management tool. The method does not refer directly to the liquidation processes used in SRK S.A. therefore, it can also be used by any entity in mine liquidation process as a comparative tool for detailed and multi-criteria estimation of the costs of planned mine liquidation.

Keywords: costs management, restructuring of mining plants, liquidation of a hard coal mine



## 1. Introduction

Life of a mine is not only the time of mining, but also its liquidation period [1-3]. Revitalization and restructuring of post-mining areas are realized by Spółka Restrukturyzacji Kopalń S.A. ([www.srk.com.pl](http://www.srk.com.pl)). The mine liquidation project is very complicated and expensive due to the large scope of work required. One of the reasons limiting the improvement of liquidation efficiency is the lack of instruments and tools supporting the cost management. In hard coal mines, comprehensive solutions adapted to the specificity of the industry have not been developed so far. The developed solutions concern only the selected issues related mainly to the efficiency of the mining process or preparatory work [4-7].

## 2. Research work problem

Rational expenditure on restoring the post-mining areas to society has not been the subject of comprehensive scientific research work so far [8-11]. Available studies in this area are few and concern only the selected issues [12-17]. The article presents the results of the next stage of research work on tools to support the management of the costs of liquidation processes [8, 11]. A method of preliminary estimation of the time and expenditure necessary in liquidation of the mining plant, which will support the company planning the mine liquidation, has been suggested.

## 3. Research work method

The aim of the research work was to develop and propose a tool for a preliminary estimation of time and expenditure necessary for the planned liquidation process based on a small group of parameters characterizing the liquidated mines. The research plan was implemented based on the analysis of updated mine liquidation programs completed or still carried out by Spółka Restrukturyzacji Kopalń S.A. (SRK) in the years 2015 to 2023.

After analyzing the available literature and statistical analysis of the mining plant restructuring processes broken down into subsequent years, a list of potential evaluation parameters was proposed and their real impact on the estimation of the final cost and time of mine liquidation was checked. Questionnaire surveys among the experts (people designing the liquidation and people managing the liquidation processes) allowed for the selection of a list of the most important assessment parameters.

The correct operation of the proposed assessment tool was verified for the hypothetical mining plants. The verification of the method consisted in comparing the estimates of the method with the experience gained by SRK S.A. Consultations in the form of interviews with the experts managing the liquidation processes confirmed correctness of the results and allowed to explain the reasons of more significant deviations from the expected values.

## 4. Results of the research work

### 4.1. Determination of the assessment parameters

Programs and liquidation plans for 19 mines or their parts from 2015 to 2023 were analyzed. The surveyed group included 9 already closed mines and 10 currently liquidated mines grouped in 5 Departments of SRK S.A. Each case of liquidation of a mining plant is individual, however, there are certain regularities [18-20]. Liquidation process at SRK S.A. lasts from 2 to 8 years (in average 5 years). The cost of liquidation is also very diverse and, for example, for the largest mine it is forty times higher than the cost of liquidating the smallest mine. The average cost of liquidation a mine is 300 to 400 million PLN (calculated to the costs from the first quarter of 2023). This is due to the large scope of work necessary during the task realization.

For better consistency in the cost ratio, it was proposed to divide the liquidated mines into 5 groups due to the amount and structure of their liquidation costs. The mines were divided into Large Mines (KD), Larger Medium Mines (KSW), Smaller Medium Mines (KSM), Small Mines (KM) and a group of Micro Mines (KMikro) [8, 10, 11].



The intention of the method was to link several parameters characterizing the mine with the final cost and time of its liquidation. The determined evaluation parameters were to be easy to read, not requiring major calculations and easy to understand. When selecting the parameters, a certain functional similarity of the analyzed mining plants was assumed. It was assumed that each of the analyzed mines has a similar set of objects, differing only in scale.

In accordance with the adopted assumptions, potential parameters were determined, the analysis of which would make it possible to initially determine the scope of costs and the duration of the mine liquidation processes. During the analysis, the size of analyzed parameter was assigned to the corresponding reference group. In the calculations, the analyzed parameters were treated as "de-stimulants", and then as "stimulants". The standardized values of the assessment parameters were calculated in accordance with formula 1. Based on the analysis, it was found that in the analyzed research problem, the following three parameters read at the time of the decision to liquidate the mine are best correlated with the costs and liquidation time (Table 1):

- the total length of excavation gates, regardless of their size, structure and the fact whether they are to be liquidated or remain as the skeleton of the left pumping station,
- volume of all mine shafts, regardless of their number and regardless of whether they will be liquidated or developed as a pumping station,
- the number of all facilities of the mining plant, regardless of their volume, technical condition or intended for liquidation or development.

**Table 1.** Single-criterion analysis of the assessment parameters

Assessment parameter		Conformity
1.	Total length of excavation gates	73.68%
2.	Volume of all mine shafts	52.63%
3.	The number of all objects of the mining plant	68.42%

The proposed parameters describe all processes related to the task of physical liquidation. Parameters less correlated with the costs and time of mine liquidation were not included in the analysis.

At the next stage of the research work, the determined parameters were correlated in pairs. As before, the standardized values of the assessment parameters were calculated in accordance with the quotient transformation. The analyzed parameters were adjusted to the corresponding group of mines by changing the weight assigned to the partial assessment and changing the range of final assessments, so as to match the parameters and groups of mines as precisely as possible [21]. The results are presented in Table 2. When all parameters are "stimulants", the multi-criteria evaluation using the quotient transformation has the following form:

$$FC_{jmax} = \sum_{i=1}^n \frac{h_{ij}}{h_{imax}} \quad (1)$$

where:

$FC_{jmax}$  - multi-criteria value of assessment parameters for the mine "j",

$i$  - number of assessment parameter,

$j$  - number of analysed mine,

$h_{imax}$  - maximum parameter "i",

$h_{ij}$  - assessment parameters for the mine "j".



**Table 2.** Multi-criterion analysis of the assessment parameters “in pairs”

Assessment parameter		Weight of the parameter	Conformity
1.	Total length of excavation gates	0.833333333	68.42%
	Volume of all mine shafts	0.166666667	
2.	Total length of excavation gates	0.265251989	73.68%
	The number of all objects of the mining plant	0.734748011	
3.	Volume of all mine shafts	0.639423077	73.68%
	The number of all objects of the mining plant	0.360576923	

Due to the fact that the compliance coefficient was too low, another attempt was made to compare the correlation of assessment parameters with the total costs of mine liquidation. This time, three assessment parameters were compared using multiple criteria, also using the quotient transformation (formula 1). The analyzed parameters were adjusted to the corresponding group of mines by changing the weight assigned to the partial assessment and changing the range of final assessments, so as to match the parameters to the appropriate group of mines as precisely as possible [8, 10, 11]. The results are presented in Table 3.

**Table 3.** Multi-criterion analysis of all assessment parameters

Assessment parameter	Weight of the parameter	Conformity
Total length of excavation gates	0.315789474	84.21%
Volume of all mine shafts	0.421052632	
The number of all objects of the mining plant	0.263157895	

Analysis of three parameters significantly improved the correctness of assigning the analysed mines to the corresponding reference groups. Adding another evaluation parameters no longer increased the conformity, and sometimes worsening the already obtained result.

#### 4.2. Method for preliminary assessment of time and costs of mine liquidation

The tool was proposed for the proposed method. The tool interface pattern is presented in Fig. 1÷4. There are fields with a white background in the interface. These fields are descriptive fields. The fields marked in light gray are the input fields, i.e. the values of the original assessment parameters. The fields marked in dark gray are the result fields, where the method reports the estimated results of the analysis.

The proposed method, based on previously determined parameters, estimates the foreseeable time and cost of liquidation. The liquidation time is assessed on the basis of a single-criteria analysis, separately for each of the assessment parameters, and a multi-criteria analysis, for three parameters at the same time. In a single-criterion analysis, a reference group is determined for the analyzed assessment parameter. Then, already within the reference group, the value of the parameter is assigned to the mine liquidation time. The tool presents the results by inserting an "x" in the column corresponding to the designated time interval.

At the next stage, the method in the multi-criteria analysis of three parameters jointly, in accordance with formula 1, classifies the analyzed set of parameters to the corresponding reference group of mines. Already within the reference group, the method estimates the foreseeable liquidation time. The results are given in the same way as in the single-criteria analysis. The "x" is bolded.



The analysis of the assessment parameters is also the basis for determining the preliminary estimated value of the mine liquidation cost. After classifying the analyzed set of assessment parameters to a specific reference group of mines, the cost of liquidating the entire mine is assigned to this set in a multi-criteria manner. The estimated preliminary liquidation cost is presented in the lower right corner of the interface. In addition, the method provides in the last line the name of the assigned reference group and the maximum, minimum and average cost of mine liquidation in this group. Based on the estimated time and cost of liquidation, the method provides the estimated average annual cost of a mine liquidation, determined for the entered set of assessment parameters.

### 4.3. Verification of the proposed method

The method was verified in two stages. At the first stage, all 19 analyzed mines were tested in terms of compliance of the calculated results with the values obtained in liquidation practice. In three cases out of 19, the results were very different from reality. Documentation analysis (liquidation plans and programs), statistical evaluation and interviews with experts (persons in charge of liquidation processes) indicated that these 3 cases are the specific cases. According to the experts, these three mining plants were excluded from the verification of the method as unusual examples. After excluding them from the analysis, according to the experts, a satisfactory estimation of liquidation costs was obtained. The method tends to slightly overestimate the liquidation costs. In most reference groups, the average overestimation of costs does not exceed 5%, only in the group of smaller medium-sized mines (KSM) it is about 16%. In extreme cases, the method overestimates the costs by up to 30% and underestimates up to 24% for larger mines (KD and KSW) and up to 13% for smaller mines (KSM and KM). For micro mines (KMikro), over 99% compliance of the forecast with the value determined by the method was obtained.

When estimating the liquidation time, in two cases the forecast indicated a much shorter liquidation time. According to the analysis of documents and the opinion of experts, this concerned the mines for which, for reasons of protection of neighboring active mining plants, the time of liquidation was artificially extended. This was the case for one of the larger medium-sized mines (KSW) and the "micro" mine (KMikro). The accuracy was considered to be sufficient for this stage of potential designing work. In the case of one of the atypical mines, the liquidation time was extended.

At the second stage of verification, four hypothetical examples of mine liquidation were analyzed. The first of the analyzed hypothetical mines was the mine marked "K1", for which the smallest parameters obtained in the entire analyzed group of 19 liquidated mines were selected. This mine turned out to be smaller than the micro mine (KMikro). The second one was the K2 mine with the shortest length of excavation gates so far, the average volume of shafts and the maximum number of mining facilities. The third analyzed example was the K3 mine with average values of assessment parameters for the group of medium-sized smaller mines (KSM). The last analyzed mine, K4, is one of the mines previously called atypical, belonging to the group of small mines (KM).

Evaluation parameters	Enter data	Expected time of liquidation [years]				
Total length of excavation gates [km]	6425					x
Volume of all mine shafts [m <sup>3</sup> ]	2310					x
Number of all minig plant facilities [items]	14					x
Multi-criteria						x
Average cost of mine liquidation per year [mIn PLN]	6,5	6 -	5-6	4-5	3-4	2-3
Cost of mine liquidation	Maximum	Minimum	Medium	Expected cost of mine liquidation [mIn PLN]		
"micro"	20,7	18,6	19,6			<b>13,1</b>

**Fig. 1.** Results of the preliminary assessment of liquidation time and costs of K1 mine

The analysis of the K1 mine (Fig. 1) classified it as expected as a micro mine (KMikro). For this mine, which is smaller than the smallest micro mine (KMikro), the liquidation cost is lower than the minimum cost for this group of mines. The mine liquidation time determined by the method in the single-criteria and multi-criteria analysis was from 2 to 3 years. Comparing the average liquidation cost with the expected liquidation cost of the K1 mine, it can be seen that the method indirectly



suggests a two-year liquidation time. In practice, such time is usually planned for liquidation processes for the analyzed set of assessment parameters.

Evaluation parameters	Enter data	Expected time of liquidation [years]				
Total length of excavation gates [km]	6425	x				
Volume of all mine shafts [m3]	10039	x				
Number of all minig plant facilities [items]	393	x				
Multi-criteria		x				
Average cost of mine liquidation per year [mln PLN]	76,6	6 -	5-6	4-5	3-4	2-3
Cost of mine liquidation	Maximum	Minimum	Medium	Expected cost of mine [mln PLN]		
"medium larger"	602	326,1	434,3	liquidation	460,4	

**Fig. 2.** Results of the preliminary assessment of liquidation time and costs of K2 mine

As expected, the multi-criteria method classified the K2 mine (Fig. 2) to the group of medium-large mines (KSW) and indicated a 5 to 6-year liquidation period, determining the liquidation cost of PLN 460.4 million. This value slightly exceeds the average value for the indicated reference group. The single-criteria analysis of the liquidation time also, as expected, determined the minimum time of liquidation of excavation gates (from 2 to 3 years), the maximum time of liquidation of facilities (over 6 years) and the time of liquidation of shafts resulting from the scope of tasks (from 5 to 6 years). Comparing the cost of liquidation with the cost of one year of mine liquidation indirectly suggested a 6-year liquidation time. Also the experts (persons managing liquidation processes) confirmed the compliance of the results with the current practice.

Evaluation parameters	Enter data	Expected time of liquidation [years]				
Total length of excavation gates [km]	22931	x				
Volume of all mine shafts [m3]	7320	x				
Number of all minig plant facilities [items]	71	x				
Multi-criteria		x				
Average cost of mine liquidation per year [mln PLN]	49,6	6 -	5-6	4-5	3-4	2-3
Cost of mine liquidation	Maximum	Minimum	Medium	Expected cost of mine [mln PLN]		
"medium smaller"	252,6	170,4	198,3	liquidation	213,3	

**Fig. 3.** Results of the preliminary assessment of liquidation time and costs of K3 mine

The analysis of the model object which is the K3 mine (Fig. 3) did not differ from the assumptions. According to the assumptions, the method classified the mine to a group of medium-sized smaller mines (KSM). The liquidation cost of the mine was set at PLN 213.3 million, which is 107.55% of the average value in this reference group. A discrepancy of this order at such an initial stage of cost estimation is not significant. The single- and multi-criteria analysis of the assessment parameters unanimously indicated 4 to 5 years of liquidation. Comparing the cost of liquidation with the cost of a year of a mine liquidation indirectly points to a 4-year liquidation time. Statistical analysis and expert opinions in this case also confirmed the correctness of the method assessment.

Evaluation parameters	Enter data	Expected time of liquidation [years]				
Total length of excavation gates [km]	32235	x				
Volume of all mine shafts [m3]	8125	x				
Number of all minig plant facilities [items]	102	x				
Multi-criteria		x				
Average cost of mine liquidation per year [mln PLN]	76,6	6 -	5-6	4-5	3-4	2-3
Cost of mine liquidation	Maximum	Minimum	Medium	Expected cost of mine [mln PLN]		
"medium larger"	602	326,1	434,3	liquidation	441,1	

**Fig. 4.** Results of the preliminary assessment of liquidation time and costs of K4 mine

The assessment of the K4 mine pointed it to medium-sized larger mines (KSW) as a reference group and assigned a liquidation cost of PLN 441.1 million (Fig. 4). In the single-criteria analysis, the method suggested, due to the total length of the excavation gates and the total volume of the shafts, 5 to 6 years of liquidation time, and due to the number of surface objects, 4 to 5 years. The multi-



criteria assessment confirmed the assessment of the first two assessment parameters. Comparing the cost of liquidation with the cost of one year of mine liquidation indicated a period of 6 years. In the opinion of experts, if this example of the mine is a typical one, the assessment of the method would be correct.

## 5. Discussion

Based on the analysis, it was found that when estimating the preliminary cost and time of liquidation, the length of excavation gates, the volume of the shafts and the number of surface objects should be taken into account. The parameters adopted for the assessment represent the components of the processes of shafts liquidation, excavation gates and surface objects, for which a statistical liquidated mine spends about 11% of the amount allocated for its liquidation. The remaining part of the cost ensures the correct mine liquidation processes, requiring additional spending of the remaining approximately 89% of the costs [8, 9, 10, 11].

When verifying the correct operation of the method, at the first stage, the scope of loosening and management of hypothetical mines was assessed, with the exception of K4, which has its liquidated counterpart. The real mine corresponding to the analyzed parameters belonged to small mines (KM) and was liquidated for 4 years. The liquidation cost assigned in the method is as much as 317.73% of the true value. The prototype of the K4 mine was a mine merged several times, consisting of many small surface objects, many short shafts and a simple network of long excavation gates. Therefore, unexpected results of the analysis were obtained. This confirmed the fact that the method gives correct results only for typical mine conditions.

At the second stage of verification, hypothetical examples of mine liquidations were presented for assessment to the people who manage the SRK S.A. Branches. Experts confirmed the correct operation of the method with the accompanying software.

## 6. Conclusions

The proposed method of preliminary assessment of the time and costs of mine liquidation can be used as a tool for estimating time and costs in the planned processes of liquidation of mines or their parts. The method can be used by any mine liquidation company, because it only requires the acquisition of a few basic parameters of the liquidated mining plant and it does not refer to the structure of liquidation processes developed by SRK S.A.

The described method is based on a statistical analysis of costs broken down into years of the ongoing liquidation processes. The tool allows optimization independent of the scale of the liquidation task.

Estimation of time and costs of liquidation, also taking into account the cases of untypical main processes of liquidation of a mining plant is an unresolved problem. Only unsystematized knowledge of practitioners is used.

The proposed method requires further research work, but already in its current form it can be a very useful auxiliary tool in an engineering work and in the initial design work of restructuring post-mining assets.

## References

- [1] Mhlongo S. E., Amponsah-Dacosta F.: A review of problems and solutions of abandoned mines in South Africa. *International Journal of Mining, Reclamation and Environment*, 30:4, 279-294, 2016
- [2] Salom A. T., Kivinen S.: Closed and abandoned mines in Namibia: a critical review of environmental impacts and constraints to rehabilitation. *South African Geographical Journal*, 102:3, 389-405, 2020
- [3] Smith F. W., Underwood B.: Mine closure: the environmental challenge. *Mining Technology*, 109:3, 202-209, 2000
- [4] Jonek-Kowalska I.: Analiza i ocena kosztów w cyklu istnienia wyrobiska wybierkowego - wnioski dla



- rachunkowości zarządczej. Scientific Papers of Silesian University of Technology, series: Organization and Management, vol. 66, pp. 195-206. 2013
- [5] Turek M.: Analiza i ocena kosztów w górnictwie węgla kamiennego w Polsce. Warszawa Difin, 2013
- [6] Turek M.: Techniczna i organizacyjna restrukturyzacja kopalń węgla kamiennego. Wydawnictwo GIG, Katowice, 2007
- [7] Turek M., Lubosik Z.: Identyfikacja resztkowych parcel pokładów węgla kamiennego. Wiadomości Górnicze, nr 3, pp. 182-189, 2008
- [8] Chmiela A., Smoliło J., Gajdzik M.: A Multifaceted Method of Analyzing the Amount of Expenditures on Mine Liquidation Processes in SRK S.A., Management Systems in Production Engineering, Vol. 30, Issue 2, pp. 130-139, 2022
- [9] Chmiela A., Smoliło J., Gajdzik M.: Analiza struktury kosztów realizacji procesów składowych restrukturyzacji, rewitalizacji i likwidacji zakładów górniczych w SRK S.A., Przegląd Górniczy 2/2022 r., pp. 34-42, 2022
- [10] Smoliło J., Chmiela A.: The mine liquidation processes in SRK S.A. in a cost approach, Scientific Papers of Silesian University of Technology, series Organization and Management 153, 2021
- [11] Smoliło J., Chmiela A., Gajdzik M., Menéndez J., Loredó J., Turek M., Bernardo Sánchez A.: A New Method to Analyze the Mine Liquidation Costs in Poland. Mining 2021, 1, 351-363, 2021 <https://doi.org/10.3390/mining1030022>
- [12] Bijańska J., Wodarski K.: Model of process management system in enterprises of the hard coal mining industry. Management Systems in Production Engineering, Volume 28, Issue 2, pp. 112-120, 2020
- [13] Bijańska J., Wodarski K.: Process management in a mining enterprise - basic areas and research problems. Scientific Papers of Silesian University of Technology, series: Organization and Management, vol. 120, pp. 35-50, 2018
- [14] Bluszcz A., Smoliło J.: Uwarunkowania transformacji rejonów górniczych, [W:] Wybrane problemy środowiska przyrodniczego w ujęciu naukowym. Lublin: Wydaw. Naukowe Tygiel, 2021
- [15] Dźwigoł H.: Model restrukturyzacji organizacyjnej przedsiębiorstwa górnictwa węgla kamiennego. Warszawa, Difin, 2007. ISBN: 978-83-7251-735-7
- [16] Grmela A., Harat A., Adamczyk Z.: Proces likwidacji kopalń jako problem środowiskowy, ekonomiczny i prawny. Ecological Engineering vol. 18, 2018
- [17] Harat A., Grzesik B., Adamczyk Z.: Ocena oddziaływania na środowisko i jej zastosowanie w procesie inwestycyjnym likwidacji kopalni, Budownictwo 23, pp. 110-115, 2017
- [18] Chmiela A.: Procesy restrukturyzacji i rewitalizacji kopalń postawionych w stan likwidacji. Systemy Wspomagania w Inżynierii Produkcji, vol. 11, issue 1, pp. 28-39, 2022
- [19] Korski J., Korski W.: Underground mine as a system of processes. Mining - Informatics, Automation and Electrical Engineering, 2 (522), pp. 19-27, 2015
- [20] Smoliło J., Chmiela A., Lubosz A., Wróblewski P.: Dynamics of bearing of costs in processes leading to revitalization of mine assets in SRK S.A., Scientific Papers of Silesian University of Technology, series: Organization and Management vol. 153, 2021
- [21] Przybyła H., Chmiela A.: Projektowanie rozwiązań techniczno-organizacyjnych stosowanych w wyrobiskach ścianowych. Gliwice, Wydawnictwo Politechniki Śląskiej, 1997



<https://doi.org/10.32056/KOMAG2023.2.2>

## Proper control of working conditions as a stimulator for reducing the incidence of pneumoconiosis in the coal mining industry

Received: 25.05.2023

Accepted: 13.07.2023

Published online: 31.07.2023

### Author's affiliations and addresses:

<sup>1</sup> Pomeranian Medical University in Szczecin, Faculty of Medicine and Dentistry, Rybacka 1, 70-204 Szczecin, Poland

<sup>2</sup> Silesian University of Technology, Faculty of Mining, Safety Engineering and Industrial Automation, Akademicka 2a, 41-100 Gliwice, Poland

### \* Correspondence:

e-mail: [piotr.mocek@polsl.pl](mailto:piotr.mocek@polsl.pl)

**Kinga MOCEK <sup>1</sup>, Piotr MOCEK  <sup>2\*</sup>**

### Abstract:

Statistical data on occupational diseases recorded by the Institute of Occupational Medicine in Lodz, Poland, indicate a renewed increase in the number of cases of pneumoconiosis in Poland in recent years, especially in the PKD section of mining and quarrying industries. At the same time, in 2018 as a result of the implementation of directives of the European Parliament and the Council of the European Union, the changes were introduced to the Polish legislation in the area of protection of workers from the risk of exposure to carcinogenic or mutagenic agents related to the respirable fraction of crystalline silica found, among others, in mine dust. As a result of these solutions, since 2020 we have seen a spike in the number of miners employed in conditions of risk of carcinogenic dust. These facts indicate that despite the wide measurement of harmful factors in coal mines, the effectiveness of preventive measures taken does not bring tangible benefits, and OSH services have problems with the proper assessment of industrial dust hazards at workplaces. In the article, based on surveys, diagnostic (health) tests of workers and verification of the risk assessment methods used, the authors try to point out the most common mistakes made in estimating the level of risk associated with exposure to industrial dust.

**Keywords:** coal mine, hazards, mine dust, preparation departments, pneumoconiosis, preventive measures, surveys, occupational risk assessment



## 1. Introduction

According to the Institute of Occupational Medicine in Łódź [1], industrial dust, including asbestos-containing dust and coal and lignite containing free silica, is mentioned most often (36.7% of cases of occupational diseases) as the reason of occupational diseases in Poland in 2021. In addition to various types of pneumoconiosis (N = 490 - 2020), industrial dusts have also been indicated as a factor contributing to the development of pleural diseases, asthma, allergic rhinitis and extrinsic allergic alveolitis.

Exposure to industrial dust is also the most common cause of malignant tumour recognized as an occupational disease. Among the 193 cancer cases diagnosed in 2018-2020, 164 (85.0%) were caused by asbestos dust, and 36 (18.7%) by dust containing free crystalline silica. These dusts are responsible for 106 confirmed cases of lung cancer and all cases of mesothelioma (67 cases). Although the overall number of occupational diseases in Poland has been decreasing in recent years, the incidence of pneumoconiosis is increasing. The leader in this respect is traditionally the Silesian Voivodship, where every year more than 50% of all diagnosed cases of pneumoconiosis in Poland are recorded. This regularity is related to the structure of the industry in the Silesian Voivodship and the highest percentage of people employed in the mining industry in the Poland [2].

According to the Central Statistical Office [3], in the NACE – in section of mining and quarrying – in dusty conditions, in 2020 there were 38,823 employees (an increase of 39% compared to 2019), of which the largest number were employed in the hard coal mining section - 34,876 (89.8 %), i.e. more than every second case of a person exposed to dust in Poland. Hard coal mining industry has the highest rate of dust exposure per 1,000 employees in the plants covered by the research, which increased by 175.5% over the last 5 years from 263.6 in 2016 to 462.5 in 2020. Miners in hard coal mines are most often employed in conditions of exposure to fibrosing dusts 20,479 people - 70.2% exposed to fibrosing dusts in Poland and carcinogenic dusts 14,397 people - 69.4% exposed to carcinogenic dusts in Poland [4].

Considering the above facts, the constant increase in the number of cases of pneumoconiosis among miners of Polish mines and the fact that despite many actions taken by mining companies, the mines themselves and health and safety services, it should be worrying that we are still unable to effectively reduce this trend. To find out the reasons for this situation, the employees of the Department of Safety Engineering at the Silesian University of Technology, together with students of the Pomeranian Medical University in Szczecin and a specialist in the field of pulmonology, conducted a series of environmental, medical and surveys in one of the mines, trying to find the answer to the question: "How to limit unfavourable trends and reduce the incidence of for occupational diseases caused by industrial dust in the mining industry.

## 2. Materials and Methods – basis for the hazard assessment

The legal basis for recognizing and ascertaining occupational diseases in Poland is the Act of June 26, 1974 on the Labour Code and implementing regulations in this regard, which include, among others, Regulation of the Council of Ministers of 30 June 2009 on occupational diseases, as amended. Pursuant to Art. 235<sup>1</sup> of the Labour Code Act (Journal of Laws of 1974 No. 24 item 141), an occupational disease is considered to be a disease listed in the list of occupational diseases, if, as a result of the assessment of working conditions, it can be stated unquestionably or with high probability that it was caused by exposure to factors harmful to health in the working environment or in connection with the way work is performed, referred to as "occupational exposure". An integral part of the said regulation is the list of occupational diseases, in which pneumoconiosis was placed in item 3, including Item 3.2 pneumoconiosis of hard coal miners and the rules for documenting disease symptoms authorizing the diagnosis of an occupational disease. Another equally important regulation on exposure to industrial dust is the Regulation of the Minister of Health of February 2, 2011 on tests and measurements of factors harmful to health in the work environment, as amended, and the Regulation of the Minister of Health of January 24, 2020 amending the regulation in on chemical substances, their mixtures, factors or technological processes with a carcinogenic or mutagenic effect



in the work environment [5,6]. Both cited regulations contain guidelines for the correct assessment of the harmfulness of dust to the human body. In the assessment of occupational exposure to dust, the concentration of dust contained in the air in a given work environment (quantitative analysis) and the assessment of the chemical composition of dust present in a given workplace (qualitative analysis) are taken into account. Qualitative analysis is of particular importance in testing the mixed dusts, such as mine dust, the chemical composition of which is uncertain.

Qualitative analysis of the collected sample is performed by X-ray diffraction or with the use of absorption spectrophotometry. Obtained measurement results and calculated exposure factors refer to arbitrarily determined maximum allowable concentrations (MAC) for identified hazard factors in occupational exposure conditions.

MAC is determined for the following dusts:

- total dust (applies to all types of dust),
- respirable dust (applies only to dusts containing less than 2% of crystalline silica, natural graphite, talc without asbestos fibres, Portland and metallurgical cement dusts, apatite and phosphorite dusts and amorphous silicas),
- respirable fibrous (applies only to dusts with a fibrous structure, e.g. asbestos, artificial mineral fibres, ceramic fibres).

Working conditions should be considered safe if the calculated exposure factor does not exceed the MAC value for a given dust, and dangerous when concentration exceeds them. These indicators are also the basis for the employer to fulfil another very important obligation contained in Article 226 of the Labour Code, according to which "the employer: assesses and documents the occupational risk related to the work performed and applies the necessary preventive measures to reduce the risk; informs employees about the occupational risk associated with the work performed, and about the rules of protection against hazards".

Risk assessment, also known as the process of analyzing and determining the acceptability of risk, consists of five basic stages:

- STAGE I - collecting information,
- STAGE II - identification of hazards,
- STAGE III - risk assessment and determination of its acceptability,
- STAGE IV - development of corrective and/or preventive measures,
- STAGE V - documenting the risk assessment.

Its proper procedure and the computational methods used may affect the accuracy of preventive measures taken by workplaces management and effectively counteract occupational morbidity, e.g. pneumoconiosis among hard coal miners, which the authors will try to prove in the presented publication.

### 3. Tests results and discussion

#### 3.1. Characteristics of the tested object in the environmental tests

The subject of tests carried out as part of the cooperation of employees of the Department of Safety Engineering of the Silesian University of Technology, with employees from the Central Laboratory for Work Environment Research "Stanisław Bielaszka" from Jastrzębie Zdrój and representatives of the medical community of the Pomeranian Medical University in Szczecin were, among others, roadways of the GRP-2 preparatory work department of the X mine and its employees. During the measurements of air dust concentration at the workstations of the GRP-2 department, mining operations were related to the drilling of a coal-stone slope using the AM-75 roadheader (Fig. 1) between the 900 m and 850 m levels.





**Fig. 1.** Face GRP-2 of X mine

Employees of the preparatory department were employed in a three-shift system according to the work schedule presented in Table 1, in six mine workings, to which the following letter designations were assigned: A – slope 3 (face); B – roadway 4, C – roadway 7, D – roadway 11 (working connected with transport of the run-of-mine from the face to the central main); E - slipway 12, F - loading ditch (transport working), and at six workstations: shearer operator - 1, shearer operator assistant - 2, miner - builder - 3, miner in transport - 4, conveyor operator - 5, miner in the face - 6, shot miner - 7, driller - 8.

**Table 1.** Work schedule of the GRP-2 department team

Activities	Duration [min]	Total duration of the shift
Going down and up	20	450 min
Transfer by passenger train	30	
Getting to and from the workplace	35	
Preparatory and transport work	60	
Mining with a shearer and operation of conveyors	200	
Construction of the frame of the roof support	105	

Results of measurements of airborne dust concentration at each working and at the workstations of the GRP 2 department of the X mine showed that the level of dust concentration and the content of carcinogenic crystal silica in many cases significantly exceed the new hygienic standards both in the mining face with a shearer and blasting work, as well as in transport workings (Table 2). The respirable dust is a greatest threat to employees, as its concentration exceeded the allowable value at each workstation by 3.7 to 5.1 times, and in the face and transport roadways by 4.6 to 6.0 times. In turn, in the case of free crystalline silica, hygienic standards are exceeded even 9.0 times (Table 3).

**Table 2.** The results of measurements of hard coal airborne dust concentration in each working and at the workstations of the GRP-2 department using the dosimetry method

Department	Position	Dust concentration in fractions [mg/m <sup>3</sup> ]		Indicator W <sub>E</sub> [mg/m <sup>3</sup> ]		MAC		Indicator W <sub>N</sub> (multiplicity of MAC)	
		inhalable	respirable	inh.	resp.	inh.	resp.	inh.	resp.
<b>Workings</b>									
GRP-2	A	0.94-39.40	0.43-12.36	38.32	11.95	10	2	3.8	6.0
	B	0.78-41.18	0.35-11.95	40.79	11.03	10	2	4.1	5.5
	C	0.58-42.60	0.28-10.50	41.55	9.70	10	2	4.2	4.9
	D	0.27-44.31	0.20-9.73	44.01	9.13	10	2	4.4	4.6
	E	0.46-32.64	0.26-7.20	31.95	6.75	10	2	3.2	3.4
	F	0.23-28.24	0.14-5.18	27.84	4.89	10	2	2.8	2.4



Workstations									
GRP-2	1	0.51-35.10	0.26-9.11	33.82	10.20	10	2	3.4	5.1
	2	0.48-33.22	0.20-9.64	31.36	9.34	10	2	3.1	4.7
	3	0.28-26.46	0.11-7.30	24.29	7.28	10	2	2.4	3.6
	4	0.09-21.13	0.07-6.35	19.21	6.13	10	2	1.9	3.1
	5	0.23-31.77	0.15-8.38	31.20	8.96	10	2	3.1	4.5
	6	0.12-26.30	0.04-6.33	24.78	7.47	10	2	2.5	3.7

**Table 3.** Results of measurements of the chemical substance - crystalline silica in each working and at the stations of the GRP-2 department using the dosimetry method

Department	Position	Range of concentration of crystalline silica in the respirable fraction [mg/m <sup>3</sup> ]	Indicator W <sub>E</sub> [mg/m <sup>3</sup> ]	MAC of the respirable fraction	Indicator W <sub>N</sub> (multiplicity of MAC)
<b>Workings</b>					
GRP-2	A	0,066-0,945	0,912	0,1	9,1
	B	0,058-0,873	0,826	0,1	8,3
	C	0,056-0,764	0,703	0,1	7,0
	D	0,049-0,614	0,596	0,1	6,0
	E	0,028-0,582	0,527	0,1	5,3
	F	0,025-0,430	0,392	0,1	3,9
<b>Workstations</b>					
GRP-2	1	0,046-0,621	0,600	0,1	6,0
	2	0,038-0,610	0,592	0,1	5,9
	3	0,026-0,555	0,514	0,1	5,1
	4	0,009-0,214	0,196	0,1	2,0
	5	0,028-0,582	0,563	0,1	5,6
	6	0,025-0,430	0,403	0,1	4,0

Medical examinations among employees of the GRP-2 department exposed to mine dust showed a many functional and health disorders in 18% of active employees of the GRP-2 department [2,4], and in the last 5 years, five cases of pneumoconiosis recognized on the basis of decision about the occupational diseases.

### 3.2. Occupational risk assessment in a selected tested object

To estimate the occupational risk, various assessment methods are used in the world depending on the prevailing hazards and the workplace specificity. They can be divided into qualitative and quantitative methods.

Qualitative risk assessment methods are very often used for immeasurable factors for which no limit values have been set. The magnitude of the risk is a combination of the hazard itself and the severity of the hazard consequences.

Quantitative risk assessment methods are used for measurable factors for which limit values have been set. They consist in comparing the value of the quantity characterizing the exposure  $P$  with the limit value  $P_{max}$ . These methods are used to calculate the concentration or intensity of harmful factors [7,8]

In Polish hard coal mines, the method of the Polish Standard PN-N-18002:2011 [9] is most often used to assess harmful factors, in which the risk ( $R$ ) is defined as a function of the probability of an event ( $P$ ) and its potential consequences ( $S$ ) referred to the value of exceeding the limit of a given harmful factor (formula 1):

$$R = f(P, S) \quad (1)$$



and the Risk Score method [10], in which the risk (R) is defined as the product of the probability of the hazard (P), exposure to the hazard (E) and the probable effects of the hazard (S), which can be written as formula 2:

$$R = P \times E \times S \quad (2)$$

The Silesian University of Technology in its research projects, proposed an assessment of the risk of harmful factors based on a number of mathematical indicators taking into account, in addition to the value of exceeding the hygienic standards, also the number of employees exposed and morbidity [11], so the health risk ( $R_{ZW}$ ) was defined as the product of exposure probability indicators ( $W_P$ ), exposure factor ( $W_E$ ), number of persons exposed ( $W_L$ ), and probability factor of loss resulting from exposure ( $W_S$ ) according to formula 3.

$$R_{ZW} = W_p \times W_E \times W_L \times W_S \quad (3)$$

The assumptions of the above-mentioned methods were used in the research part to estimate the health risk for employees of the GRP-2 department of the X mine, based on the measurement data of airborne dust concentration given in Table 2, taking into account the nominal work time of the miners of this department according to the time schedule presented in Table 1. Going down to the mine and up the crew is practically not exposed to harmful dusts. During the arrival and departure from the workplace, preparatory and transport work and other elements of the production process, the measurement of the content of harmful dust was taken using individual dust meters of the CIP-10 and AP-2000Ex type. The measurements covered workstations in all workings in the GRP-2 department.

Health risk for the GRP-2 department was assessed at the workings level using all three risk assessment methods mentioned earlier. A full health risk assessment for each method is presented in Table 4 (PN-N-18002 method), Table 5 (Risk Score method) and Table 6 (Silesian University of Technology method).

The measurements confirm the theses of other researchers [12,13] that the determination of occupational (health) risk by the method of the Polish Standard PN-N-18002:2011, depending on the considered event, has a relative error ranging from a dozen to even 60%, because this method omits many important environmental parameters depending, among others, on the time of exposure and the competence of the team assessing a given hazard. On the other hand, in the Risk Score method, the most common method used by mines, the relative statistical error exceeds 15%. The Risk Score method takes into account exposure to risk, which significantly improves its credibility, but does not take into account the human factor and pathological changes. In the teams assessing the risk using the Risk Score method, there is also no occupational medicine specialist who could assess the potential impact of a harmful factor on the actual health condition of the employee. As a consequence, the inability to take into account in both methods even small uncertainties in the calculation of the original values of losses, the probability of events and the frequency of exposure results in a small differentiation of the assessed objects in terms of the existing threat (Table 7). An underestimation of the risk may result in unnecessary human losses such as an increase in the dynamics of pneumoconiosis, while an overestimation of the risk may result in material losses for mining plants due to too costly overestimation of the necessary preventive measures aimed at reducing the risk. The method of the Silesian University of Technology, although laborious and complicated due to the multitude of variable parameters, seems to be the most desirable in the assessment of health risk. Its relative statistical error due to the use of actual variables is also the smallest due to the elimination of the free assessment of facts by the members of the assessment team, which in turn affects the final result of the occupational risk assessment and the possibility of indicating the effective preventive measures.

**Table 4.** Health risk assessment for workings of the GRP-2 department for mine X due to airborne dust using the PN-N-18002 method

	Name of the parameter	Workings of the department					
		Dip road 3 (face)	Roadway 4	Roadway 7	Roadway 11	Inclined drift 12	Loading ditch 850 m
	Symbol	A	B	C	D	E	F
1.	Average concentration of free crystalline silica SiO <sub>2</sub> [mg/m <sup>3</sup> ]	0.912	0.826	0.703	0.596	0.527	27.84
2.	Average total dust concentration in the working, C <sub>wc</sub> [mg/m <sup>3</sup> ]	38.32	40.79	41.55	44.01	31.95	30.09
3.	MAC for total dust [mg/m <sup>3</sup> ]	10	10.0	10.0	10.0	10.0	10.0
4.	Average concentration of respirable dust in the working, C <sub>wc</sub> [mg/m <sup>3</sup> ]	11.95	11.03	9.70	9.13	6.75	4.89
5.	MAC for respirable dust [mg/m <sup>3</sup> ]	2.0	2.0	2.0	2.0	2.0	2.0
6.	Multiplicity indicator of exceeding the K <sub>MAC</sub> normative	5.6	5.2	4.6	4.3	3.2	2.3
7.	Hazard probability	high	high	high	high	high	high
8.	Severity of the harmful consequences	high	high	high	high	high	high
9.	Health risk assessment	high	high	high	high	high	high
10.	Admissibility of health risk	unacceptable					

**Table 5.** Health risk assessment for workings of the GRP-2 department for mine X due to airborne dust using the Risk Score method

	Name of the parameter	Workings of the department						
		Dip road 3 (face)	Roadway 4	Roadway 7	Roadway 11	Inclined drift 12	Loading ditch 850 m	
	Symbol	A	B	C	D	E	F	
1.	Average concentration of free crystalline silica SiO <sub>2</sub> [mg/m <sup>3</sup> ]	0.912	0.826	0.703	0.596	0.527	27.84	
2.	Average total dust concentration in the working, C <sub>wc</sub> [mg/m <sup>3</sup> ]	38.32	40.79	41.55	44.01	31.95	30.09	
3.	MAC for total dust [mg/m <sup>3</sup> ]	10.0	10.0	10.0	10.0	10.0	10.0	
4.	Average concentration of respirable dust in the working, C <sub>wc</sub> [mg/m <sup>3</sup> ]	11.95	11.03	9.70	9.13	6.75	4.89	
5.	MAC for respirable dust [mg/m <sup>3</sup> ]	2.0	2.0	2.0	2.0	2.0	2.0	
6.	Multiplicity indicator of exceeding the K <sub>MAC</sub> normative	5.6	5.2	4.6	4.3	3.2	2.3	
7.	Hazard probability P	10	10	10	10	3	3	
8.	Exposure to the hazard E	10	6	6	6	6	6	
9.	Potential effects of the hazard - S	7	7	7	7	7	7	
10.	Risk factor	700	420	420	420	126	126	
11.	Category of risk	Very high				significant		
12.	Risk zone	Critical				dangerous		



**Table 6.** Health risk assessment for workings of the GRP-2 department for mine X due to airborne dust

	Name of the parameter	Workings of the department					
		Dip road 3 (face)	Roadway 4	Roadway 7	Roadway 11	Inclined drift 12	Loading ditch 850 m
	Symbol	A	B	C	D	E	F
1.	Average concentration of free crystalline silica SiO <sub>2</sub> [mg/m <sup>3</sup> ]	0.912	0.826	0.703	0.596	0.527	27.84
2.	Average total dust concentration in the working, C <sub>Wc</sub> [mg/m <sup>3</sup> ]	38.32	40.79	41.55	44.01	31.95	30.09
3.	MAC for total dust [mg/m <sup>3</sup> ]	10	10.0	10.0	10.0	10.0	10.0
4.	Average concentration of respirable dust in the working C <sub>Wr</sub> [mg/m <sup>3</sup> ]	11.95	11.03	9.70	9.13	6.75	4.89
5.	TLV for respirable dust [mg/m <sup>3</sup> ]	2.0	2.0	2.0	2.0	2.0	2.0
6.	Daily exposure for one worker [hours]	7.5	7.5	7.5	7.5	7.5	7.5
7.	Multiplicity indicator of exceeding the K <sub>MAC</sub> normative	5.6	5.2	4.6	4.3	3.2	2.3
8.	Hazard risk indicator P	<b>10</b>	<b>10</b>	<b>10</b>	<b>10</b>	<b>10</b>	<b>10</b>
9.	Average number of hours worked in exposure by a worker in a given working per one year L <sub>gw</sub>	1738	1738	1738	1680	1680	1680
10.	Number of working hours in a year L <sub>gr</sub>	1950	1950	1950	1950	1950	1950
11.	Indicator of the risk of absorption of a given harmful factor by an employee, E <sub>c</sub>	5.0	4.6	4.1	3.7	2.8	2.0
12.	Hazard Exposure Risk Index, E	<b>10</b>	<b>10</b>	<b>10</b>	<b>10</b>	<b>10</b>	<b>10</b>
13.	The average number of employees exposed daily to the harmful factor L <sub>NW</sub>	15	12	9	6	12	12
14.	Total number of employees of the department, L <sub>AZ</sub>	66	66	66	66	66	66
15.	Risk indicator of exposure of a given number of people employed in the W <sub>L</sub> excavation	0.23	0.18	0.14	0.09	0.18	0.18
16.	Risk indicator of the number of people at risk, W <sub>L</sub>	<b>4</b>	<b>2</b>	<b>2</b>	<b>1</b>	<b>2</b>	<b>2</b>
17.	Number of cases of pneumoconiosis in the last 5 years	5	5	5	5	5	5
18.	Average number of diagnosed cases of pneumoconiosis among the department employees in the last 5 years, L <sub>CH</sub>	1	1	1	1	1	1
19.	Average number of employees employed in the department in the last 5 years L <sub>ZAT</sub>	63	63	63	63	63	63



20.	Occupational morbidity rate of employees, $W_z$	0.00137	0.00137	0.00137	0.00137	0.00137	0.00137
21.	Loss risk indicator due to the hazard, $W_s$	<b>10</b>	<b>6</b>	<b>3</b>	<b>3</b>	<b>0.5</b>	<b>0.5</b>
22.	Health risk index, $W_{RZ}$	4000	1200	600	300	100	100
23.	Risk category	Not acceptable	undesired	significant	acceptable	acceptable	acceptable
24.	Risk zone	critical	Specially dangerous	dangerous	almost safe	almost safe	almost safe

The tests enabled developing the final ranking of the workings of the GRP-2 department of the X mine in terms of the risk category and the sequence of preventive actions according each method of occupational risk assessment (Table 7).

**Table 7.** Ranking of the workings of the GRP-2 department regarding the risk of harmful exposure to coal dust

Method of Polish PN-N-18002 Standard							
Acceptance of risk in the working							
Unacceptable		Acceptable		Acceptable		Acceptable	
Dip road 3 (face)							
roadway 4							
roadway 7							
roadway 11							
Inclined drift 12							
Loading ditch 850m							
Risk Score Method							
Critical workings		Specially dangerous workings		Dangerous workings		Almost safe workings	
Risk factor	Workings name	Risk factor	Workings name	Risk factor	Workings name	Risk factor	Workings name
700	dip road 3			126	inclined drift 12		
420	roadway 4			126	loading ditch		
420	roadway 7						
420	roadway 11						
Method of Silesian University of Technology (Poland)							
Critical workings		Specially dangerous workings		Dangerous workings		Almost safe workings	
Risk factor	Workings name	Risk factor	Workings name	Risk factor	Workings name	Risk factor	Workings name
4000	dip road 3	1200	roadway 4	600	roadway 7	300	roadway 11
						300	inclined drift 12
						100	loading ditch

### 3.3. Questionnaire inquiry among GRP-2 department employees

68 employees of the GRP-2 preparatory department of the X mine took part in the inquiry. The vast majority of the respondents were still active employees of the mine - 92.1%.

In addition to answers to basic questions related to age, seniority, professional status, the respondents were also asked to indicate the department of the mine in which they worked for the longest time and to answer the following 25 more detailed questions:

- a) exposure to industrial dust at work,



- b) the type of sources of industrial dust that accompanies them at work,
- c) changes that have recently taken place in the method of assessing the dust hazard at the workplace,
- d) health effects that may appear in connection with long-term exposure to industrial dust,
- e) preventive measures taken by the employer to reduce the dust hazard.

The answer to the above issues gave an image of an average employee of the GRP- 2 preparation department who:

- 1) Is in an average age of around 43 years old and has been working in a mine for 17 years, with an average of 16.5 in preparation departments.
- 2) Is aware of the health issues, which might be caused by long-term exposure to mine dust.
- 3) Is exposed to dust, whose main source is the process of excavating and hauling, for about 5 hours per day in their workplace.
- 4) Mining and rock dust influences their wellbeing and they feel its influence on the respiratory system.
- 5) Is informed by their employer of the dusting level at the workplace and is equipped with personal protective equipment (Graph No. 1).
- 6) Knows about collective dust protection methods, although associates them mostly with reducing dust's explosive properties, rather than its harmful effect.
- 7) Isn't aware of any additional obligations the employer has in view of the change in regulations, which count crystalline silica as a carcinogen.
- 8) Performs a chest X-ray once every few years, sometimes a spirometry test, during the periodic examinations, but is unlikely to have heard of any other diagnostic lung tests.
- 9) Shows interest in their actual health condition only when retired or when experiencing severe respiratory ailments (Graph No. 2).

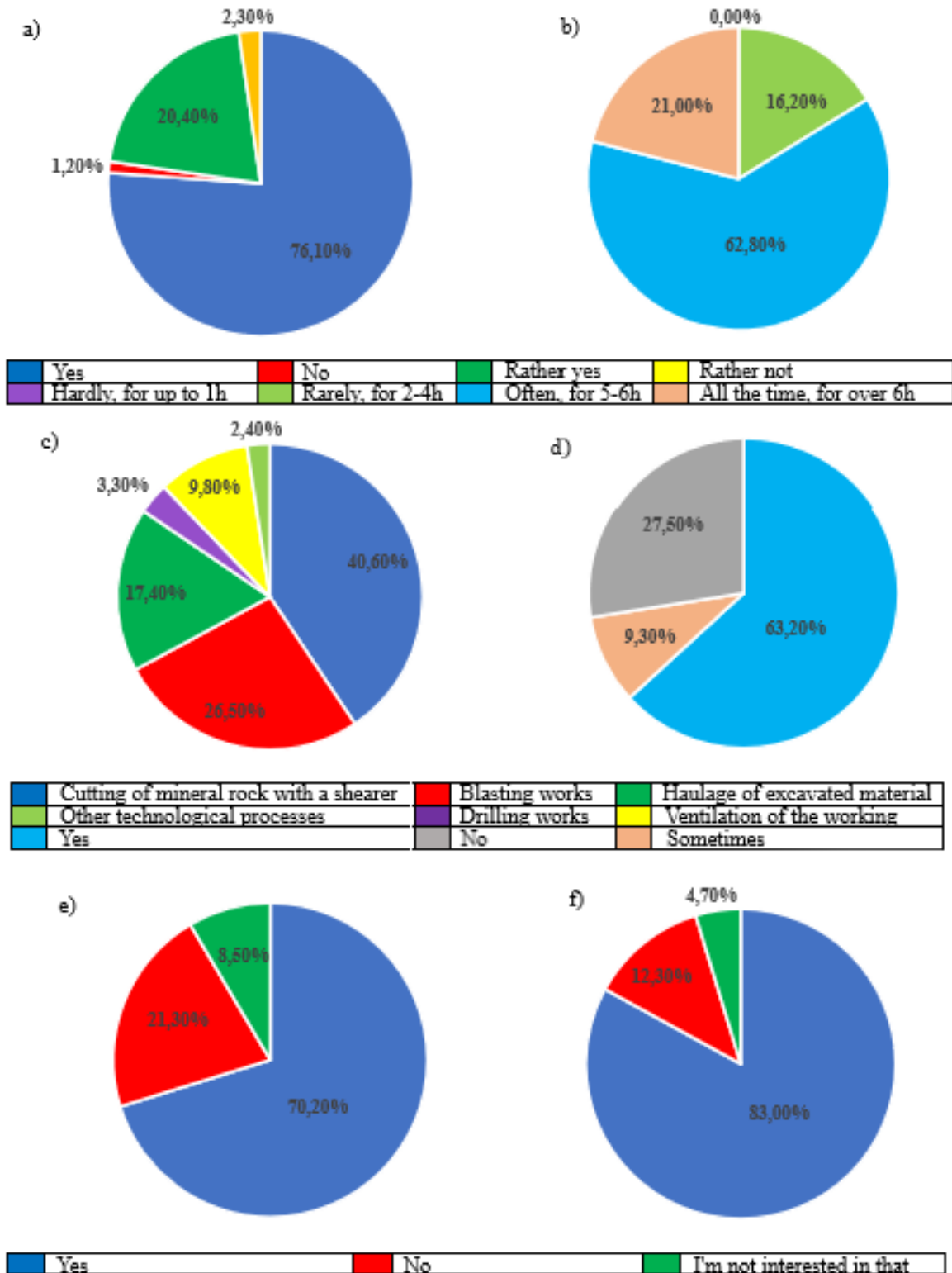
Doesn't pay much attention to the occupational risk assessment, because usually doesn't understand the meaning of it.

#### 4. Conclusions

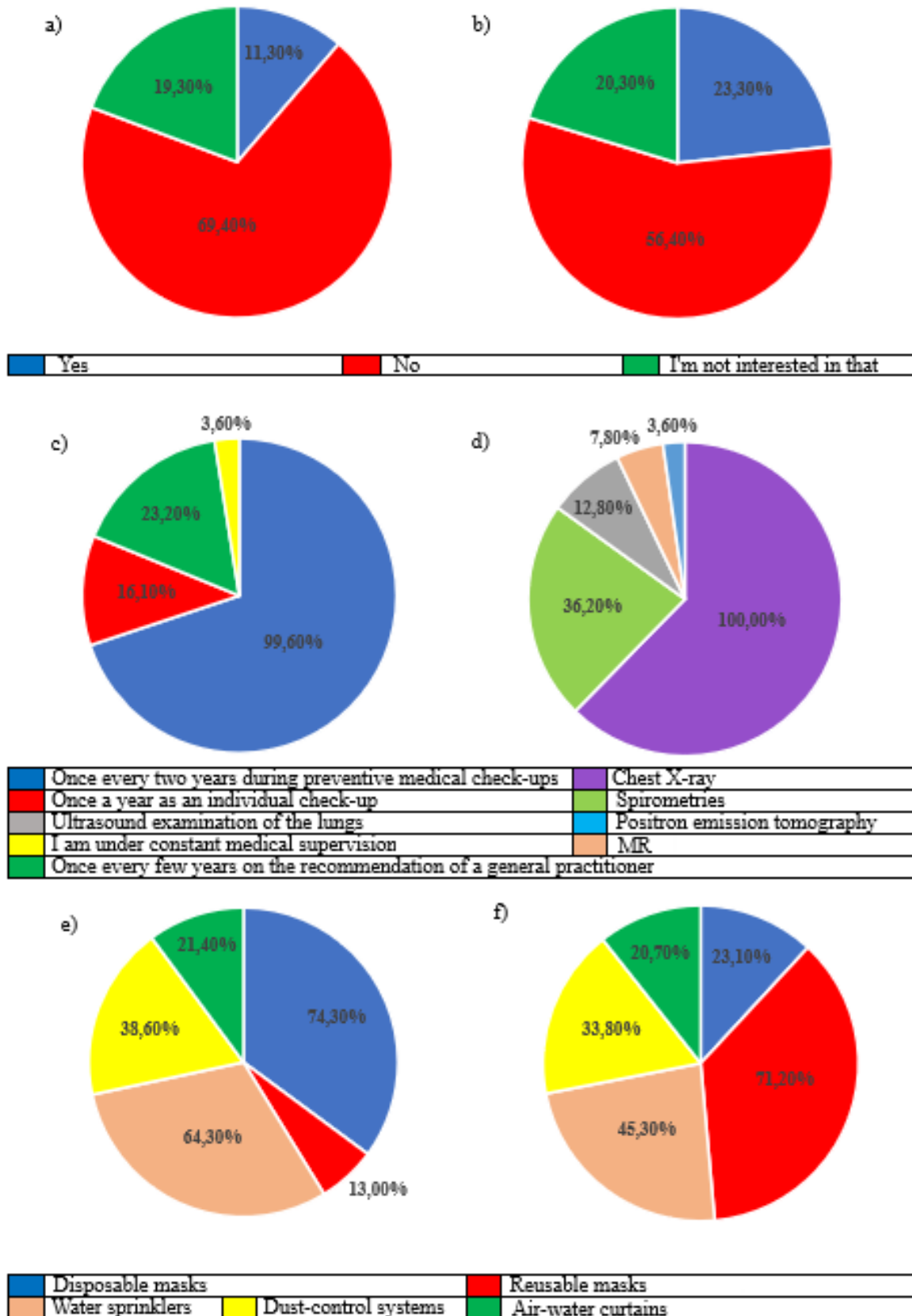
Despite the international efforts and actions taken in order to reduce the exposure of coal mine workers to harmful dust from mining process, there are still tens of thousands of miners exposed to its harmful effects. One of the results of this exposure is pneumoconiosis, an illness commonly occurring amongst miners, which has been the subject of research and scientific publications for many researchers over the years. Apart from personal protective equipment provided for workers exposed to dust-forming processes, other technical solutions such as sprinklers or dust control systems installed on mining machines and in mine workings of hard coal mines are used in order to reduce the risk. Those installations are designed to reduce the amount of dust in the workplace.

The results of the questionnaires are presented below in the form of graphs 1 and 2.





**Graph No.1.** Answers to the questionnaire questions: a) Is there a high level of dust in your workplace?, b) How often during the day are you exposed to dusty air at work?, c) What is the main source of dust at your workplace?, d) Does the dusty air at your workplace adversely affect your wellbeing?, e) Are you sufficiently informed about the dust levels at your workplace (you know the results of dust measurements)? f) Do you know how long-term exposure to coal dust and dust containing crystalline silica can influence your health?



**Graph No. 2.** Answers to the questionnaire questions: a) Do you know the employer's obligations in relation to the change in the maximum concentration limits for dust and chemicals?, b) Is the crystalline silica contained in mine dust classed as a carcinogen?, c) How often do you perform

respiratory health checks? d) What type of respiratory tests were performed on you? e) What type of dust protection equipment is most commonly used at your workplace? f) How would you rate the effectiveness of the dust control measures in place at your workplace?

As shown by environmental studies carried out by employees of the Department of Safety Engineering at the Silesian University of Technology and medical examinations of miners of the GRP-2 division of mine X, the individual and collective protection measures currently used in mining, despite advances in knowledge and new technical solutions, are not able to completely eliminate the risk of illness among workers. This problem is particularly apparent for dusts containing free crystalline silica, which is why most European countries have reduced the limit values for respirable silica to no more than  $0.1 \text{ mg/m}^3$ . These changes were introduced in Poland as a result of the Directive (EU) 2017/2398 of the European Parliament and of the Council of 12 December 2017, amending Directive 2004/37/EC on the protection of workers from the risks related to exposure to carcinogens or mutagens at work (OJ EU L 345, 27.12.2017) [29] and extending the record of the Regulation of the Minister of Health on chemicals, their mixtures, agents or technological processes with a carcinogenic or mutagenic effect in the working environment to include "work involving exposure to crystalline silica - respirable fraction generated at work." The clause introduced imposes additional obligations on employers and physicians providing preventive health care to employees working in conditions of exposure to harmful dusts, involving not only an increase in environmental measurements of air dust, but also an extension of preventive medical care.

A well-conducted occupational risk assessment is also an important element in combating existing health risks in the production process. The research presented in this publication has shown that the use of simplified expert occupational risk assessment methods that omit some of the important measurable parameters of the working environment can adversely affect the valuation of existing risks and be subject to significant statistical errors, resulting in underestimation or overestimation. Therefore, occupational health physicians should be included in the health risk assessment teams, who will be able to estimate the health effects and implement appropriate medical prevention, which should, in the long term, reduce the incidence of pneumoconiosis and other occupational diseases not only in the mining industry.

## References

- [1] Świątkowska B., Hanke W.: Choroby zawodowe w Polsce w 2020 r. Instytut Medycyny Pracy. Centralny Rejestr Chorób Zawodowych, Łódź 2021
- [2] Mocek P., Mocek K.: Environmental impact of noise from mining operations. Scientific Journals of the Maritime University of Szczecin 2023, 73 (145), 15–28. DOI: 10.17402/551
- [3] Akusztol J. i inni. Warunki pracy w 2020 r. Informacja Statystyczna. Główny Urząd Statystyczny. Warszawa, Gdańsk 2021. str. 1-39 plus załączniki.
- [4] Mocek P., Mocek K.: Mine dust – as a cause of respiratory diseases of mines. Mining Machines, 2022, vol. 40 nr 2, s 98-109. DOI:10.32056/KOMAG2020.2.5
- [5] Rozporządzenie Ministra Zdrowia z dnia 2 lutego 2011 r. W sprawie badań i pomiarów czynników szkodliwych dla zdrowia w środowisku pracy Dz. U. 2023 poz. 419
- [6] Rozporządzenie Ministra Zdrowia z dnia 24 stycznia 2020 r. zmieniające rozporządzenie w sprawie substancji chemicznych, ich mieszanin, czynników lub procesów technologicznych o działaniu rakotwórczym lub mutagennym w środowisku pracy. Dz.U. 2020 poz. 197
- [7] Rączkowski B.: BHP w praktyce. Wyd.: Oddk, Gdańsk 2012, s. 1018- 1019, 1029.
- [8] Krause M.: Bezpieczeństwo i higiena pracy. Podstawowe wymagania i wytyczne. Wyd. Poznań 2012, s.71
- [9] Polska Norma: PN-N-18002:2011 Systemy zarządzania bezpieczeństwem i higieną pracy - Ogólne wytyczne do oceny ryzyka zawodowego
- [10] Kinney G. F., Wiruth A. D.: Practical Risk Analysis for Safety Management. US Naval Postgraduate School, Security Department China Lake, Kalifornia 1976



- [11] Mocek P.: Ocena ryzyka powstawania chorób zawodowych u pracowników zatrudnionych w wyrobiskach podziemnych kopalni węgla. Politechnika Śląska. Wydział Górnictwa i Geologii Praca doktorska. Gliwice 2002. Promotor dr hab. inż. Stanisław Krzemień
- [12] Smolarkiewicz M.: Analiza niepewności oceny ryzyka w metodach ilościowych i półilościowych. Uniwersytet Łódzki, 2022; [https://imul.math.uni.lodz.pl/wp-content/uploads/2017/11/MMSmolarkiewicz\\_Analiza-niepewnos%CC%81ci-oceny-ryzyka-w-metodach-ilos%CC%81ciowych-i-po%CC%81%C5%82ilos%CC%81ciowych.pdf](https://imul.math.uni.lodz.pl/wp-content/uploads/2017/11/MMSmolarkiewicz_Analiza-niepewnos%CC%81ci-oceny-ryzyka-w-metodach-ilos%CC%81ciowych-i-po%CC%81%C5%82ilos%CC%81ciowych.pdf)
- [13] Smolarkiewicz M.: Niepewność identyfikacji i wyznaczenia ryzyka w metodzie analizy Risk Score, str. 107-118, Zeszyty Naukowe SGSP, nr 41, Warszawa 2011, ISSN 0239-5223



## Monitoring of belt floating under controlled belt transmission load

Received: 17.07.2023

Accepted: 28.07.2023

Published online: 31.07.2023

### Author's affiliations and addresses:

<sup>1</sup> Technical University of Kosice,  
Bayerova 1, Presov, 080 01, Slovak  
Republic

### \* Correspondence:

e-mail: [jozef.mascenik@tuke.sk](mailto:jozef.mascenik@tuke.sk)

tel. +421 51 772 6337

Jozef MASCENIK <sup>1\*</sup>, Tomas CORANIC <sup>1</sup>,  
Juraj RUZBARSKY <sup>1</sup>, Tibor KRENICKY <sup>1</sup>

### Abstract:

The paper focuses on experimental monitoring of tightening and floating of the belt at controlled loading of belt gear. In general, the belt gear is referred to as friction gear in practice the primary function of which is to transfer the performance as a consequence of frictional forces occurring between a driven belt pulley, a driving belt pulley and a flexible element. In experimental measurements, the flexible element is represented by a V-belt. The main advantages of the belt gears are peripheral speed, flexible engagement, silent running, vibration absorption and their price. Standard operation of the belt gear requires correct belt tightening which is achieved by movement of a pulley and a tension roll. At the same time, the belt tightening can be achieved by changing the spacing of the shaft axes used in experiments. In the case of belt gears use, specific principles must be observed. The principles include tightening of the belt with particular force which represents, in fact, primary condition of transmission of motion and force. At rest, the tension of both belt parts is identical. Complex analysis of belt gears was followed by experimental measurements on the stands designed for testing and monitoring of belt gears. For the purposes of monitoring of the belt floating there was a system designed which used a high precision sensor to measure distance between the belt and the sensor. At the same time, a device designed to determine the belt tightening was used as well. All measurements were analysed and collected data and facts were used to determine dependencies possible to be applied when the monitored parameters are evaluated. The results of experimental monitoring of the selected parameters at controlled loading of the belt gear can be useful in practice for designing, checking and maintenance operations.

Keywords: monitoring, belt floating, strength, belt gear, tension, load



## 1. Introduction

Currently, the frequency of utilization of V-belts is higher compared to standard flat belts. The reason rests in capability to transmit higher torque. Frequently, they have of trapezoidal section which creates friction in a keyseat of the pulley on the side faces. The keyseat in the pulley must be correctly shaped to prevent the belt from reaching the bottom of the keyseat. Contrary to standard conditions, by means of the V-belts it is possible to transmit relatively high performances with considerably shorter axis distances and with higher gear ratios [1]. The gears with V-belts considerably damp strokes and flexibility of the belts. An exceptional advantage is rather silent running, soft engagement and negligible slippage. In practice, the customers are supplied with the open-ended V-belts in enclosed circle which means that the belt length is determined either by technical conditions of the manufacturer or by a respective standard. The gear containing more V-belts placed side-by-side require replacement of the entire set of the belts. In the case of such belt types, there are not any modifiers to increase the friction between the belt and pulley used.

The belt gears are commonly used in passenger vehicles as some types of vehicles are designed with a friction gearbox. The gearbox in a passenger vehicle consists of two pulleys and of axially moving bevel gear with the V-belt running in between. One of the pulleys is connected with an input shaft and the other one is connected with an output shaft. Moving the cones closer and further results in change of diameter, which the belt draws, along with gear ratio. During run-up, when the highest gear ratio or tensile force is required, the lowest diameter is set in primary pulley [2]. The belt of such gear has fixed length yet slight deformations are taken into consideration. With regards to the fact that the belt gears are frequently used in different spheres and that the precision tolerance constantly increases, it is inevitable to deal with the issue.

The belt gears are used in case of diverse industrial applications for their versatility, reliability and low costs. However, floating of the belt may occur due to different reasons such as insufficient tension, incorrect alignment, wear and tear and excessive loading. Floating of the belt may result in decreased efficiency, increased energy consumption and premature failure of the belt gear system [3].

The designed monitoring system will include measurement and analysis of frequency of the belt floating to detect and diagnose potential defects in the belt gear system. The system will use sensors to measure vibrations of the system of the belt gear and the data will be processed and analysed in order to identify frequency of the belt floating and other abnormalities. The results of analysis will be used to determine the cause of the belt floating and to provide recommendations for rectifying measures.

The monitoring system was designed to allow simple installation and maintenance and to be applicable in case of diverse types of the belt gears. The implementation of the designed system will contribute to increase efficiency and reliability of the belt gear systems, to decrease maintenance costs and to extend service life of the device [4].

## 2. Analysis and design of the belt gears

Analysis of the belt gears deals with examination of different aspects of function and performance. Within the frame of the analysis the following factors are examined:

1. Torque capacity - it refers to the torque which can be transmitted by the gear with zero belt damaging. The factor depends on width, material and tightening of the belt.
2. Efficiency – it refers to energy being transmitted from side to side. The efficiency of the belt gears depends on many factors such as belt tightening, used belt type, belt width and gear speed.
3. Speed – gear speed depends on belt diameter, belt width and speed of shaft rotation. It is important to remember that speed must be sufficient enough to reach required performance, yet it cannot be too high to prevent belt damaging.
4. Noise level – belt gears can achieve high noise level, especially when using older models. Noise level depends on type and material of the used belt.



5. Service life – service life of the belt gears depends on many factors such as type, quality, use and maintenance of the belt. Correct maintenance and regular check-ups can extend service life of the belt gears [5].

Designing and checking of the belt gears is preceded by proposal of their dimensions. Significant dimension is arithmetic diameter of the pulley referred to as “ $d_p$ ” for input pulley and “ $D_p$ ” for output pulley. Arithmetic length is referred to as “ $L_p$ ” which is applicable both for the flat belts and for the V-belts. In fact, it is the length of the tightened belts in the plane of the neutral fibre. The length of fibres remains the same at constant tension and deformation of cross-section by deflection. The arithmetic length of the belt can be expressed as follows:

$$L_p \cong 2a + \frac{\pi}{d}(d_p + D_p) + \frac{(D_p - d_p)^2}{4a} \quad (1)$$

With “ $a$ ” referring to axial distance of the pulleys. Consequently, it is possible to determine approximate length based on the equation as follows:

$$L_p = 2a \frac{\alpha}{2} + \frac{\pi}{2}(d_p + D_p) + \frac{\pi\gamma}{180^\circ}(D_p - d_p) \quad (2)$$

With  $\alpha$  referring to angle of contact of smaller pulley and the value  $\gamma$  can be calculated according to the following equation:

$$\gamma = \left(90^\circ - \frac{\alpha^\circ}{2}\right) = \arcsin\left(\frac{D_p - d_p}{2a}\right) \quad (3)$$

Consequently, standardized belt length can be determined according to the standard and approximate axial distance of the individual pulleys can be expressed by means of the following equations:

$$a \approx p + \sqrt{p^2 - q} \quad (4)$$

Then  $p$  and  $q$  can be calculated as follows:

$$p = \frac{1}{4}L_p - \frac{\pi}{8}(d_p + D_p) \quad (5)$$

$$q = \frac{1}{8}(D_p - d_p)^2 \quad (6)$$

Initial solution for calculation of the force was its calculation in tensile  $F_1$  and relieved  $F_2$  branch of the belt gears (Fig. 1). In these calculations a perfectly flexible fibre was taken into consideration and at the same time the angle of contact was defined along with coefficient of friction  $f$ . When taking into consideration an elementary particle, an elementary normal  $dF_N$ , tangential  $dF_t$  tension, it is possible to opt for relations for elementary tangential  $F_T$  and normal  $F_N$  force [6].



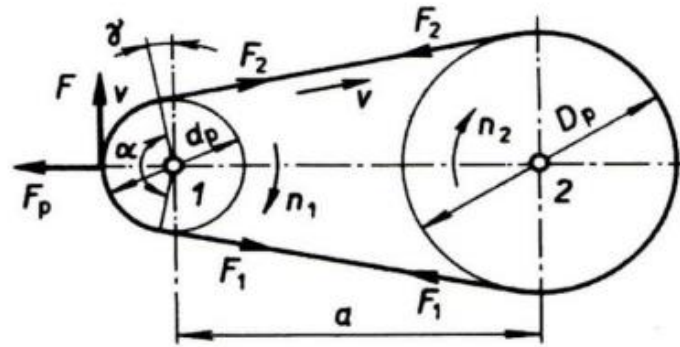


Fig. 1. Force ratio in the belt gear

Euler’s formula is applicable for the forces  $F_1$  and  $F_2$  in relieved and tensile branch of the belt gear:

$$F_1 = F_2 \cdot e^{f \cdot \alpha} \tag{7}$$

with:

- $\alpha$  – angle of contact of small pulley,
- $f$  – coefficient of friction stipulated by the standard,
- $e$  – Euler’s number - 2.718...

Checking the force ratios requires calculation of circumferential force of the small pulley according to following equation:

$$F_o = \frac{2 \cdot Mk_1}{d_p} \tag{8}$$

Then the torque can be defined according to the following equation:

$$Mk_1 = \frac{P_1}{\omega_1} \tag{9}$$

Consequently, based on resultant force balance of the selected belt the following relationship can be detected:

$$F_o = F_1 - F_2 \tag{10}$$

The following relation is then applicable for force  $F_1$ :

$$F_1 = F_o \frac{e^{\alpha \cdot f}}{e^{\alpha \cdot f} - 1} \tag{11}$$

Consequently, it is inevitable to calculate the belt tightening during installation. The respective tightening is necessary to derive adherence force between the belt and the pulley. The following relation is applicable:

$$F_p = \frac{F_1 + F_2}{2} \tag{12}$$

Consequently, it is suitable to select actual prestress to increase prevention of slippage according to the equation as follows:

$$F_{ps} = (1,2 \div 1,6) \cdot F_p \quad (13)$$

Resultant of the individual forces will be geometrical sum according to the equation as follows:

$$F_v = \sqrt{F_1^2 + F_2^2 + 2 \cdot F_1 \cdot F_2 \cdot \cos \gamma} \quad (14)$$

So angle  $\gamma$  is possible to be calculated according to the equation as follows:

$$\gamma = 90^\circ - \frac{\alpha}{2} \quad (15)$$

The aforementioned force causes transverse stress of the shaft.

### 3. Floating of the belt

Vibrations of the belt gear can cause diverse problems including increased noise, premature wearing of the belt and of the pulley and decreased efficiency [7]. As regards the belt drives different types of the floating can occur (Fig. 2) including the following phenomena:

1. Torsional floating occurs when the belt and pulleys are incorrectly adjusted which causes torsional deflection of the belt. The slippage of the belt, excessive wearing and noise can be caused by torsional vibrations.
2. Transverse floating to sides caused by excessive stress, incorrect adjustment or resonance is referred to as transverse vibrations. Excessive wear of the belt, of the pulley and of the bearings as well as increased noise level can be caused by transverse vibrations.
3. Axial floating occurs when the belt moves back and forth along its axis which is frequently caused by insufficient tightening or incorrect adjustment. Axial floating can result in excessive wear and noise of the belt and pulleys.

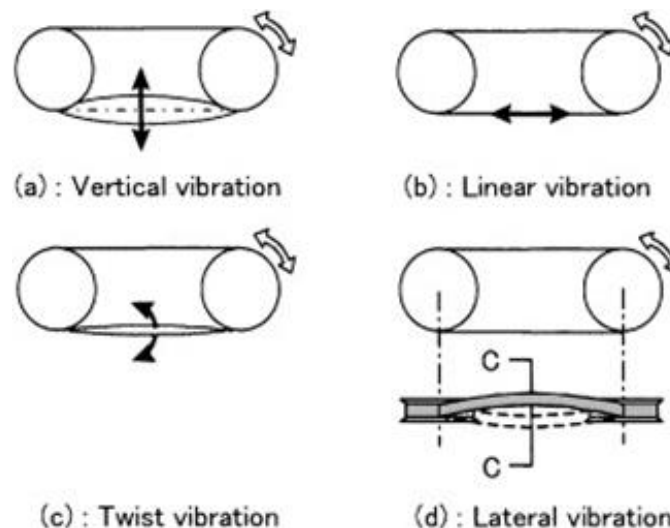


Fig. 2. Types of the belt floating

Floating of the belt drive can be caused by different causes such as incorrect tightening, incorrect adjustment, worn out or ruptured belts, damaged pulleys or bearings and resonance. Correct tightening

and adjustment are indispensable to minimize vibrations and preservation of optimal performance of belt and pulleys.

Except for the aforementioned facts, a selection of high-quality belts and pulleys, regular lubrication and maintenance, and also a prevention against resonance risk can forestall floating in the belt drive. Regular check-ups and monitoring can contribute to an identification of possible problems with vibrations before making them more complicated.

Floating in the belt drive can be caused by other factors apart from aforementioned types of vibrations. Those can include the following cases:

- Belt resonance occurs when inherent frequency of the belt is identical with operating frequency of the system which results in increased amplitudes of floating. Belt resonance can be decreased by changing the belt tightening or by using different belt material.
- Bearing resonance occurs when inherent frequency of the bearing is identical with operating frequency of the system which results in increased amplitudes of floating. Bearing resonance can be decreased by using better bearings or by extending the system by absorption.
- Toughness of the belt: contrary to softer belts, the stiffer ones are more prone to floating. Selection of the belt with accurate toughness is crucial for the respective application.
- Eccentricity of the pulley: Eccentric or diverging pulley can cause the floating of the belt. It can be eliminated by changing the adjustment of the pulley or by using a new one [8].

Generally, a reduction of floating in the belt drives is crucial for improving the performance and for decreasing maintenance costs. Regular check-ups and maintenance can help detect possible problems and prevent excessive wearing and damaging of the system.

#### 4. Design of belt floating monitoring system

While designing the belt floating monitoring system with highly precise sensor of distance, it is indispensable to deal with different issues influencing performance and reliability.

1. The first factor includes a determination of correct positioning of the distance sensor. The sensor should be positioned to be able to detect floating of the belt in both motors and at the same time it should be isolated from external influence such as vibration or impacts.
2. The second aspect is a selection of suitable distance sensor with broad range of measurement and high precision.
3. The third aspect is to build an algorithm for processing input data collected by sensor and for determining the belt floating. The algorithm should be able to process the input data in real time and to pre-set data related to belt floating in easily applicable interface [9].
4. The system should be designed to provide easy assembling and dismantling.

#### 5. Measurement and evaluation of the belt floating

Procedure of the belt floating measurement in the belt gear by means of highly precise distance sensor includes the following stages:

1. Preparation of the measuring system (Fig. 3): prior to measurement it is necessary to prepare the measuring spot. It is recommended to conduct the measurement in clean space, adequately illuminated by light, with minimal disturbance. At the same time, it is important to ensure correct installation and calibration of the sensor.





Fig. 3. Measuring system designed for the belt gear testing

2. Removal of the gear cover: installation of the sensor on the belt must be preceded by a removal of the gear cover. Safety measures must be observed when removing the cover.
3. Installation of the sensor SICK OD2000-0501T15 (Fig. 4): the sensor must be positioned on one side of the gear by means of universal magnetic stand and must be parallel with the belt. The distance must be minimal. Installing of the sensor will ensure precise measurement of the floating of the belt in the belt gear. It is recommended to position the sensor in the proximity of the centre line of the belt which should enable a more precise measurement.



Fig. 4. Sensor SICK OD2000-0501T15

4. Fixation and adjustment of the distance sensor: the sensor should be firmly fixed on its position to minimize influence of vibrations or of other external factors on the measurement.
5. Tightening of the belt by a tightening pulley to the first value of 105 N. The required value is set by the belt tension meter SKF PHL FM10/400/A (Fig. 5).

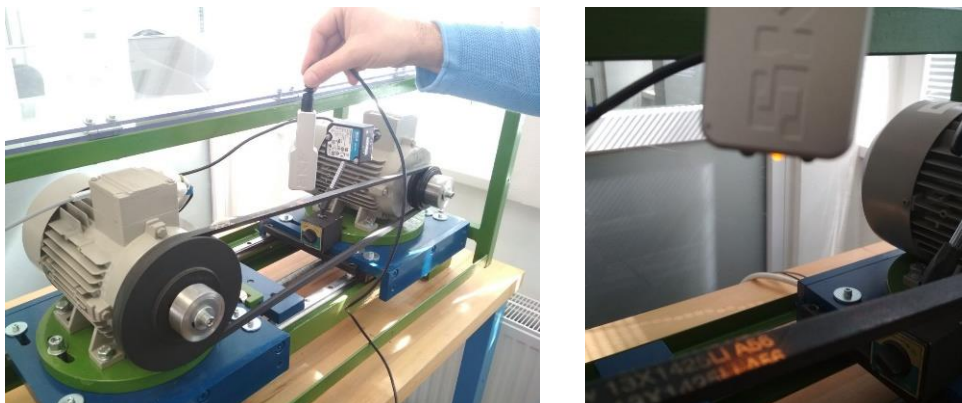


Fig. 5. Adjustment and tightening of the belt by means of contactless belt tension meter SKF



6. Preparation of the table environment to record the measured values: rotations with the values are 500 rev/min, 1000 rev/min, 1500 rev/min, 2000 rev/min, 2500 rev/min. Selected tightening is approximately 100 N, 200 N, 300 N.
7. Measurements: by means of the distance sensor the values of the belt floating are obtained. The results should be recorded in real time along with all relevant data [10].

**Table 1.** Measured values

Revolutions [rpm]	Tension [N]	0%			25%			50%			75%		
		MAX	MIN	STR									
500	105	-0.5	-1.4	0.9	-0.5	-1.5	1.1	-0.7	-1.9	1.2	-0.6	-2.2	1.6
	202	2	1.3	0.7	1.8	1.3	0.5	1.9	0.8	1.1	1.9	1.1	0.8
	306	2.4	1.7	0.8	2.3	1.6	0.7	2.4	1.4	1	2.3	1.5	0.9
1000	105	-0.3	-1.5	1	-0.2	-2.2	2	-0.7	-1.9	1.4	-0.8	-2.2	1.4
	202	2.1	1.2	0.9	1.9	1.2	0.7	2	1.2	0.8	2.2	0.8	1.3
	306	2.4	1.5	0.9	2.3	1.5	0.8	2.2	1.7	0.6	2.2	1.5	0.7
1500	105	-0.3	-1.6	1.5	-0.5	-1.8	1.3	-0.6	-2	1.4	-0.5	-2.2	1.7
	202	2	1.4	0.6	2.1	1.3	0.8	2.1	1.2	0.9	2.2	1.1	1.1
	306	2.8	1.2	1.6	2.6	1.2	1.4	2.4	1.6	0.7	2.2	1.7	0.6
2000	105	1	-2.6	3.6	2.7	-1.7	4.4	1.8	-0.1	1.9	2.4	-0.7	3.1
	202	2	1.2	0.8	2.1	1.1	1	4.1	-0.9	5	3	0	3
	306	2.5	1.7	0.8	2.4	1.7	0.8	2.5	1.6	1.1	2.8	1.3	1.5
2500	105	2.9	-0.7	3.6	1.3	0.3	1	1	0.3	0.7	0.8	0.2	0.6
	202	5.3	-2	7.3	2.2	0.8	1.4	2.5	0.5	2	2.3	0.7	1.5
	306	2.4	1.5	0.9	2.3	1.6	0.8	2.2	1.5	0.8	2.3	1.5	0.8

8. Repetition of the measurements: the measurements are repeated using different values of tension such as 105, 202 and 306 N (Table 1), or using different values of rotations and motor loading.
9. Data processing.

## 6. Data analysis

Measurement 1 – Input rotations 500 rev/min

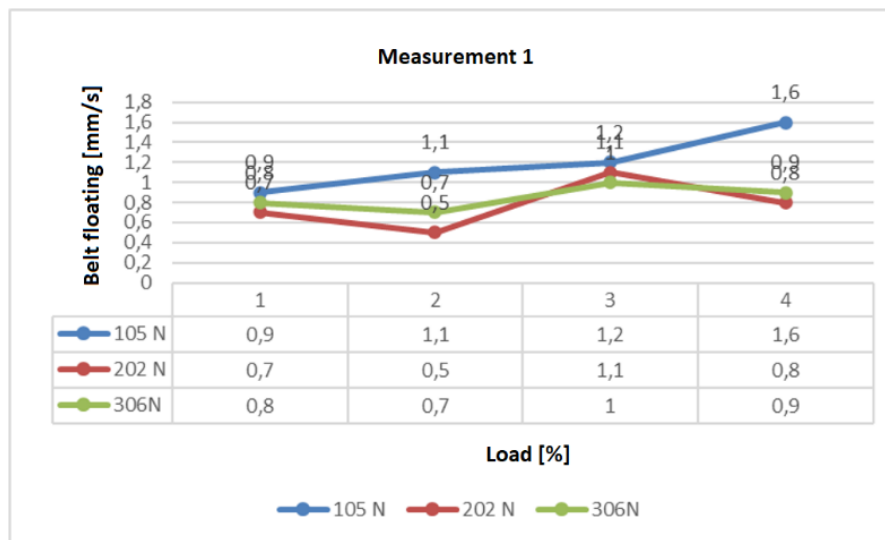


**Fig. 6.** Dependence of the belt floating on gear loading and the belt tightening at 500 rev/min

Fig. 6 shows that at 500 rev/min and with the belt tightening to 105 N and with increasing percentage value of the motor loading (ranging from 0 to 75%), the value of the belt floating increases. Furthermore,



it is obvious that in the case of the belt tightening to 202 N and 306 N and with increasing gear loading, the belt floating decreases.

Measurement 2 – Input rotations 1000 rev/min



Fig. 7. Dependence of the belt floating on gear loading and the belt tightening at 1000 rev/min

Fig. 7 shows that floating vibrations decrease with increasing values of tightening and loading of the motor. For instance, in the case of tightening to 105 N for percentage loading of 0%, the belt floating is 1 mm/s. In the case of percentage loading of 75% the belt floating is 1.4 mm/s. In the case of tightening to 306 N, the belt floating is 0.9 mm/s for percentage loading of 0%. In the case of percentage loading of 75% the belt floating is 0.7 mm/s.

At the same time, it can be seen that the value of the belt floating for each tension differs in relation to percentage representation of tightening [11]. For instance, when tightening is 202 N, the belt floating value is of 0.7 m/s for percentage representation of 25%, yet the belt floating value of 1.3 mm/s is typical for percentage representation of 75%.

Measurement 3 – Input rotations 1500 rev/min



Fig. 8. Dependence of the belt floating on gear loading and the belt tightening at 1500 rev/min



Fig. 8 shows that the amplitude of the belt floating increases when tightening reaches 105 N and 202 N and it also increases with increasing percentage loading of the motor.

For instance, in the case of tightening value of 105 N and percentage ratio of 0%, the amplitude of the belt floating reaches 1.5 mm/s and in the case of percentage ratio of 75%, the tightening value is 1.7 mm/s. In the case of tightening of 202 N and percentage ratio of 0%, the amplitude of the belt floating reaches 0.6 mm/s and in the case of percentage ratio of 75%, the belt floating amplitude reaches the value of 1.1 mm/s.

However, in the case of tightening of 306 N, the values of the belt floating decrease with the increasing percentage loading of the motor. For instance, in the case of tightening of 306 N and percentage ratio of 0%, the belt floating amplitude reaches 1.6 mm/s and in the case of percentage ratio of 75% the values reach 0.6 mm/s.

Following the aforementioned facts, it is clear that the more tightened the belt is, the lower the floating value drops.

Measurement 4 – Input rotations 2000 rev/min

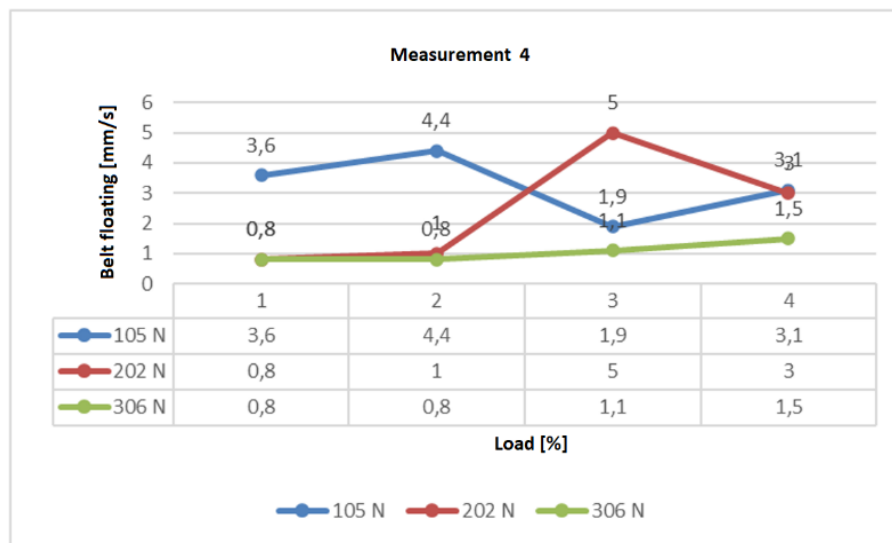


Fig. 9. Dependence of the belt floating on gear loading and the belt tightening at 2000 rev/min

Measurement 5 – Input rotations 2500 rev/min

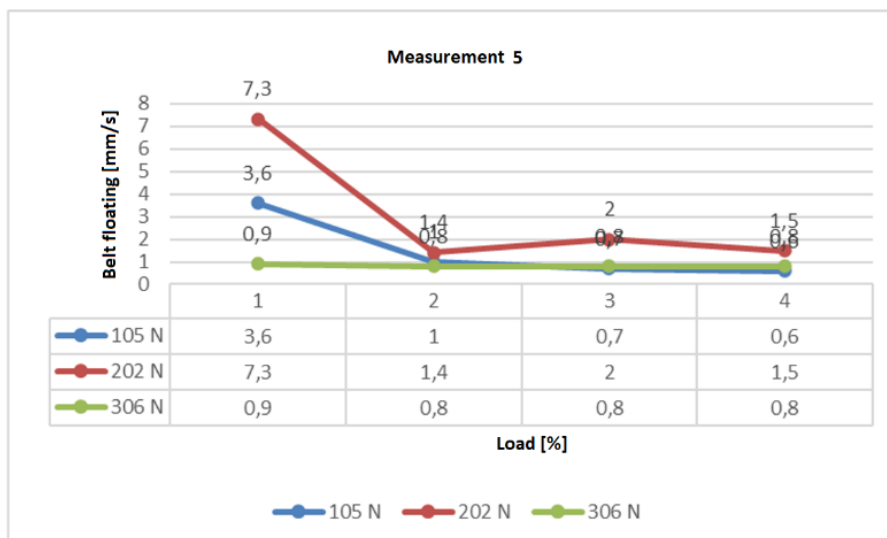


Fig. 10. Dependence of the belt floating on gear loading and the belt tightening at 2500 rev/min



According to the aforementioned measurements (Fig. 9, 10), it is possible to evaluate the results of the belt floating measurement when changing the rotations, the belt tightening and loading at the output by adjusting the load torque.

## 7. Conclusion

The paper points out that the design of the monitoring system for the belt floating in the belt gear represents an important prevention tool of potential defects and failures of the motor. The system uses sensors for measuring vibrations and temperature of the belt and for their processing by means of algorithms applied to detect the belt floating. The designed system was verified by means of experimental devices and the results proved its efficiency in detection of the belt floating as well as options of further use in present gears. In the future, the system could be improved by using automatic control of the belt tightening based on obtained data and thus its reliability and efficiency might increase as well.

The design of the monitoring system for the belt floating in the belt gear has high potential in the field of machine and device operation as it allows the operators to prevent an occurrence of serious failures and to increase efficiency of operation. As regards the fact that the belt floating in the belt gear represents one of the main factors causing wear of the belt as well as of other gear elements, it is important to have a reliable and precise system for monitoring this parameter.

## Acknowledgement

This research was funded by the Ministry of Education, Science, Research and Sport of the Slovak Republic within the project KEGA 017TUKE-4/2021.

## References

- [1] Mascenik J., Pavlenko S.: Gear production using nonconventional technologies Technika i technologii: innovacii i kačestvo Baranoviči p. 55-57 ISBN 978-9-8549-8092-8
- [2] Mascenik J., Coranic T., Panda T.: CA technology as an effective tool in the design and control of springs, 2022. In: Top Layer in Manufacturing Process. Poznań, PL: Polish Academy of Sciences s. 34-39. ISBN 978-83-66246-52-2
- [3] Mascenik J., Vojtko I.: Experimental monitoring and diagnostics of belt gears in testing device. MM Science Journal, Vol. 2016, No. September, pp. 964-968. ISSN 1803-1269, DOI: 10.17973/MMSJ.2016\_09\_201641
- [4] Mascenik J., Pavlenko S., Bičejová L.: A device designed to monitor new belt types with application of diagnostic system. MM Science Journal, 2016, Vol. September, pp. 931-934. ISSN 1803-1269
- [5] Husar J., Knapcikova L.: Exploitation of Augmented Reality in the Industry 4.0 Concept for the Student Educational Process. In: INTED 2019: Valencia (Spain): IATED, 2019, pp. 4797-4805, ISBN 978-84-09-08619-1, ISSN 2340-1079
- [6] Coranic T.: Design and Manufacturing of an Optimized Mould Insert by DMLS Technology. MM Science Journal, 2021(December), pp. 5492-5496
- [7] Mascenik J., Pavlenko S., Husar J.: Inovatívne skúšanie a monitorovanie remeňových prevodov (Innovative testing and monitoring of belt drives), 1. vyd. – Brno, Tribun EU - 2018. 90 pp. [CD-ROM]. ISBN 978-80-263-1436-3
- [8] Straka L., Dittrich G.: Design of manufacturing process of mould for Die Casting by EDM technology with the computer aided. International Journal of Engineering and Management Sciences, 2020, Vol. 5, pp. 57-63
- [9] <https://grabcad.com/library/roller-chain-drive-and-sprockets-16b-type-iso-606-din-8187-1> [accessed: 26.05.2023]



- [10] Mascenik J.: Monitoring of parameters directly influencing performance transfer by belt gear, 2017. In: MM Science Journal. Vol. 2017, no. December (2017), p. 1959-1962. ISSN 1803-1269
- [11] Pavlenko S., Mascenik J. and Krenicky T.: Worm gears: general information, calculations, dynamics and reliability, Lüdenscheid: RAM-Verlag - 2018. - 167 p. [print]. ISBN 978-3-942303-80-4



## Identification of dynamic forces in the chain during the steady operation of a rescue scraper conveyor

Received: 12.06.2023

Accepted: 11.07.2023

Published online: 31.07.2023

### Author's affiliations and addresses:

<sup>1</sup> KOMAG Institute of Mining Technology, Pszczyńska 37, 44-101 Gliwice, Poland

<sup>2</sup> Silesian University of Technology, Akademicka 2A, 44-100 Gliwice, Poland

### \* Correspondence:

e-mail: [mwojcicki@komag.eu](mailto:mwojcicki@komag.eu)

Mateusz WÓJCICKI <sup>1\*</sup>, Andrzej N. WIECZOREK <sup>2</sup>, Krzysztof NIEŚPIAŁOWSKI <sup>1</sup>

### Abstract:

The article presents a study of the dynamic forces occurring in the chain of a rescue scraper conveyor during its steady operation. It describes the characteristics of the test stand in the form of a scraper conveyor for investigating dynamic forces in the chain, moreover, the results of these tests are presented. Based on the values obtained during the dynamic tests, the characteristic parameters of the above mentioned measurements were determined.

Keywords: plain link chain, scraper conveyor, tests of dynamic forces



## 1. Introduction

The collaboration of the chain links with the drum, the joint interaction between the individual links in the articulated joint area, and the impact of aggressive environmental factors, account for the complexity of the wear processes of link chains. The most important factors that increase the degradation of chains and entire scraper conveyor assemblies are the following [1-7]:

- the occurrence of stone and coal dust in the chain link collaboration zone (articulated joints) [7-8],
- corrosive effects of mine water coming from sprinkler units and flowing out of goafs [9-16],
- dynamic loads from, among others, conveyor drive start-ups, uneven loading, frequent overloading and blocking [17].

The interaction between the aforementioned factors usually leads to the occurrence of synergy effect [18]. In order to determine the effect of synergy, it is necessary to determine the impact of a single degradation factor and the aggregate effect of their combined impact.

One of the above-mentioned factors that can act synergistically on the wear process of link chains includes variable dynamic forces. The impact is complex and often stochastic in nature, resulting from the uneven loading of the conveyor itself, the frictional nature of the movement of the conveyor belt and scraper elements in the trough, as well as other factors that are difficult to identify. Therefore, in order to represent the synergism of the aforementioned factors in the best way, an identification of the dynamic forces occurring in the chain tendon during steady-state operation of the rescue conveyor was carried out. For this purpose, a dedicated test stand was developed and built at the KOMAG Institute.

This article is part of a broader study related to the synergistic effects of environmental factors on chain link wear depending on the exploitation factors juxtaposed. In the work presented here, the determination of forces acting on the tendon system of a rescue scraper conveyor during its steady-state operation, for the above-mentioned research work, was carried out using a dedicated test stand (description in [19]).

## 2. Materials and Methods

### 2.1. Test stand

The test stand (Fig. 1-6) was built based on the rescue scraper conveyor possessed by the KOMAG Institute, equipped with the 14x50 chain strand. The research scraper conveyor under testing was composed of 10 trough sections and equipped with the main (active) drive and the return drive. The conveyor propulsion wheel was powered by a hydraulic motor, supplied by a hydraulic power pack and controlled from a separate station. The load-inducing element was a friction brake bolted to the scraper. In addition, the chain nominal load was varied by the chain pre-tension, adjusted through the turnbuckle installed in the chain strand.



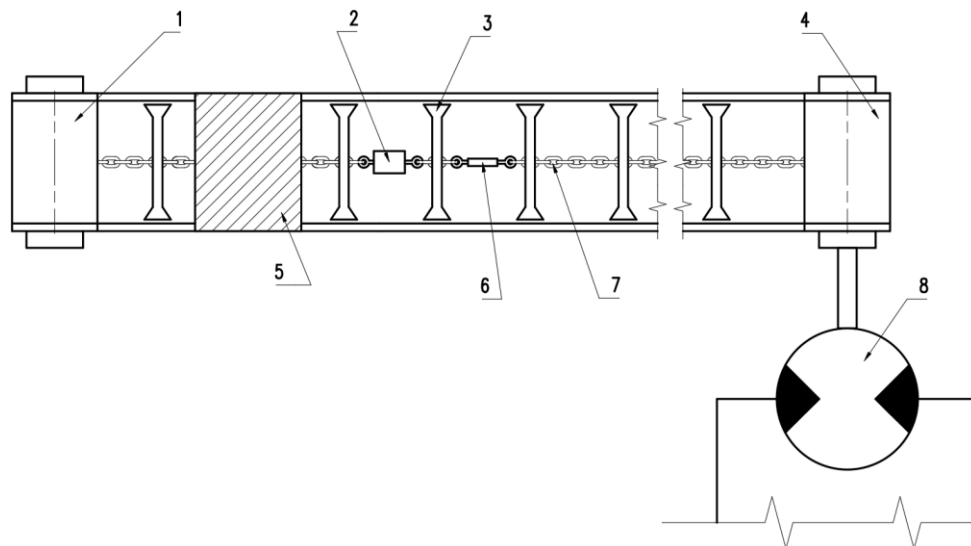


**Fig. 1.** Diagram of the test stand for dynamic forces in the rescue scraper conveyor (1- return wheel, 2- force sensor, 3- scrapers, 4- drive wheel, 5- friction brake, 6- turnbuckle, 7- chain, 8- hydraulic motor)

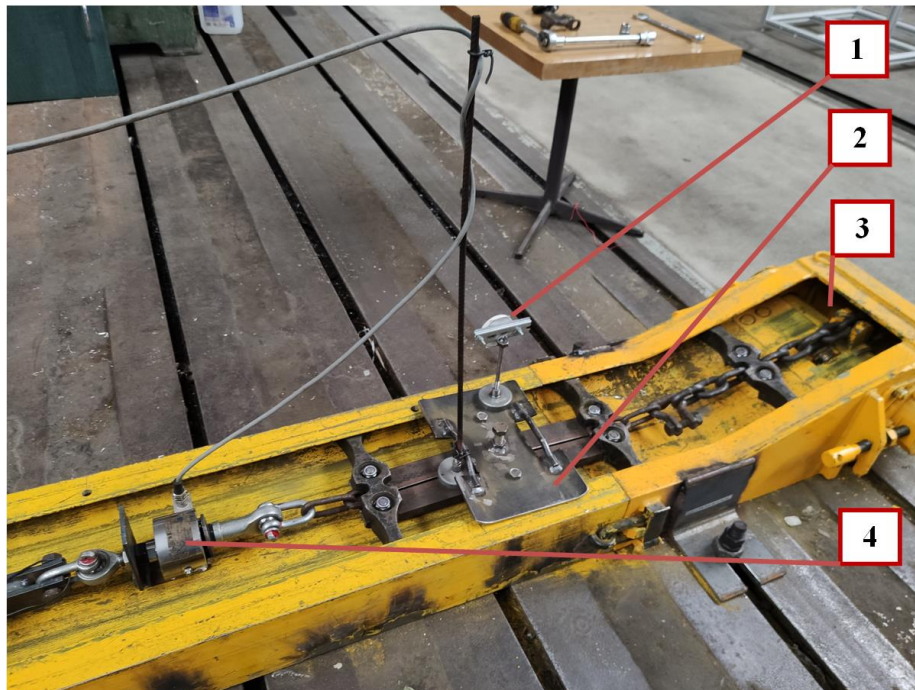


**Fig. 2.** Dynamic forces test stand – view from the return drive side (1- reflector, 2- friction brake, 3- return wheel, 4- force sensor)

## 2.2. Testing method

Tests of dynamic forces, occurring in the link chain, were conducted on a straight section of the conveyor. A U2A-2T force sensor manufactured by Hottinger Messtechnik Baldwin was used as the force measuring element. The sensor parameters are shown in the following Table 1.

**Table 1.** Technical parameters of the force sensor U2A-2T Hottinger Messtechnik Baldwin [20]

Parameter/physical quantity	Unit	Value
Nominal load	kg	2000
Construction material	-	Stainless steel
Accuracy class	-	0.2%
Sampling frequency (set)	Hz	50
Type	-	can-type weight transducer
Number of strands	-	6
Bridge constant	mV/V	2

**Fig. 3.** Stand for testing dynamic forces – view from the drive wheel side, markings: 1- hydraulic motor, 2- drive wheel**Fig. 4.** Hydraulic control unit



**Fig. 5.** Measurement sensors, markings: 1- force sensor, 2- turnbuckle

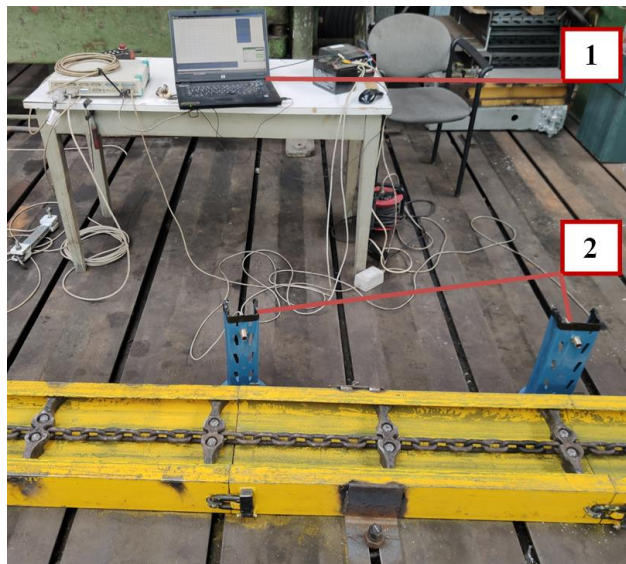


**Fig. 6.** Instrumentation for speed measurement and data processing, markings: 1- data processing and recording unit, 2- speed measurement sensors

The force sensor was mounted in the line of the link chain. In order to prevent it from being damaged, it was installed on a slide developed and manufactured at KOMAG, the design of which allowed the sensor to move smoothly along the conveyor without causing additional dynamic impacts when passing at the joints of the troughs. In addition, the test stand was equipped with a travel speed measurement system to allow testing at a constant conveyor speed. For this purpose, two optical sensors were used, installed along the route, at known spacing, calculating the speed of travel based on the time difference in the reading of the signal from the reflector mounted on the friction brake moving with the chain. The tests were carried out at a constant conveyor speed of  $\sim 1.3$  m/s. The base (constant) load was generated by a friction brake installed on the route, and the load differentiation was carried out by the degree of chain tension set by the turnbuckle (read from the data provided by the force sensor). The tests were performed in 8 series - from an unstrained chain (initial load - 0 N) to the initial load of about 3237 N. Above this value, the operation of the conveyor was non-stationary due to the stick-slip effect occurring when the friction brake was moved. The parameters of the test series are shown in Table 2.

**Table 2.** Parameters of the test series

Series number	The pre-tension of the tested chain S
1	0 N
2	490.5 N
3	686.7 N
4	1275.3 N
5	1863.9 N
6	2746.8 N
7	2943 N
8	3237.3 N

Each of the test series consisted of 10 principle runs and 10 return runs of the measuring element. By principle run the movement of the chain with the sensor in the direction of the drive wheel, and the return run - in the opposite direction are meant. A total of 160 runs were made, during which the value of the tensile force was recorded, as well as the control value of the supply pressure to the hydraulic motor of the drive unit. The series were started with a basic run in the drive direction, which were characterized by the presence of higher forces than for the sensor return movement (Fig. 7).

### 3. Results and discussion

The obtained results of measurements of dynamic forces in the chain and supply pressure are shown in Figures 8÷15 for All the test series (1÷8).

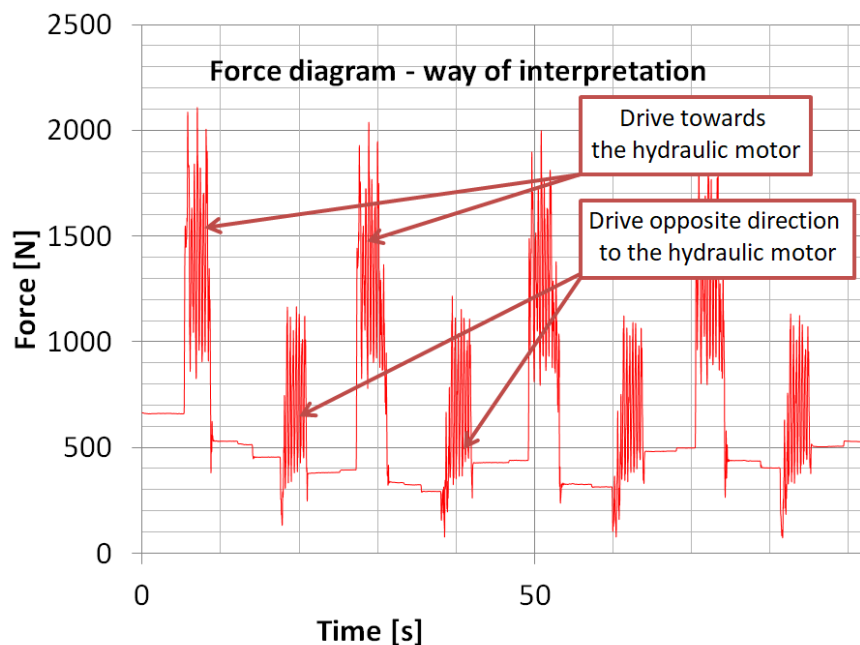


**Fig. 7.** Variation of the results of dynamic force measurements for basic and return movement.

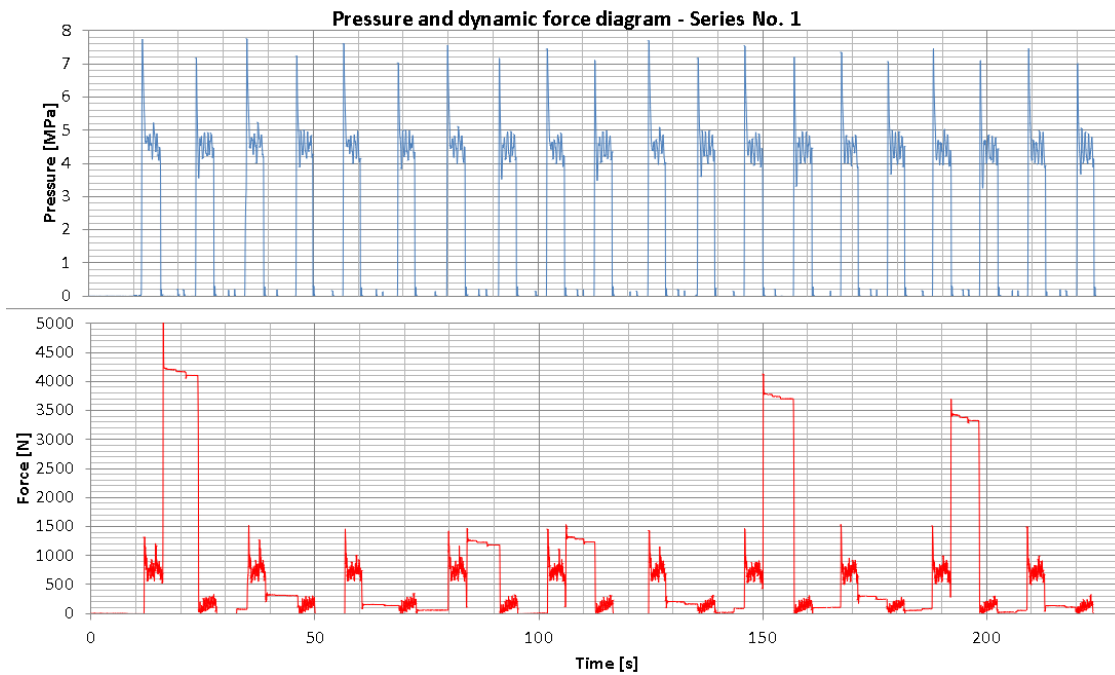


**Fig. 8.** Graphs of supply pressure (upper figure) and dynamic forces in the chain (lower figure) obtained for pretension  $S=0$  N (Series 1)

Based on Figures 8÷15, it is possible to determine the basic parameters of the dynamic force in the chain strand during the travel of the rescue conveyor depending on the chain pre-tension. In addition to the differences in the values of the extreme dynamic forces depending on the initial load, significant differences in the forces depending on the direction of movement are also noticeable. Each time, higher force values are observed in the case of the movement direction corresponding to the tensioning of the part of the chain located in the upper compartment of the conveyor trough (the basic direction of the conducted tests). This phenomenon is directly related to the design of the conveyor itself and the orientation of the drive and return wheels in relation to the travel direction.

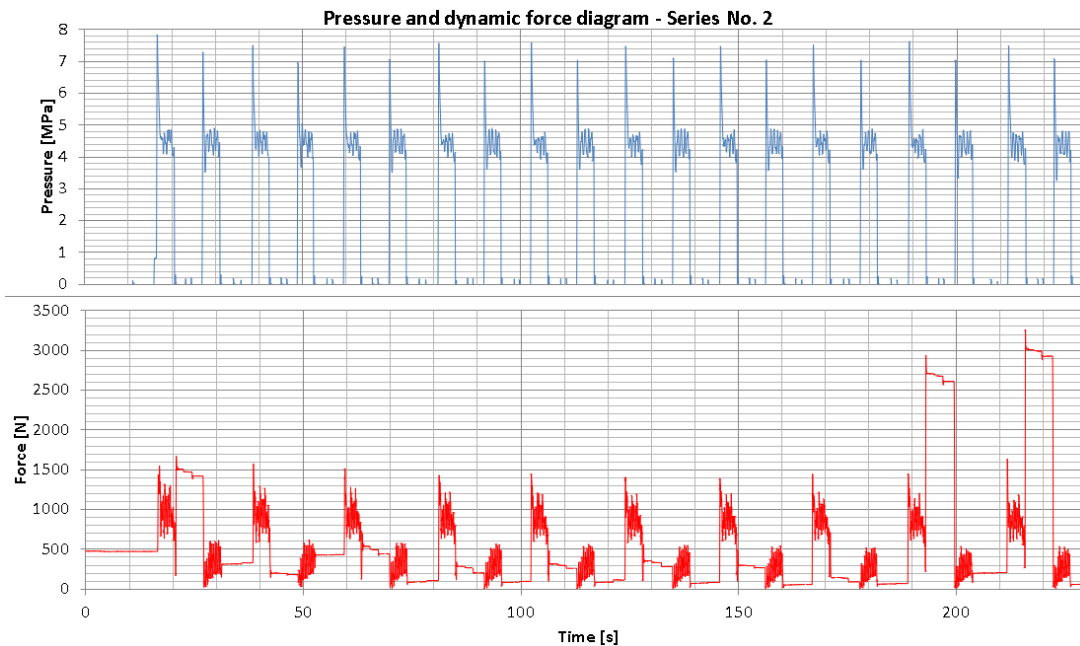


**Fig. 9.** Graphs of supply pressure (top figure) and dynamic forces in the chain (bottom figure) obtained for pretension  $S=490.5$  N (Series 2)

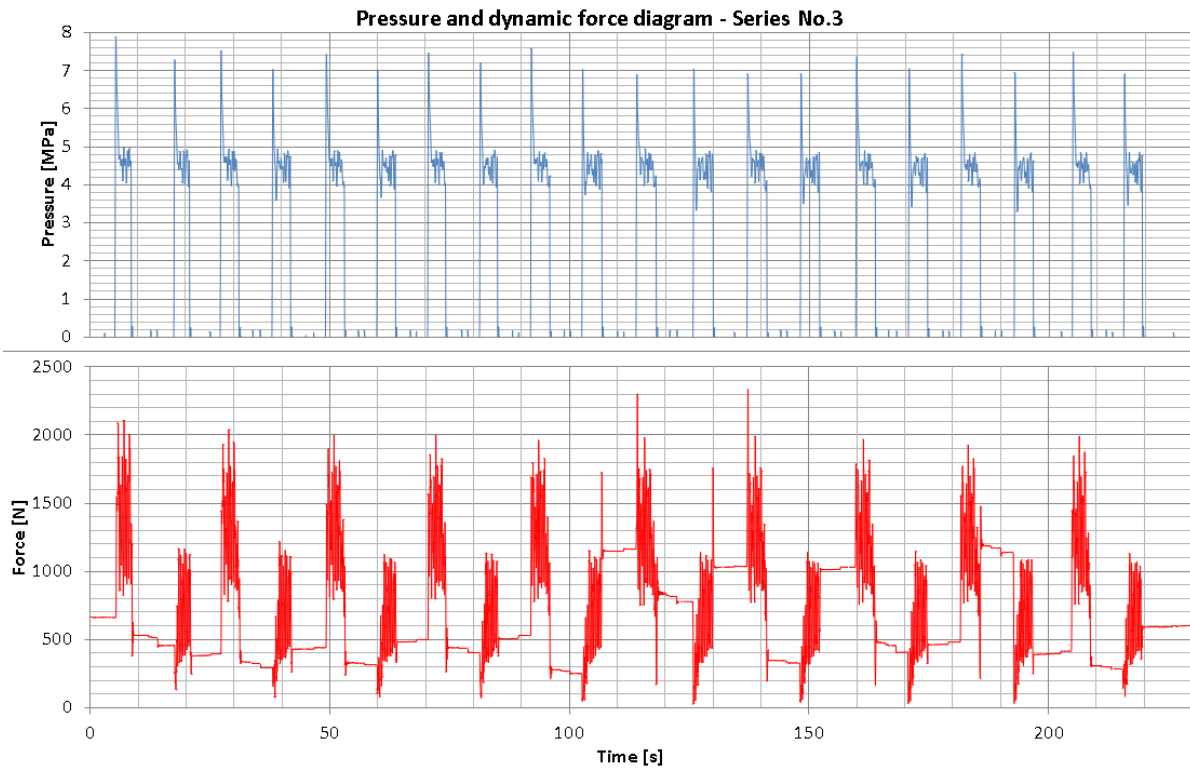


**Fig. 10.** Graphs of supply pressure (top figure) and dynamic forces in the chain (bottom figure) obtained for pretension  $S=686.7$  N (Series 3)

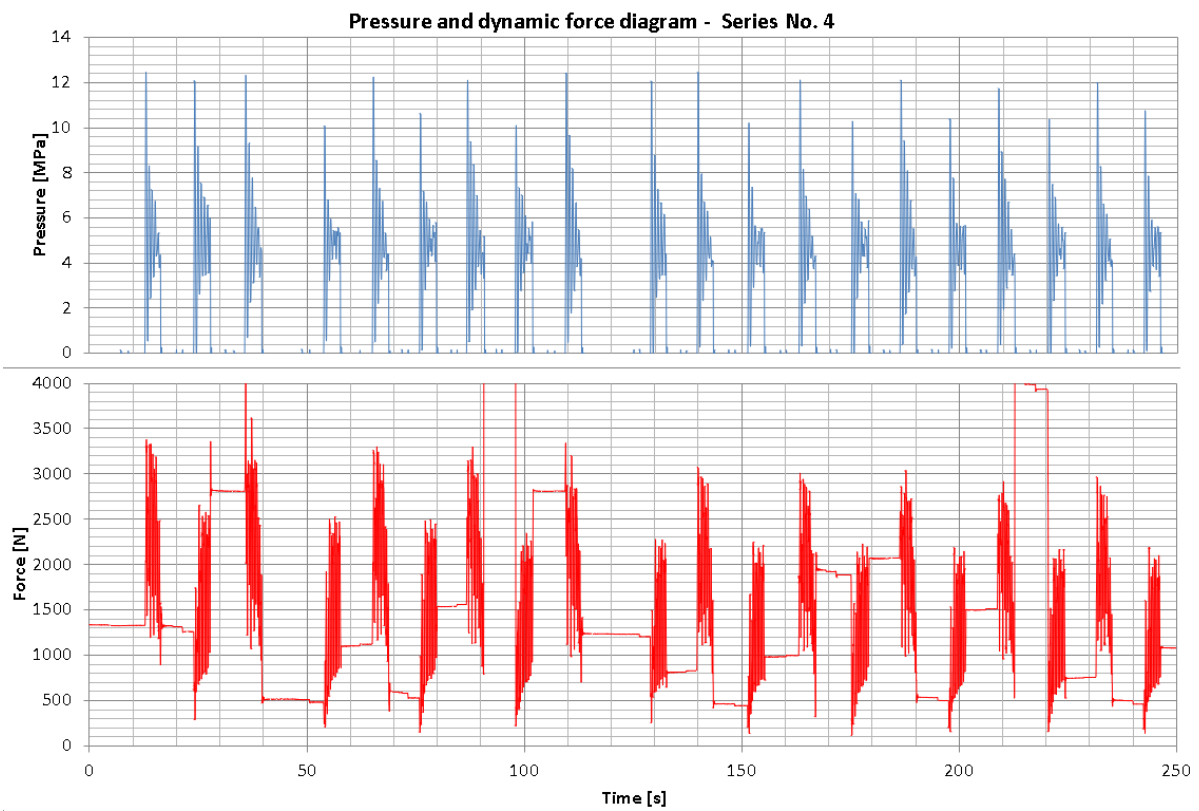


**Fig. 11.** Graphs of supply pressure (top figure) and dynamic forces in the chain (bottom figure) obtained for pretension  $S=1275.3$  N (Series 4)

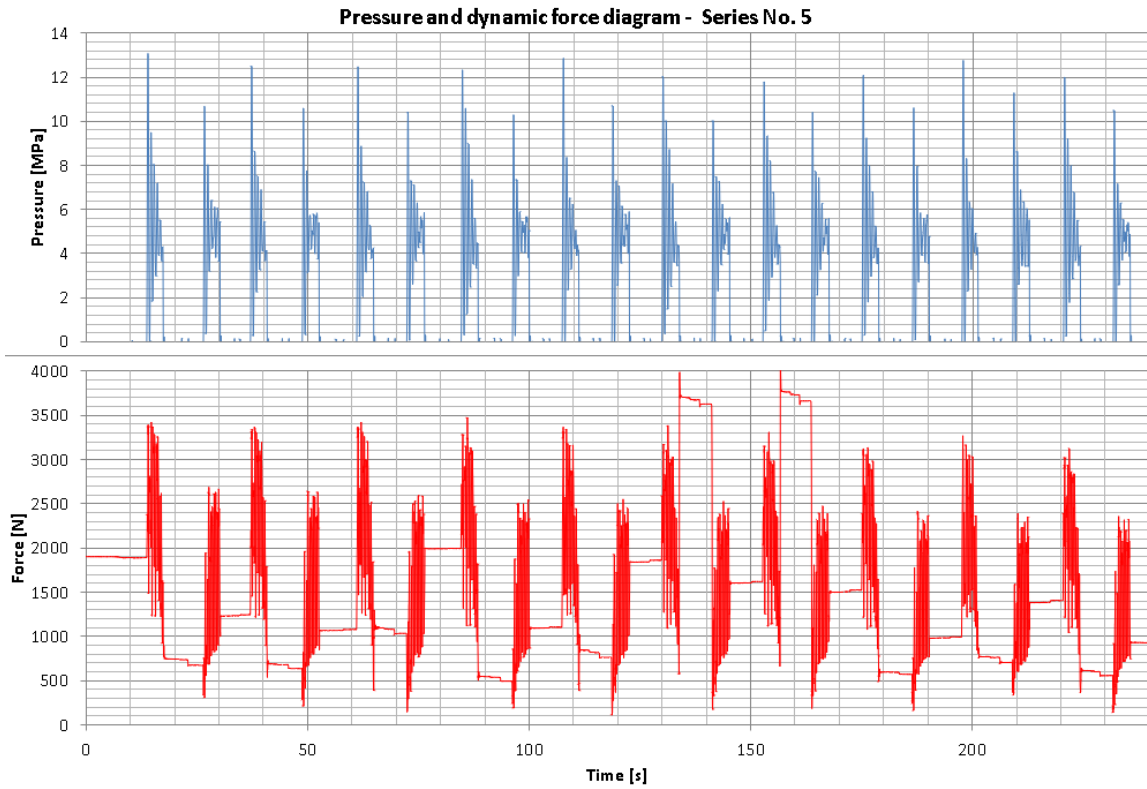


**Fig. 12.** Graphs of supply pressure (top figure) and dynamic forces in the chain (bottom figure) obtained for pretension  $S=1863.9$  N (Series 5)

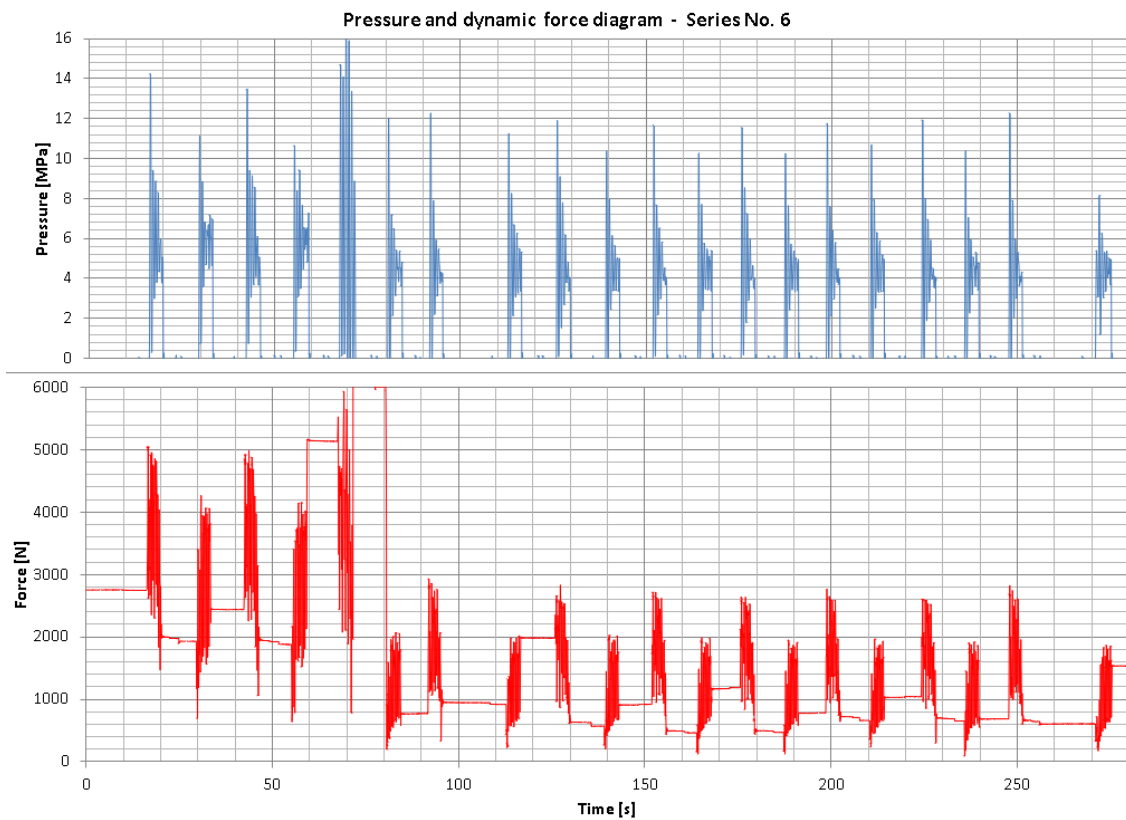


**Fig. 13.** Graphs of supply pressure (top figure) and dynamic forces in the chain (bottom figure) obtained for pretension  $S=2746.8$  N (Series 6)

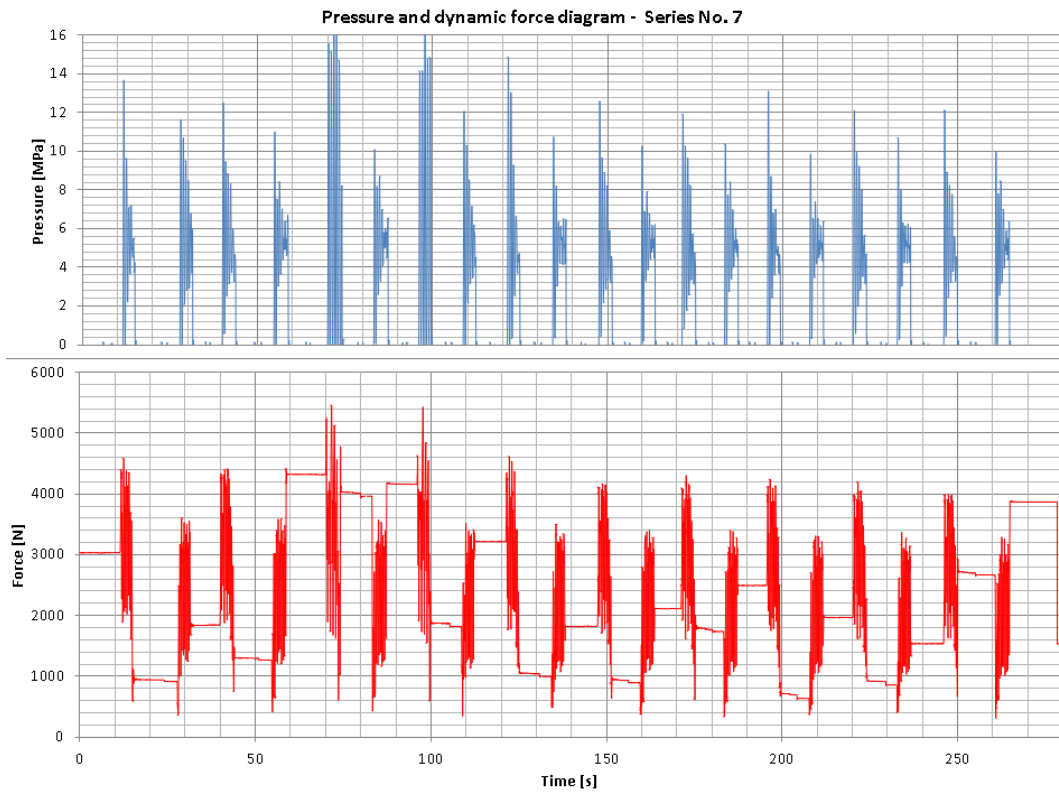


**Fig. 14.** Graphs of supply pressure (top figure) and dynamic forces in the chain (bottom figure) obtained for pretension  $S=2943$  N (Series 7)

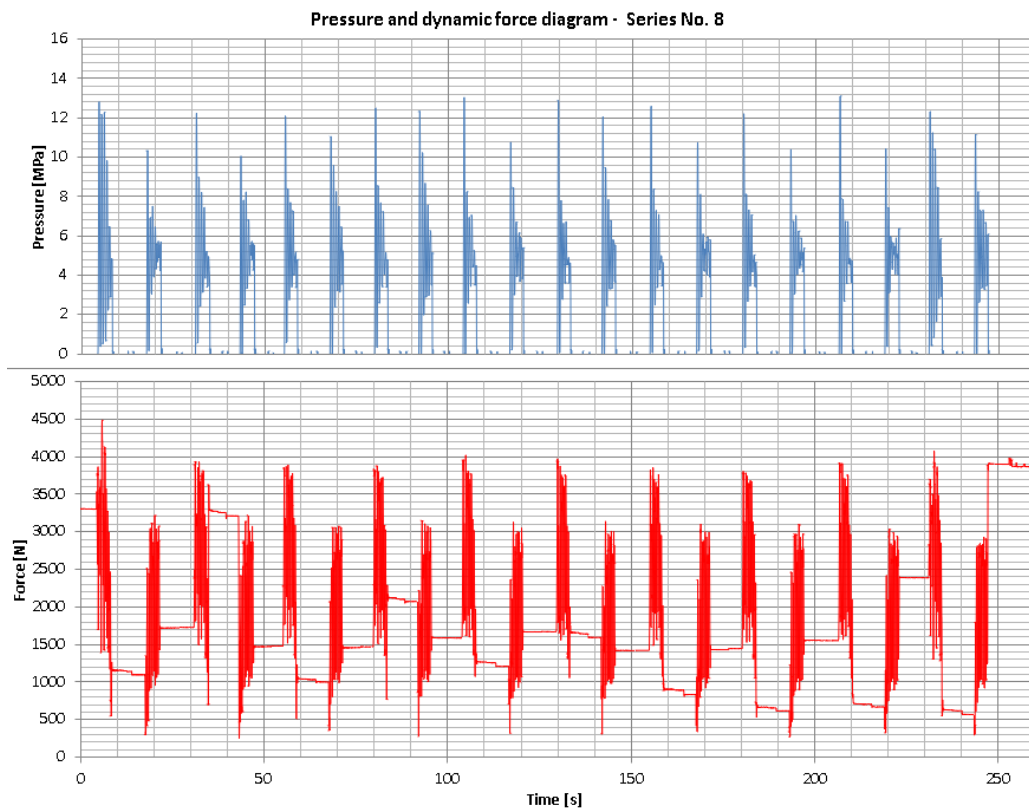


**Fig. 15.** Graphs of supply pressure (top figure) and dynamic forces in the chain (bottom figure) obtained for pretension  $S=3237.3$  N (Series 8)

As it has already been mentioned before, the primary objective of the tests is an identification of dynamic forces in the chain of a rescue scraper conveyor for the purpose of mapping dynamic forces on a test stand for chain link wear synergism. The basic values characterizing the dynamic forces (Fig. 16) are the maximum ( $Max\_F$ ) and minimum ( $Min\_F$ ) estimates of the dynamic forces.

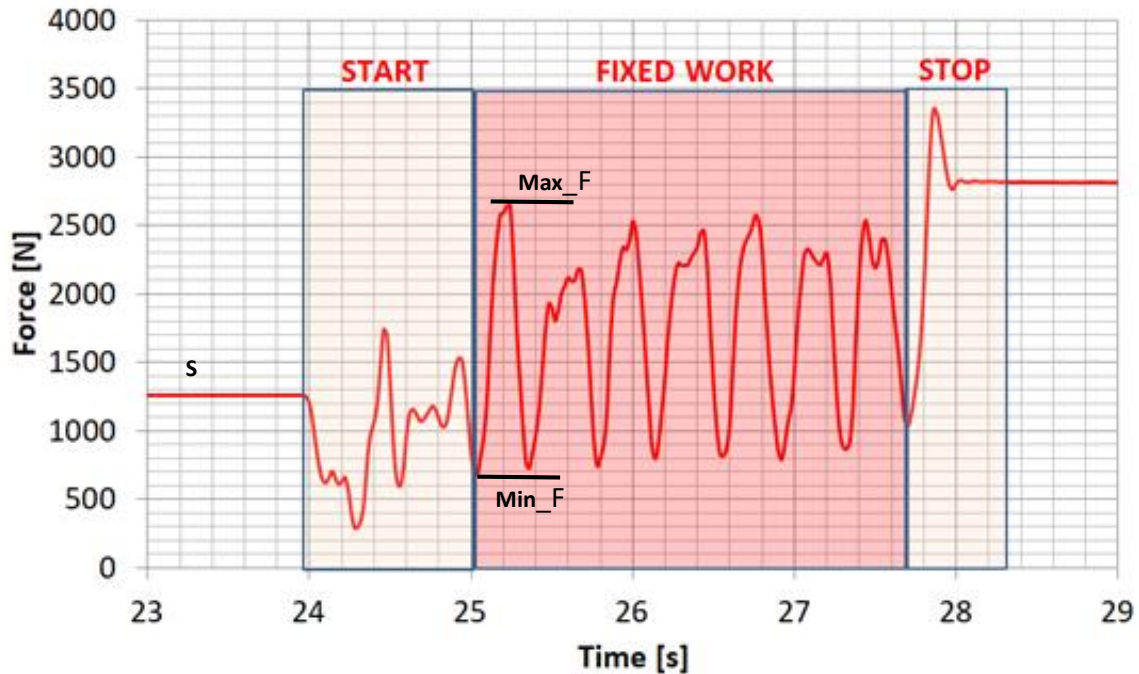


**Fig. 16.** An exemplary course of dynamic forces for one travel of the measuring head at the basic direction

Based on them, the amplitude  $A$  of changes in dynamic forces can be determined according to the relationship (1):

$$A = \frac{Max\_F - Min\_F}{2} \quad (1)$$

It is obvious that the actual forces loading the scraper conveyor will be different from the forces loading the test stand due to the inability of the test stand construction to carry big loads. As an adequate parameter, representing the actual variation of instantaneous forces acting in the chain, the ratio of the amplitude to the initial force  $A/S$  and the dynamic surplus defined by the following relation are accepted (2):

$$DS = \frac{Max\_F}{S} \quad (2)$$

The obtained values of dynamic forces and coefficients characterizing them are summarized in Table 3. In addition to the amplitude of the force, the frequency of dynamic forcing will be important for the proper presentation of the actual state, however, this issue will be the basis of further research work conducted by the authors.

**Table 3.** Results of measurements of forces and dynamic parameters

Base motion						
Series number	S [N]	Max_F [N]	Min_F [N]	A [N]	A/S	DS
1	0.00	1400	500	450	-	-
2	490.5	1500	600	450	0.92	3.06
3	686.7	2000	800	600	0.87	2.91
4	1275.3	3400	1000	1200	0.94	2.67
5	1863.9	3500	1200	1150	0.62	1.88
6	2746.8	5000	1000	2000	0.73	1.82
7	2943.00	5000	1000	2000	0.68	1.70
8	3237.3	4500	1500	1500	0.46	1.39
Return motion						
Series number	S [N]	Max_F [N]	Min_F [N]	A [N]	A/S	DS
1	0.00	300	0	150	-	-
2	490.5	600	50	275	0.56	1.22
3	686.7	1100	300	400	0.58	1.60
4	1275.3	2400	500	950	0.74	1.88
5	1863.9	2600	400	1100	0.59	1.39
6	2746.8	4000	400	1800	0.66	1.46
7	2943.00	3600	400	1600	0.54	1.22
8	3237.3	3400	600	1400	0.43	1.05

As the chain pretension increases, there is a noticeable increase in the minimum and maximum estimates for both the basic and return movements. For the basic movement, the minimum estimate ranges from ~500 to 1500, while for return movement it ranges from ~0 to 600. The maximum estimate is ~1400 to 5000 for the basic movement and ~300 to 4000 for the return movement.

The above results thus show an increase in the amplitude with increasing chain pretension. For the basic movement it varies from 450 to 2000 while for the return movement it varies from 150 to 1800. Thus, the ratio of amplitude to initial force in the A/S chain for the basic movement ranged from 0.46 to 0.94, while for the return movement it ranged from 0.43 to 0.74. Also the differences in the dynamic surplus, varying from 3.06 to 1.39 for the basic movement and from 1.88 to 1.05 for the return motion are noticeable.

#### 4. Conclusions

The paper presents the test results of the dynamic forces acting in the chain during the steady operation of the rescue scraper conveyor. Based on them, the following conclusions were drawn:

- The values of the dynamic forces in the chain of the rescue scraper conveyor depend on the direction of the conveyor movement.
- The coefficients characterizing the dynamic forces, regardless of the direction of movement of the strand, decrease as the pretension of the chain increases.
- The ratio of amplitude to initial force in the A/S chain for the basic movement ranged from 0.46 to 0.94, while for the return movement it ranged from 0.43 to 0.74.

Based on the determined values of the relative coefficients, characterizing the dynamic forces in the chain of the rescue scraper conveyor, in particular the A/S parameter, a method of applying a variable load in the contact area if chain links will be developed.



## References

- [1] Wieczorek A.N.: Badania skojarzonego oddziaływania górniczych czynników środowiskowych na degradację powierzchni bębnowych chodnikowych przenośników zgrzeblowych, Wydawnictwo Politechniki Śląskiej; Gliwice 2018; ISBN978-83-7880-571-7
- [2] Wieczorek, A.N.; Wójcicki, M.: Synergism of the Binary Wear Process of Machinery Elements Used for Gaining Energy Raw Materials. *Energies* 2021, 14, 1981. <https://doi.org/10.3390/en14071981>
- [3] Antoniak J., Suchoń J.: „Górnice przenośniki zgrzeblowe”; Wydawnictwo Śląsk; Katowice 1983
- [4] Suchoń J.: Górnice przenośniki zgrzeblowe. Budowa i zastosowanie. ITG KOMAG, Gliwice 2012; ISBN 978-83-60708
- [5] Remiorz E., Mikuła S.: Podstawowe formy degradacji własności użytkowych łańcuchów ogniowych górniczych stosowanych w maszynach ścianowych. *Maszyny Górnicze* 2017(151) nr 3
- [6] Kocańda S.: Zmęczeniowe niszczenie metali. WNT, Warszawa 1972
- [7] Mikuła S.: Trwałość zmęczeniowa ciągów łańcuchowych górniczych maszyn urabiających i transportowych. *Prace badawcze CMG KOMAG*, Gliwice 1978
- [8] Cheluszka P., Dolipski M., Remiorz E., & Sobota, P. Follow-Up Chain Tension in an Armoured Face Conveyor. *Arch. Min. Sci.*, 2015, Vol. 60, No 1, p. 25–38 2015
- [9] Celis J.-P.; Ponthiaux P.: Testing tribocorrosion of passivating materials supporting research and industrial innovation. *European Federation Corrosion by Maney Publishing*; 2011
- [10] Landolt D.: Electrochemical and materials aspect of tribocorrosion systems. *J. Phys. D Appl. Phys.* 2006, 39, 3121–3127
- [11] Celis J.-P., Ponthiaux P.: Tribocorrosion. *Wear* 2006, 261, 937–938
- [12] Jemmely P., Mischler S., Landolt D.: Electrochemical modeling of passivation phenomena in tribocorrosion. *Wear* 2000, 237, 63–76
- [13] Mischler S., Debaud S., Landolt D.: Wear-accelerated corrosion of passive metals in tribocorrosion systems. *J. Electrochem. Soc.* 1998, 145, 750–758
- [14] Landolt D.: Electrochemical and materials aspects of tribocorrosion systems. *Journal of Physics D: applied physics*, 2006. 39(15), 3121
- [15] López-Ortega A., Arana J. L., Bayón R.: Tribocorrosion of passive materials: a review on test procedures and standards. *International Journal of Corrosion*, 2018
- [16] Munoz A. I., Espallargas N.: Tribocorrosion mechanisms in sliding contacts. In *Tribocorrosion of passive metals and coatings* (pp. 118-152). Woodhead Publishing. 2011
- [17] Dolipski M., Remiorz E., Sobota P.: Determination of dynamic loads of sprocket drum teeth and seats using mathematical model of a scraper conveyor. *Archives of Mining Sciences* 2012, volume 57 issue 4
- [18] Burakowski T.: Rozważania o synergizmie w inżynierii powierzchni. Wydawnictwo Politechniki Radomskiej. Radom 2004
- [19] Wójcicki M.; Wieczorek, A.N.; Głuszek G.: Concept of the facility for testing the wear of chain links in the aspect of synergism of environmental factors. *Mining Machines*, 2021
- [20] Materiały katalogowe firmy Hottinger Messtechnik



<https://doi.org/10.32056/KOMAG2023.2.5>

## Modelling the suspended monorail route stresses and deflections during the transport of heavy loads with use of diesel locomotives

Received: 02.06.2023

Accepted: 24.07.2023

Published online: 31.07.2023

### Author's affiliations and addresses:

<sup>1</sup> Dnipro University of Technology,  
19 Yavornytskoho Ave., 49005,  
Dnipro, Ukraine

Leonid SHYRIN <sup>1</sup>, Andrii HERASYMENKO <sup>1</sup>,  
Ivan INYUTKIN <sup>1</sup>

### \* Correspondence:

e-mail: herasymenko.an.o@nmu.one

tel.: +38 066 488 04 31

### Abstract:

Based on the results of tests of the monorail transport system using suspended diesel locomotives with traditional transport beams and with the use of an innovative system of transport beams for the delivery of heavy loads, it was found that to reduce the dynamics of the load to the elements of the suspended route segments fastened to the arches of the arch support, it is beneficial to use the proposed an innovative technical solution that increases the reliability of the route catches to the support arches, which is important when transporting heavy loads. The new solution significantly reduces the dynamic loads to the route catches to the support arches by redistributing the load over a greater number of sections of the suspended monorail route. It has been proven that during the period of intensification of preparatory work, these technical solutions make it possible to keep to the timely preparation of new mining pillars and are perceived as a promising direction for improving the existing transport system for the mines of the region and ensuring the operational parameters of mining transport equipment at a high technical level in the specific conditions of the mines of Western Donbass

Keywords: arch support, heavy loads, dynamic loads, auxiliary transport, lifting and transport system, transport and technological system, solidworks simulation



## 1. Introduction

The use of suspended monorail diesel locomotives (PDM) as the only vehicle in the coal mining industry significantly increases the advance of longwall mining at coal mines. However, in the specific conditions of thin coal seams of the Western Donbass mines the traditional schemes of attaching the monorail route to the arch support lead to bending the arches and changes the profile of the SMR route. Tests [1] showed that when transporting the heavy loads on a deformed monorail route, dynamic loads occur, which initiate the roof fall [2]. Moreover, in the conditions of intensification of mining operations, traditional auxiliary transport required the development and implementation of innovative technical solutions improving the technical condition of the route [3]. The expediency of implementing such solutions is especially relevant when preparing new mining pillars. This is due to the need of transporting heavy loads such powered roof supports, shearers, etc. to the assembly chambers and to the workplaces. In the foreign practice of coal seams development by high-performance mechanized systems, similar problems are solved by introducing alternative types of auxiliary transport and methods for determining their technical condition [4]. Suspended monorail with diesel locomotives is currently one of the most effective types of transport in the coal mining industry. In the specific conditions of WD mines, transport effectiveness is determined by improvements of technological solutions in the area of transport-technological system PDM – route fastening – rock mass, hereinafter referred to as “PDM-KV-GM”

## 2. Materials and Methods

It has been experimentally confirmed that the parameters of interaction between the elements of the technological system PDM-KV-GM are currently poorly investigated [5]. In this regard, the problems regarding the operational control of the monorail route technical condition and a determination of their maximum permissible dynamic loads in real conditions of the mine environment require special observations and theoretical studies.

It is recommended to solve non-traditional technical tasks for the industry by modelling the conditions of interaction of the elements of the PDM-KV-GM system using the methods of mathematical analysis of technical systems and the licensed SolidWorks Simulation software. The gained experience of transporting the heavy loads through extensive networks of workings allowed to define the tasks related to the special mine studies of the parameters of the new generation SMR in the specific conditions of WD mines, namely:

- features of monorail route profile changes under the impact of dynamic loads and deformations
- the amount of deflection and the technical condition of the monorail beams;
- the consequences of the negative impact of dynamic loads to the route sections and centers of beams of a monorail route sections during the transportation of heavy loads.

According to the results of testing the technical condition of the route of the SMR monorail route, it was established that the main deformations in its profile, deflections in the arch support and the roof fall of the rock mass are concentrated in the zones of the supporting arches to which the monorail route section is suspended (Fig. 1). In the zones of intermediate arches, rockfalls were not observed. Thus it can be stated that during the transportation of heavy loads, the areas of frontal contact of the monorail route sections are the zones of increased dynamic loads to the arch support and the rock mass. This is caused primarily by the design features of monorail route sections, the ends of which are beveled to compensate the longitudinal deformations during the transport operation. The negative factors also include emergency braking of the railway, which initiate dynamic overloads to the monorail beams, which are transmitted through suspensions to the support arch and in the result to the roof rock.





**Fig. 1.** Mechanical failure due to dynamic loads and local deformation of the roof

Currently, the most available methods of analyzing the loads and the resulting deformations of the route of suspended transport systems in the conditions of their installation in mine workings are the methods of mathematical and computer modeling using SolidWorks Simulation and Multi Body System (MBS) software [6].

### 3. Results

#### 3.1. Problems of interaction among the components of the PDM-KV-GM system

According to the observations of the actual routes of suspended monorails, focusing on the deformations of the route sections and support arches, and based on the SolidWorks Simulation software, the interaction of the "PDM-KV-GM" transport system and its strength reserves for typical operating conditions were determined. It was found that the support arches and the middle sections of the route are the most susceptible to mechanical damage in a result of dynamic loads (Fig. 1).

The actual data on the conditions of cooperation of the components of the "PDM-KV-GM" transport system and the results of modelling its technical condition using the SolidWorks Simulation software allowed to determine the specificity of transporting the large, heavy loads along the suspended monorail route and to develop assumptions as to how to reduce the dynamic loads to route sections of the suspended monorail and arches of the support to increase capacity of the transport and technological system in specific conditions of mining the coal seam.

Tests of the operating parameters of the suspended rail routes [7, 8] showed that to reduce the dynamic loads to the fasteners of the route sections, it is necessary to ensure redistribution of dynamic loads to the adjacent beams of the monorail route during the passage of the rolling stock, so that only the minimum permissible deflection of the route segments occurs as a result.

In this regard, the method of modelling deformations of the monorail route sections joints under the impact of heavy loads provides:

- identification of zones of maximum deflection of route segments when transporting heavy loads;
- forecasting possible negative consequences and methods to prevent them.

### 3.2. Input data for interaction among the components of the PDM-KV-GM system

According to recommendations [1], the tasks were realized in stages.

At the first stage, to determine the technical condition of the track of suspended monorail, a base of input data is formed, which includes physical and mechanical properties of the steel I-beam in operation, as well as data characterizing the mine environment has been created.

The most important factors include: deformation of the roof rocks, which lead to a forced spatial displacement of the monorail route from the assumed position; physical and mechanical properties of steel monorail sections; mass of heavy loads and their dimensions, which significantly affect the speed of transportation especially at the route turns.

Design, construction and operational documentation of mines [9, 10], monitoring and diagnostics of the technical condition of the monorail route, as well as the results of testing the deformation characteristics of the rock mass in the real conditions of the mine environment are the main sources for the collection of input data.

In accordance with the program and methodology of comprehensive tests, in order to obtain initial information about the technical condition of the suspended monorail transport system and stresses of its components, it was necessary to determine the most heavily loaded sections of the monorail track as well as the real forces acting on them, to establish the compliance of the calculated indicators of the safety margin of these sections with the normative ones.

According to recommendations [11], spatial changes in the track of suspended monorail roads are considered taking into account the isotropic properties and physical and mechanical characteristics of steel monorail beams, which are deformed in all directions equally. In this regard, the deformations of their material in the process of spatial change of the route of mine suspension roads are analysed identically, but taking into account the impact of the rock mass behavior.

To generate the initial data on the components of the PDM-KV-GM system operation in real conditions of the mine environment and to analyse the monorail route, a linear-elastic model of the I-beam material was adopted, and the parameters of the elastic properties of the material ( $G$ ) were described by standard parameters, such as Young's modulus and Poisson's ratio [12]:

$$G = \frac{E}{2 \cdot (1 + \nu)} \quad (1)$$

where:

- $E$  – Young's modulus,
- $\nu$  – Poisson's ratio.

The formed database enabled assessment of the loads, the impact of which leads to plastic deformation and destruction of the integrity of the I-beam structure.

In fundamental studies [13, 14], the Huber-Mises-Genki hypothesis of deformation energy is used to describe the deformation models of a monorail track. Practical calculations and the equivalent stresses are determined by the following relationship:

$$\sigma_i = \frac{1}{\sqrt{2}} \cdot \sqrt{(\sigma_1 - \sigma_2)^2 + (\sigma_2 - \sigma_3)^2 + (\sigma_3 - \sigma_4)^2} \quad (2)$$

where:

- $\sigma_1, \sigma_2, \sigma_3, \sigma_4$  – Main values of the stress tensor.

According to (2), the equivalent stresses arising in the linear parts of the I-beam monorail joint lead to the transition of the material to the plastic state and at ( $\sigma_i = \sigma_T$ ) reach the yield point, and at ( $\sigma_i = \sigma_\sigma$ ) the strength limit and can lead to the destruction of the structure.

Thus, this model of plasticity can be successfully used as a criterion for determining the limit states and failures of I-beam sections of the SMR monorail joint under different conditions of their operation.



For the mathematical modeling of the interaction conditions of the PDM-KV-GM system, a section of the monorail route is represented as a beam of length  $L$ , fixed on both sides, and a weight ( $F$ ) is applied to it. The deformation energy of the PDM I-beam joint is determined by the following relationship:

$$\delta V = \frac{1}{2} EL \left( \frac{d\theta}{dx} \right)^2 \delta x \quad (3)$$

where:

$E$  – modulus of elasticity;

The potential energy of a curved I-beam is determined by the following expression:

$$V = U - \frac{1}{2} F \int_0^1 \varphi^2 dx \quad (4)$$

where:

$U$  – potential energy of deformation;

$F$  – compressive force.

Previous studies [5] established that as a result of the deformations of the rock mass, spatial changes occur in the mine monorail route, which leads to an increase in dynamic loads in the butt joints of I-beam beams and the deflection of the monorail route and, as a result decreasing the carrying capacity of the transport and technological systems.

It should be noted that the interactions among the components of the PDM-KV-GM system is an understudied problem of mining production and requires special tests to establish the maximum stresses and deformations in the linear parts of the monorail route and its nodal connections. In this regard, the further examination of the technical task, which is not traditional for the mining industry, was carried out comprehensively, through testing the interactions among the components of the PDM-KV-GM system and their simulation using the SolidWorks Simulation software.

The initial data for modeling the linear deformations of the PDM route under the impact of dynamic loads arising during the transportation of heavy loads were obtained from the results of testing the deformations of rock mass and the arch attachment as well as changes in the profile of the monorail route (Fig. 2).



**Fig. 2.** Measuring station for recording the deformations of arch fastening during transportation of heavy loads

In the process of modeling, the deformed section of the I-beam was analysed in the SolidWorks Simulation program using the finite element method (FEM) [15]. The tests consisted in determination of maximum allowable deflections and stresses in the butt joints of the sections of the track using the generated CAD models. A similar approach enabled a structural analysis of the behavior of the system under dynamic loads and predict changes in the technical condition of the beams of the monorail route in the complex conditions of the mine environment.

The simulated section of the monorail track consists of I-beams 3.0 m long. I-beams are made of alloy steel without any special coating. The physical and mechanical properties of the I-beam material included in the generated CAD models are shown in Table 1.

**Table 1.** Parameters of the alloy steel

Properties	Amount	Unit
Modulus of elasticity	2.1e+11	N/m <sup>2</sup>
Shear modulus	7.9e+10	N/m <sup>2</sup>
Mass density	7800	kg/m <sup>3</sup>
Tensile strength limit	8·10 <sup>8</sup>	N/m <sup>2</sup>
Poisson's ratio	0.28	
Yield point	590593984	N/m <sup>2</sup>
Coefficient of thermal expansion	1.1e-0,5	
Thermal conductivity	14	W/(m·K)
Specific heat capacity	440	J/kg·K

To simulate the conditions of interaction of the components of PDM-KV-GM technical system in the CAD environment, the straight line section of the route of the underground monorail, as in Fig. 3, was assumed.

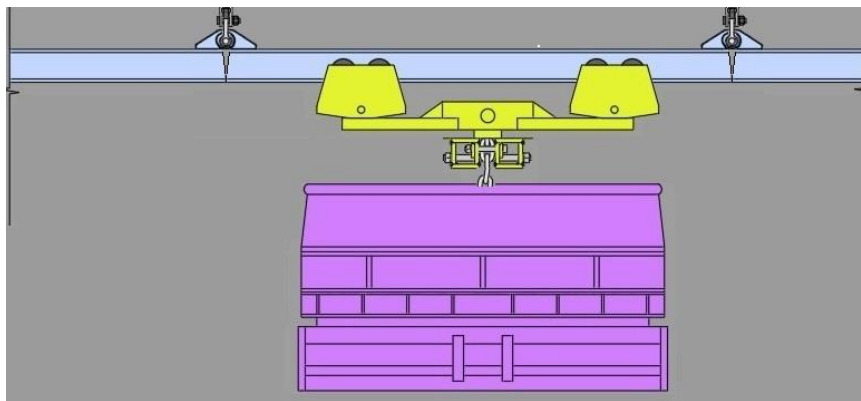


**Fig. 3.** Load diagram of a route segment using a traditional transport trolley

### 3.3. Modeling the technical condition of a monorail using SolidWorks Simulation software

A straight section of the monorail track consists of I-beams with a length of  $l = 3$  m, which are attached to the arches of the support with chain slings. The route segments are connected to each other in such a way that the bending moments at the connections are equal to zero. Such a constructive solution allows to treat each segment of the route as a beam, attached individually, end-to-end, to the arches of the support.

The tests of the technical condition of the suspended monorails in the mine showed that the areas most exposed to deformations are the butt joints of the route sections and the central sections of the route. The tests results were used as the basis for theoretical analyses on the conditions of interaction of the PDM-KV-GM technical system components during the transport of heavy loads. In order to

calculate the loads and deformations in the characteristic nodes of the butt joints of the route sections, they were divided into elementary meshes. The CAD model of dynamic loads in the articulated nodes of the monorail beams is shown in Fig. 4.

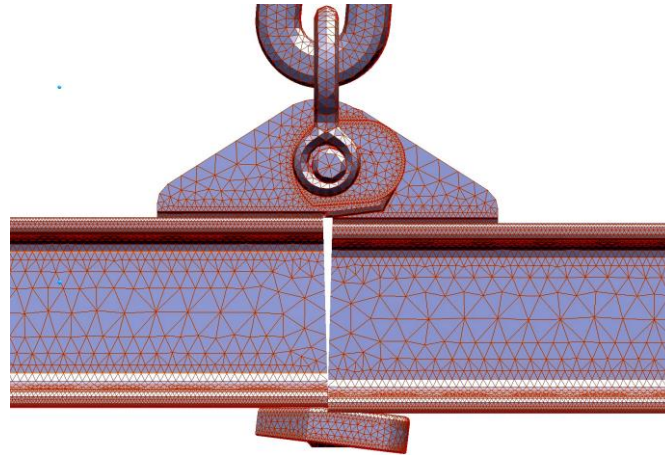


**Fig. 4.** CAD tetrahedral finite element mesh at route segment junction developed to analyze stresses and strains

Loads to the central parts of the sections was modelled for the traditional transport trolleys (Fig. 3) and for a new lifting and transport system, the principle of operation of which is described below.

Using the SolidWorks Simulation software, the maximum deformations in the segments of the monorail route (Fig. 5) and stresses (Fig. 6) during the transport of a heavy loads were determined.

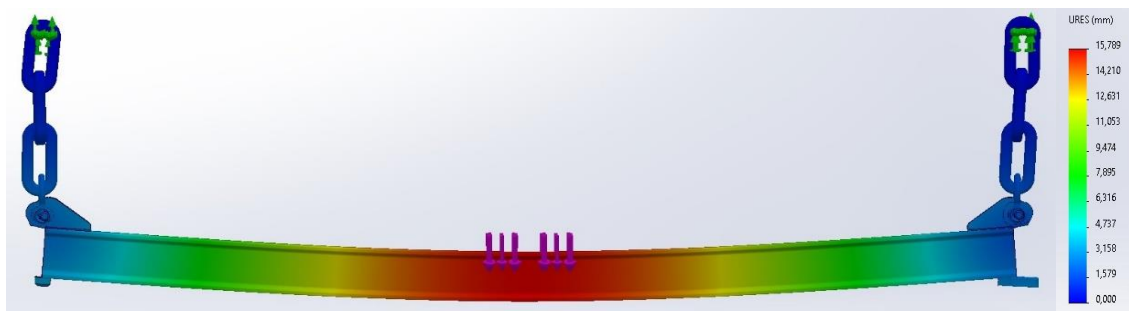


**Fig. 5.** Deflection of the monorail beam when transporting heavy loads in a traditional way

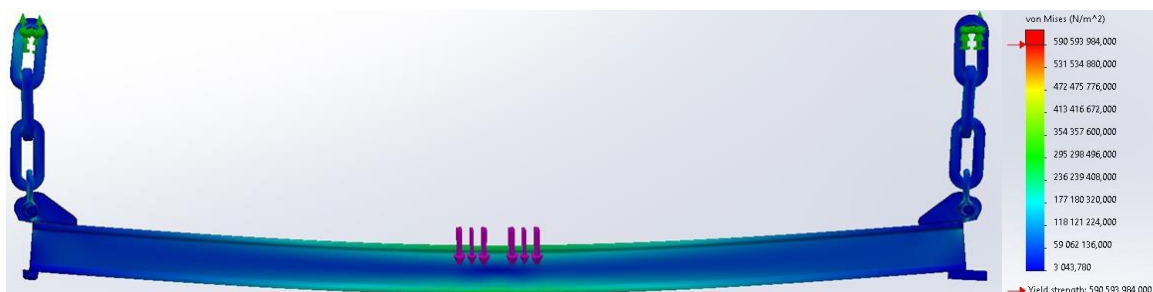


**Fig. 6.** Stresses in the beam of the monorail track resulting from the transportation of heavy loads in a traditional way

Equivalent stresses at the centers of monorail joint beams (Von Mises stresses) are shown in Fig 6. The Von Mises stresses obtained from the simulation results are calculated according to the following formula:

$$VON = \{0.5 \cdot [(SX - SY)^2 + (SX - SZ)^2 + (SY - SZ)^2] + 3 \cdot (TXY^2 + TXZ^2 + TYZ^2)\}^{(1/2)} \quad (5)$$

where:

- VON* - Von Mises stress;
- SX* - the normal stress along X;
- SY* - the normal stress along Y;
- SZ* - the normal stress along Z;
- TXY* - Y-displacement in the YZ plane;
- TXZ* - displacement along Z in the YZ plane;
- TYZ* - displacement along Z in the XZ plane.

$$VON = \{0.5 \cdot [(P1 - P2)^2 + (P1 - P3)^2 + (P2 - P3)^2]\}^{(1/2)} \quad (6)$$

where:

- P1* - the first major stress (the largest);
- P2* - the second main tension;
- P3* - the third main tension.

Based on the obtained equivalent stresses, it was found that the centres of I-beam chains, where the stresses reach 413 MN/m<sup>2</sup> are the most susceptible to fracture.

Based on the analyses of the obtained stresses, it was found that the most susceptible to damage are the middle fragments of the route section, in which the stresses reach 413 MN/m<sup>2</sup>.

In order to reduce the loads during the transport of heavy loads, a technical solution was developed and an application for a Ukrainian patent was submitted [16]. The idea behind this solution is to distribute the load over a larger number of route sections, which reduces the deflection of each section and increases operational reliability during the transport of heavy loads. The diagram of the lifting and transport system for moving heavy loads (1) consisting of load-carrying trolleys (2), rolling trolleys (3) and suspensions to the support arches is shown in Fig. 7.

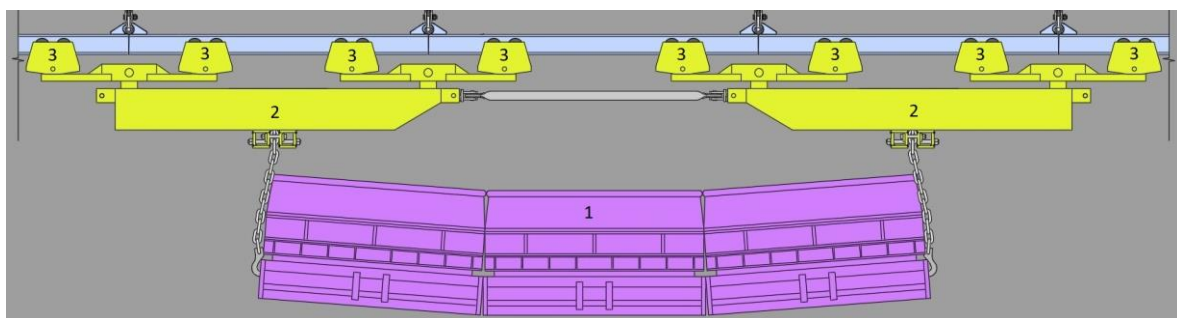


**Fig. 7.** Diagram of the crane and transport system with the load on the suspended monorail track

The results of simulation of interaction of the components of the lifting and transport system with the arch support enabled determining the zones of equivalent deformations and indicators of the safety margin of the monorail sections joints. Fig. 8, 9 show the equivalent stresses and deflection of a monorail beam during the transportation of heavy loads ( $M \geq 4000$  kg) using a lifting and transport system.

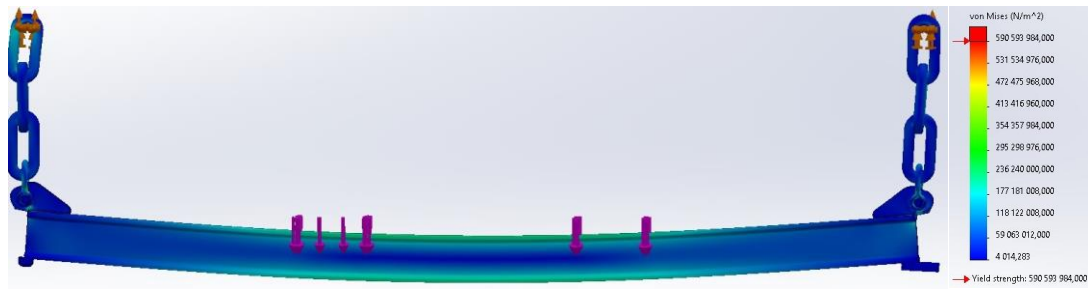


**Fig. 8.** Equivalent stresses of the beam of the monorail route from transportation of heavy loads when using the lifting and transport system

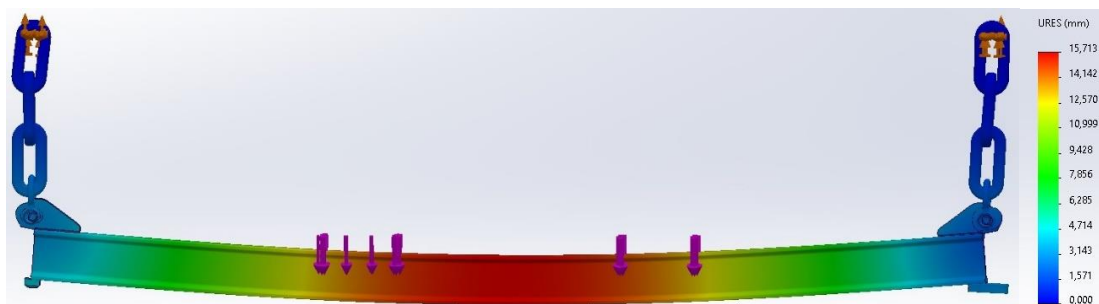


**Fig. 9.** Deflection of the monorail beam during transportation of large-tonnage cargo using the lifting and transport system

Based on the results of the simulation of the deflection of the monorail beams, it was found that the redistribution of loads to the monorail route due to the introduction of a lifting and transport system will allow safe transportation of heavy loads weighing up to 16 tons in the difficult conditions of the mine environment. The results of testing the deflection of monorail beams and forecasting their technical condition using the traditional transportation scheme and with the use of a lifting and transport system are shown in Fig. 10.

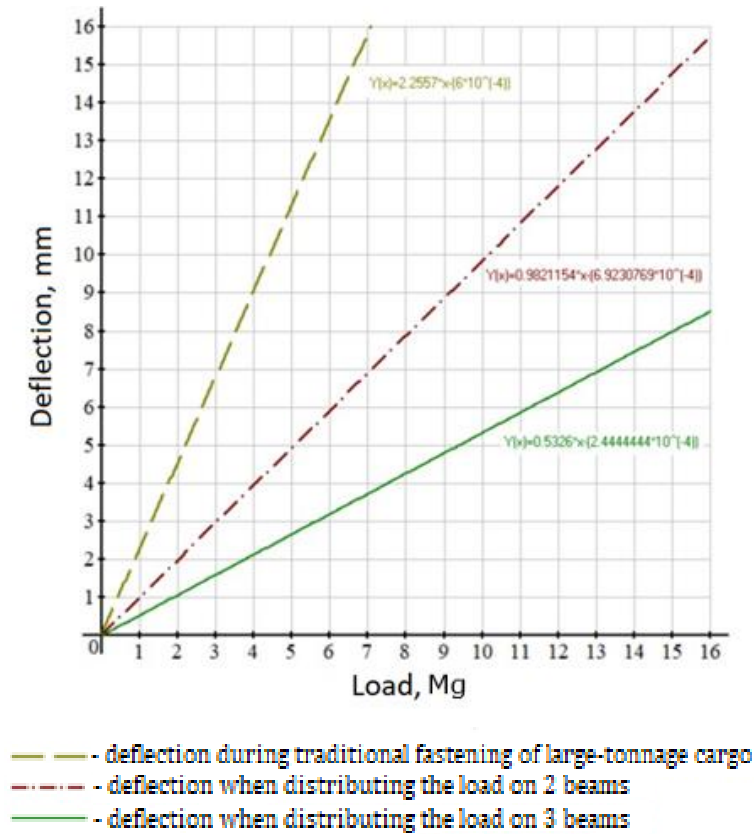


**Fig. 10.** Comparative curves of deflection of route sections during the transport of heavy loads by the traditional and lifting-transport system with load distribution into 2 and 3 route sections

#### 4. Conclusions

Based on the results of modeling the interaction of the system components, the strength reserves of the suspended monorail route sections were determined for typical operating conditions. It has been experimentally proven that the most susceptible to dynamic loads and mechanical damage are the butt connections of the route sections and the middle parts of these sections of the suspended monorail route.

The analysis of the results of the simulation of interaction of system components shows that dynamic loads appear during the transport of heavy loads, the negative impact of which on the beam route sections and arch fastening is significantly reduced when using the developed lifting and transport system

The obtained parameters of cooperation of the system components and the results of the assessment of the technical condition of the connections of the monorail route segments allowed to conclude that in the real conditions of the mine environment, the designed profile of the suspended monorail track is a complex transport and technological system, which, under the impact of dynamic loads, continuously changes its initial state both in vertical and horizontal planes. Based on the results of mathematical and computer modeling of the PDM-KV-GM transport system, it was found that dynamic loads can be significantly reduced by distributing them over several segments of the suspended monorail route.

The recommended technical solutions allow to increase the potential reserves and the area of effective use of suspended monorails in the real conditions of the mine environment and to predict the permissible loads to the monorail route when moving the heavy loads.

#### References

- [1] Shyrin L.M., Rastsvietaiev V.O., Koval O.I.: Pidvyshchennia efektyvnosti roboty monoreikovykh dorih pid chas pidhotovky zapasiv vuhillia do ochysnoi vyimky. Monohrafiia. Nats. horn. un-t. D.: NHU. 2014, 144 s.



- [2] Dychkovskiy R., Bondarenko V.: Methods of Extraction of Thin and Rather Thin Coal Seams in the Works of the Scientists of the Underground Mining Faculty (National Mining University). International Mining Forum 2006, New Technological Solutions in Underground Mining, 2006, 21–25. <https://doi.org/10.1201/noe0415401173.ch3>
- [3] Tokarczyk J.: Metodyka identyfikacji wybranych zagrożeń mechanicznych w pomocniczym transporcie podziemnych zakładów górniczych. Prace Naukowe – Monografie KOMAG, Monografia nr 52, Instytut Techniki Górniczej KOMAG, Gliwice 2017; ISBN 978-83-65593-08-5
- [4] Dychkovskiy R., Falshtynskiy V., Ruskykh V., Cabana E., Kosobokov O.: A modern vision of simulation modelling in mining and near mining activity. E3S Web of Conferences 2018, (60): 00014. <https://doi.org/10.1051/e3sconf/2018600001>
- [5] Herasymenko A.O., Rastsvietaiev V.O., Shyrin A.L.: Selection of the means of auxiliary transportation facilities and adaptation of their parameters to specific operation conditions. Naukovyi Visnyk Natsionalnoho Hirnychoho Universytetu 2023, (2): 40–46. <https://doi.org/10.33271/nvngu/2023-2/040>
- [6] Szewerda K., Krenicky T.: Use of the MBS method in mining industry R&D projects. Mining Machines, 2022, Vol. 40 Issue 2, pp. 110-120 <https://doi.org/10.32056/KOMAG2022.2.6>
- [7] Shyrin A., Rastsvetaev V., Morozova T.: Estimation of reliability and capacity of auxiliary vehicles while preparing coal reserves for stoping. Paper presented at the Geomechanical Processes during Underground Mining – Proceedings of the School of Underground Mining 2012, 105-108. <https://doi.org/10.1201/b13157-18>.
- [8] NPAOP. Safety requirements for the technology of installation and dismantling of mechanized complexes for gentle and inclined layers. Luhansk: Vuhlemekhanizatsiia. 2011 Retrieved from [http://mpe.kmu.gov.ua/minugol/control/publish/article?art\\_id=210138](http://mpe.kmu.gov.ua/minugol/control/publish/article?art_id=210138)
- [9] SOU-P 10.1.00174088.018:2009 Sistema upravleniya proizvodstvom i ohranoj truda v ugolnoj promyshlennosti Ukrainy (tipovoe rukovodstvo): Utverzhdeno Prikazom Ministerstva ugolnoj promyshlennosti Ukrainy ot 21.01.2010 g. № 7. Kiev, 2010. 200 s.
- [10] Shyrin L. N., Koroviaka Ye. A., Posunko L. M., Rastsvietaiev V. O., Sharina B. C.: Poshyrennia oblasti efektyvnoho zastosuvannya pidvisnykh monoreikovykh dorih v umovakh vidpratsiuvannya pokhylykh vuhilnykh plastiv. Zbirnyk naukovykh prats Natsionalnoho hirnychoho universytetu № 55. 2018, (pp. 255–266). [http://nbuv.gov.ua/UJRN/znpngu\\_2018\\_55\\_27](http://nbuv.gov.ua/UJRN/znpngu_2018_55_27)
- [11] Stalevi konstruksii. Normy proektuvannya: DBN V.2.6-198:2014. – K.: Minrehion Ukrainy, 2014. – 199 s.
- [12] Gavrić L.J.: Computation of propagative waves in free rail using a finite element technique / L. J. Gavrić // Sound and Vib. - 1995. - №185(3). - P. 531-543. – ISSN 0022-460X.
- [13] Shmyh R. A.: Rozrakhunok budivelnnykh konstruksii v obchysliuvalnomu kompleksi SCAD: navch. posib. / R. A. Shmyh, I. M. Dobrianskyi; za zah. red. R. A. Shmyha. – Lviv: Liha Pres, 2015. – 79 s.
- [14] Han H. Teoriya uprugosti: Osnovy linejnoy teorii i ee primenenie: Per. s nem. / H. Han. – M.: Mir, 1988. – 344 s. 12 Gere J. M. Mechanics of materials / J. Gere, B. Goodno. – Stamford: Cengage Learning, 2012. – 620 p.
- [15] Ovcharenko V.A., Podlyesnij S.V., Zinchenko S.M.: Osnovi metodu kincevih elementiv i jogo zastosuvannya v inzhenernih rozrahunkah: Navchalnij posibnik. – Kramatorsk: DDMA, 2008. – 380 s. ISBN 978-966-379-224-8
- [16] Shyrin L.N., Herasymenko A.O., Shyrin A.L., Yehorchenko R. R., Koptovets O.M., Diachkov P.A., Iniutkin I.V.: Pidiomno-transportna systema dlia dostavky vantazhiv (Ukraina/Dnipro Zaiavka na vynakhid a2022 02487 vid 14.07.22). Natsionalnyi tekhnichnyi universytet «Dniprovska politekhnika».



## Development of a prototype shredder for WEEE equipped with NdFeB magnets

Received: 04.07.2023

Accepted: 25.07.2023

Published online: 31.07.2023

### Author's affiliations and addresses:

<sup>1</sup> KOMAG Institute of Mining Technology, Pszczyńska 37, 44-101 Gliwice, Poland

### \* Correspondence:

e-mail: pfriebe@komag.eu

tel.: +48 322 374 608

Pawel FRIEBE  <sup>1\*</sup>

### Abstract:

Waste Electrical and Electronic Equipment (WEEE) that contains neodymium magnets (NdFeB) has the potential to serve as a valuable source of elements, including critical ones. These magnets contain Rare Earth Elements (REEs) like Neodymium, Dysprosium, and Praseodymium. A noteworthy method of recycling REEs involves the magnet-to-magnet process, wherein the NdFeB alloy is separated from WEEE and directly reused in the production of new products, specifically new NdFeB magnets. The initial step in this recycling process involves disintegration, a procedure aimed at reducing and segregating the materials within the WEEE. The conventional process of disintegrating WEEE for recycling faces challenges due to the presence of magnetic materials, making it ineffective with existing equipment. To address this, a specialized device called a disintegrator, using counter-rotating cutting shafts, has been developed for efficient shredding of WEEE containing NdFeB. The goal of the research is to develop a prototype shredder to effectively recover valuable metals, including REEs, from WEEE. Specific sub-objectives include motor and gearbox selection, shaft bearings selection, gear design, and cutting blades design. The work involved calculations and 3D modelling of the disintegrator components using Autodesk Inventor 2020 software.

Keywords: NdFeB magnet, recycling, physical processing of electronic waste, shredding



## 1. Introduction

An alternative approach to mining for obtaining Rare Earth Elements (REEs) is through recycling [1, 2]. Waste Electrical and Electronic Equipment (WEEE) that contains NdFeB magnets (composed of  $\text{Nd}_2\text{Fe}_{14}\text{B}$  alloy) exhibits significant potential for reuse [3, 4]. These magnets consist of REEs such as Neodymium (Nd), Dysprosium (Dy), and Praseodymium (Pr) [5, 6, 7]. Efficiency studies conducted on NdFeB magnets produced from recycled raw materials have demonstrated similar performance to conventionally produced magnets [8, 9, 10]. Furthermore, a comparative Life Cycle Assessment (LCA) analysis comparing the production of new and recycled NdFeB magnets revealed lower emissions and energy requirements in the case of recycling [11].

The currently conducted process of disintegration of hard drives causes many difficulties related to the characteristics of the material [12]. The presence of magnetic materials poses difficulties as the existing equipment used for shredding is constructed with ferromagnetic components, making it ineffective for shredding WEEE containing NdFeB magnets [13]. This is because the magnetic particles adhere to the ferromagnetic elements of the machine, resulting in reduced shredding efficiency and requiring manual interruption and cleaning of the machine.

In order to facilitate the initial shredding process in magnet-to-magnet recycling, a specialized device known as a disintegrator has been developed. Disintegrators operate on the principle of counter-rotating pairs of cutting shafts. The functioning of this equipment is as follows: materials placed on the shafts are captured by blades attached to the cutting shafts. The material is then pressed against the adjacent shaft surfaces and shredded. The resulting fragmented material is further transported by the blades and subsequently discharged from the machine after passing over the shafts. The primary components of the machine consist of the cutting shafts and the shaft casing. The cutting shafts are composed of inner shafts on which cutting knives in the form of discs are mounted. The fundamental concept of the design revolves around employing paramagnetic and robust materials, along with optimizing the design parameters of the machine components, to ensure an efficient shredding process for WEEE containing NdFeB magnets. The shredded product is then directed for further recycling. Recycling enables the recovery not only of REEs but also of other metals, including precious metals, and other component materials from WEEE. The closed-loop magnet-to-magnet recycling approach facilitates the reuse of REEs. Assuming selective separation and reuse of other components in the processed equipment, the amount of waste generated will be significantly reduced, aligning with the principles of a closed-loop economy policy.

The objective of the research presented in this publication is to develop a prototype shredder with the capability to effectively shred WEEE containing NdFeB magnets, thus enabling the recovery of valuable metals, including REEs. To achieve this primary goal, the project has established the following specific sub-objectives:

- Motor and gearbox selection: The appropriate motor and gearbox will be carefully chosen to ensure optimal performance and efficient power transmission within the shredder system.
- Shaft bearings selection: The selection of suitable bearings for the shredder's shafts will be conducted to ensure smooth operation and enhance the longevity of the equipment.
- Gears design: Thorough design work will be carried out to develop efficient gears that will enable reliable operation of the shredder, facilitating the effective shredding of WEEE materials.
- Cutting blades design: The design phase will focus on developing cutting blades that enhance the shredder's cutting efficiency, enabling the successful separation of valuable metals from the WEEE material.

## 2. Materials and Methods

In sections 2.1 to 2.4, the most important stages of designing the aforementioned device were presented, including motor and gearbox selection, shaft bearing selection, gear design, and the selection of construction material and shape of cutting blades. These tasks involved conducting calculations to determine the minimum torque of the device or to determine the geometric parameters of the components. Subsequently, based on the conducted calculations, 3D models of the parts comprising



the disintegrator were designed. The 3D modelling was carried out using Autodesk Inventor 2020 software, which includes functions related to 3D mechanical modelling, CAD design, and visualization of the developed elements. In section 2.5, the designed device is presented.

This project was developed taking into account the specifications described in the patent application titled "Disintegrator for shredding used electrical and electronic equipment" [14].

## 2.1. Motor and gearbox selection

The selection of the motor and gearbox for driving the device began with calculating the minimum force required to crush the target material. The following dimensions for the cutting blades were assumed: blade diameter - 129 mm, cutting blade thickness - 12 mm. It was also assumed that the material to be shredded would be a 3.5" hard disk drive (HDD). The components of the HDD include neodymium magnets, a positioner arm with a head, disks, and a PCB (Printed Circuit Board). The components that may pose difficulty in the shredding process due to their high durability are the casing, which has a thickness of up to 12 mm and is made of aluminium, as well as the two steel plates inside. The thickness and width of the HDD were assumed to be 12 mm x 101 mm.

The calculations began with determining the surface area on which the destructive force will act.

$$A = S_1 \cdot G \quad (1)$$

where:

A - cutting area, mm<sup>2</sup>,

S<sub>1</sub> - width of the cutting blade, mm,

G - thickness of the material being shredded, mm [15].

In the shredding process using disintegrators, the primary force acting on the material is cutting. The shear strength of the shredded materials, such as aluminium and steel, which exhibit the highest strength among the other materials contained in the HDD, was obtained from Table 1.

Based on the above calculations, the destructive cutting force for a single cutting blade was determined using the following formula:

$$R_t = \frac{F_t}{A} \quad \Rightarrow \quad F_t = R_t \cdot A \quad (2)$$

where:

R<sub>t</sub> - shear strength, N/mm<sup>2</sup>,

F<sub>t</sub> - destructive force on the material, N [15].

The calculated force F<sub>t</sub> needs to be increased due to the fact that in the actual shredding process, multiple cutting blades are involved, depending on the dimensions of the material being shredded. In the case of material with the assumed width mentioned above, the number of cutting blades will be as follows:

$$I = \frac{S_2}{S_1} \quad (3)$$

where:

I - number of blades involved in the shredding process, 1,

S<sub>2</sub> - width of the material being shredded, mm.

The total required destructive force on the material in the shredding process is the product of the required force for a single cutting blade and the number of cutting blades involved:

$$F_c = F_t \cdot I \quad (4)$$

where:

F<sub>c</sub> - total required cutting force, N.



The next parameter to be determined is the minimum torque of the device. It is a derived parameter from the cutting force  $F_c$  and the radius of the blade  $r_n$  [16]:

$$M = F_t \cdot r \quad (5)$$

$$M_a = F_a \cdot r_n \quad (6)$$

$$M_s = F_s \cdot r_n \quad (7)$$

where:

$F_a, F_s$  - destructive force of aluminium, steel, Nm,

$M, M_a, M_s$  - destructive torque of aluminium, steel, Nm,

$r_n$  – radius of the cutting shaft, mm.

The assumptions for the calculations are presented in Table 1 [17].

**Table 1.** Assumptions for the calculations

No.	Parameter	Value	
		Aluminium	Steel
1.	$S_1$ [mm]	12	
2.	$r_n$ [mm]	64,5	
3.	$G$ [mm]	9	2,5
4.	$R_t$ [N/mm <sup>2</sup> ]	75	305

where:

$r_n$ - radius of the cutting blade, mm

The previously determined torque applies to the aluminium casing and a single steel plate. Since the HDD disk contains two steel plates, the calculated torque for a single plate has been doubled. Additionally, a safety margin of 25% has been introduced.

$$M_c = (M_a + 2 \cdot M_s) \cdot 125\% \quad (8)$$

where:

$M_c$  - total required torque.

Knowing the required torque, the selection of the gearbox and motor was conducted. It was assumed that the rotational speed of the shafts should be within the range of 11-16 RPM. Firstly, the torque on the output shaft of the gearbox was converted into force.

$$F_g = \frac{M_n}{r_{wz}} \quad (9)$$

where:

$F_g$  - force generated by the gearbox,

$r_{wz}$  - radius of the input shaft of the gearbox [18].

Next, using the previously calculated force and the assumed dimensions of the cutting elements, the rotational torque of the cutting blade located on its circumference was determined.

$$M_{wt} = F_g \cdot r_{wt} \quad (10)$$

where:

$M_{wt}$  - rotational torque on the cutting shaft.



Table 2 presents the technical data of the considered transmissions, which will be used to determine the generated torque on the cutting shafts of the device [19]. This value will be compared to the previously determined required moment of torque. Based on the knowledge of the torque values on the cutting shafts, a specific variant of the gearbox and electric motor will be selected from the table below.

**Table 2.** Parameters of considered gearboxes

No.	$n_1$ [rpm]	$n_2$ [rpm]	I [1]	$P_s$ [kW]	$M_n$ [Nm]
1.	1400	20,5	68,43	11	4710
2.		18,7	74,95	7,5	3520
3.		15,1	92,53	7,5	4360
4.		13,8	101,33	5,5	3500
5.		11,6	120,33	5,5	4170
6.		11,3	123,75	5,5	4280
7.		10,6	131,78	5,5	4560

## 2.2. Selection of chamber bearings

The calculations related to the selection of bearings for the device started with determining the rotational speed and torque at which the input shaft of the gearbox would operate. Subsequently, the bearing load was calculated, which allowed estimating the bearing durability expressed in revolutions. The calculations assumed that each bearing would be subjected to half of the total torque generated by the gearbox, considering the use of two bearings on the cutting shaft. The remaining assumptions are listed in Table 3.

**Table 3.** Assumptions for determining bearing durability

No.	Parameter	Value
1.	$n_s$ [rev.]	1460
2.	I [1]	92,53
3.	P [kW]	7,5
4.	$r_n$ [mm]	64,5
5.	$L_l$ [years]	min, 5

The calculations were performed using the following equations [18]:

$$M = \frac{9550 \cdot P}{n_w} \quad (11)$$

where:

$n_w$  - rotational speed of the gearbox input shaft, RPM,

$n_s$  - rotational speed of the motor shaft, RPM,

I - gear ratio of the gearbox, dimensionless.

$$F = \frac{M}{r_n} \quad (12)$$

where:

F - bearing load, kN,

r - radius of the cutting blade, m.

$$L = \left( \frac{C}{\frac{1}{2}F} \right)^p \quad (13)$$

where:

L - bearing life, million revolutions,

C - dynamic load capacity, kN,

P - power exponent, for ball and roller bearings  $p=3$ ,

$$L_h = \frac{16660}{n_w} \left( \frac{C}{\frac{1}{2}F} \right)^p \quad (14)$$

where:

$L_h$  - bearing life, hours,

$n_w$  – calculated revolutions of cutting shafts, rev.

In the following Table 4, the data of bearings for the durability calculations are presented [20].

**Table 4.** Bearing life of the considered spherical roller bearings

No.	Bearing	Shaft diameter $\varnothing$ [mm]	C [N]
1.	22210-E1-XL	50	109 000
2.	22209-E1-XL	45	104 000
3.	22208-E1-XL	40	101 000
4.	22207-E1-XL	35	89 000
5.	22206-E1-XL	30	64 000
6.	22205-E1-XL	25	48 500

### 2.3. Gear selection

Gear parameters are essential in determining the functionality and performance of gears in various mechanical systems. Selecting appropriate gear parameters, in line with specific application requirements, is crucial for ensuring reliable and efficient performance in mechanical systems. The following assumptions were made for the gear selection calculations: pitch diameter (equal to the gear centre distance) - 110 mm, module - 5 mm. The following equations [21] were used for the calculations:

$$p = m \cdot \pi \quad (15)$$

where:

p - pitch,

m - module, mm.

The pitch of the gear refers to the distance between corresponding points on adjacent gear teeth along the pitch circle. It is commonly denoted by the symbol "p" and is a fundamental parameter used in gear design. The pitch of the gear determines the size and characteristics of the gear and is essential for proper gear engagement and transmission efficiency.

$$z = \frac{d}{m} \quad (16)$$

where:

z - number of teeth,

d - pitch diameter, mm.



The number of teeth of the gear refers to the total count of teeth present on the gear's circumference. It is a critical parameter in gear design and is typically denoted by the symbol "N." The number of teeth directly affects the gear ratio, meshing capabilities, and overall performance of the gear in various mechanical systems. Proper consideration of the number of teeth is essential for achieving desired speed and torque ratios in gear assemblies.

$$h_a = m \quad (17)$$

where:

$h_a$  - addendum height, mm.

$$h_f = 1,25 \cdot m \quad (18)$$

where:

$h_f$  - dedendum height, mm.

$$h = h_a + h_f \quad (19)$$

where:

$h$  - tooth height, mm.

The addendum is the radial distance from the pitch circle to the top of the gear tooth. It is denoted by the symbol  $h_a$  and represents the height of the tooth above the pitch circle. The dedendum is the radial distance from the pitch circle to the bottom of the gear tooth. It is denoted by the symbol  $h_f$  and represents the depth of the tooth below the pitch circle. Together, the addendum and dedendum define the overall height of the gear tooth and are crucial for ensuring proper meshing and engagement between gears in a gear system. These parameters play a significant role in determining the strength, durability, and performance of the gear during operation.

$$j = (0,015 \div 0,04) \cdot m \quad (20)$$

where:

$j$  - backlash, the highest value in the range (0.04) was chosen due to the small number of teeth in the gear.

$$s = 0,5p - j \quad (21)$$

where:

$s$  - tooth width, mm,

$j$  - backlash, mm.

$$e = 0,5p + j \quad (22)$$

where:

$e$  - gear width, mm.

Backlash, tooth width, and gear width are essential gear design parameters. Backlash is the clearance between meshing gears, tooth width affects load capacity, and gear width influences gear-tooth contact area and overall performance.

$$d_a = d + 2h_a \quad (23)$$

where:

$d_a$  - addendum circle diameter, mm.

$$d_f = d - 2h_f \quad (24)$$

where:

$d_f$  - dedendum circle diameter, mm.



The addendum circle diameter and dedendum circle diameter are important gear parameters that define the tooth profile. The addendum circle diameter represents the outermost extent of the gear tooth, while the dedendum circle diameter defines the tooth depth. These parameters ensure proper gear engagement and transmission efficiency.

$$c = h_f - h_a \quad (25)$$

where:

c - clearance at the tooth tip.

The clearance at the tooth tip refers to the gap between gear tooth tips when not in contact. It is vital for smooth gear engagement, noise reduction, and preventing tooth damage during operation.

## 2.4. Designing cutting blades

The cutting shaft consists of a set of cutting blades mounted on the inner shaft. The design of the cutting blades began with the selection of the construction material for the prototype disintegrator's blades. This material should be non-magnetic and have higher strength properties than the products intended for shredding in the disintegrator. The disintegrator will be used for shredding WEEE, including used HDDs. By using non-magnetic construction materials with appropriate strength properties and optimizing the technological parameters of the device, it will be possible to recover rare earth elements from WEEE containing NdFeB magnets and manage the remaining materials generated during recycling.

The construction material of the cutting blades should have higher strength than the materials used in the components of the HDD. It should also be non-magnetic to prevent magnets from adhering to the working elements. The most challenging components of the hard disk drive (HDD) to be shredded are its casing and NdFeB magnets. The HDD casing is made of an aluminum-silicon alloy, commonly referred to as silumin alloy. The magnets inside the HDD are made of an NdFeB alloy. The strength properties of the components are presented in Table 5 [22, 23, 24].

**Table 5.** Strength properties of HDD casing and magnet

No.	Component	Tensile strength Rm [N/mm <sup>2</sup> ]	Hardness [HRB, HRC]
1.	Casing	240-280	45,15 HRB
2.	NdFeB Magnet	82,7	51,8 HRC

Next, the shape optimization of the cutting blades was carried out using Autodesk Inventor software. Based on this, a 3D model of the cutting blades, which constitute the main working element of the disintegrator, was developed. The shape of the cutting blades should ensure effective liberation of the iron alloy with neodymium, dysprosium, and other rare earth elements from the remaining materials generated during the disintegration/shredding of WEEE. This shape should also provide sufficient fragmentation of the remaining materials generated during recycling, enabling their further recovery processes.

## 3. Results

In this chapter, the results of the conducted project work are presented, including the selection of the motor and gearbox, the choice of bearings, the selection of gears, and the design of cutting blades. The disintegrator's illustration, along with its construction description and technical data, is also provided.

### 3.1. Motor and gearbox selection

In this subsection, the determined parameters necessary for selecting a motor and gearbox that meet the previously stated requirements have been presented. Firstly, the shearing area, destructive force, total required cutting force, and destructive torque for the given material were calculated, and the results are shown in Table 6.



**Table 6.** Obtained results necessary for selecting the disintegrator drive

No.	Material	A [mm <sup>2</sup> ]	F <sub>t</sub> [N]	F <sub>C</sub> [N]	M <sub>a</sub> , M <sub>s</sub> [Nm]
1.	Aluminium	108	8100	30375	1959
2.	Steel	30	9150	34313	2213

Then, utilizing the data from the above table, the total required moment of torque amounted  $M_c = 7982$  Nm was determined.

The next step involved determining the values of the rotational torque on the cutting shafts for the given variant of the electric motor and gearbox, which are presented in Table 7.

**Table 7.** Results of torque calculations

No.	M <sub>wt</sub> [Nm]
1.	8680
2.	6487
3.	8035
4.	6450
5.	7685
6.	7887
7.	8403

### 3.2. Selection of chamber bearings

The calculated values of rotational speed, torque, and force on the gearbox input shaft, based on the above formulas, are presented in Table 8.

**Table 8.** Results of calculations for rotational speed, torque, and force on the gearbox input shaft

No.	Parameter	Value
1	n <sub>w</sub> [rpm]	15,78
2	M [Nm]	4539,36
3	F [N]	70378

Then, the hourly bearing life ( $L_h$ ) was calculated, assuming a weekly working time of 38 hours. It was assumed that the bearings should operate for at least 5 years. The results of the bearing life calculations are presented in Table 9. Due to the challenging working conditions in the shredder, only spherical roller bearings were considered.

**Table 9.** Bearing life of the considered spherical roller bearings

No.	Bearing [22]	L [rev]	L <sub>h</sub> [hours]	L <sub>t</sub> [years]
1.	22210-E1-XL	43325098	45763	25,1
2.	22209-E1-XL	37047795	39133	21,5
3.	22208-E1-XL	33603858	35495	19,5
4.	22207-E1-XL	22043705	23284	12,7
5.	22206-E1-XL	7343749	7757	4,3
6.	22205-E1-XL	2913782	3078	1,7



### 3.3. Gear Selection

Table 10 presents the calculated parameters for the gear. Based on these parameters, a 3D model of the gear was created (Fig. 1) and a 2D drawing was generated (Fig. 2). The 3D model and drawing were created using Autodesk Inventor 2022 software.

**Table 10.** Calculated parameters of the gear

No.	Parameter	Value	Parameter	Value
1.	p [mm]	15,71	s [mm]	7,65
2.	z [1]	22	e [mm]	8,05
3.	h <sub>a</sub> [mm]	5	d <sub>a</sub> [mm]	120
4.	h <sub>f</sub> [mm]	6,25	d <sub>f</sub> [mm]	97,5
5.	h [mm]	11,25	c [mm]	1,25
6.	j [mm]	0,15-0,2		



**Fig. 1.** 3D model of the gear

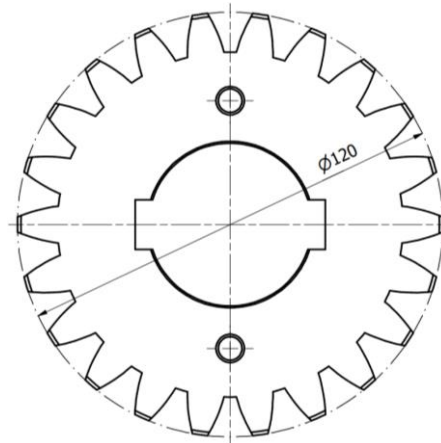


**Fig. 2.** Side view of the gear

### 3.4. Designing cutting blades

The SLM (Selective Laser Melting) method has been chosen for the production of the working components of the disintegrator, specifically the cutting blade edges. This method involves the additive manufacturing of parts by selectively melting layers of metal powder. This technology allows for the production of complex-shaped parts with high strength properties. There are various powders available, including titanium-based, nickel-based, iron-based, and others. Among the available powders, a material called PowderRange 718 has been selected, and its properties are further characterized below. This material has a granulation size of 15-45  $\mu\text{m}$ , suitable for SLM technology. It is a nickel-based alloy [25] with a composition of alloying elements presented in Table 11.

**Table 11.** Chemical composition of PowderRange 718 powder

No.	Element	Ratio [%]	No.	Element	Ratio [%]
1.	Nickel	50,00-55,00	10.	Chromium	17,0-21,0
2.	Niobium + Tantalum	4,75-5,50	11.	Titanium	0,65-1,15
3.	Cobalt	1,00	12.	Magnesium	0,35
4.	Silicon	0,35	13.	Carbon	0,08
5.	Nitrogen	0,03	14.	Phosphorus	0,015



No.	Element	Ratio [%]	No.	Element	Ratio [%]
6.	Molybdenum	2,80-3,30	15.	Sulfur	0,015
7.	Aluminum	0,20-0,80	16.	Iron	Balance
8.	Copper	0,30	17.	Oxygen	0,03
9.	Boron	0,006			

The PowderRange 718 powder allows for the manufacturing of non-magnetic components and exhibits high strength properties (Table 12) [25], surpassing the strength parameters of the materials used in other HDD components, except for the hardness of the NdFeB magnet. Neodymium magnets in hard disks are characterized by their small thickness of approximately 1.5 mm and low strength. Therefore, their disintegration using cutting blades made from PowderRange 718 powder will proceed smoothly.

**Table 12.** Strength properties of components made from PowderRange 718

Yield Strength Re [N/mm <sup>2</sup> ]	Tensile Strength Rm [N/mm <sup>2</sup> ]	Hardness [HRC]
1086	1425	43

The shape of the cutting blades, sketched using Autodesk Inventor software, was designed to ensure effective separation of NdFeB magnet particles from other HDD components such as the casing, disks, positioning arm, head, and PCBs. For this purpose, a cutting blade shape (Fig. 3) was designed with a blade edge (1) that, during operation (rotation), will cause the tip (2) to penetrate into the material being disintegrated, followed by cutting a small piece of material trapped within the surface area formed between the tip (2) and the base (3) of the blade. The remaining surfaces of the cutting blade (4) are rounded, as shown in Fig. 3. By using a small-sized blade edge (1), a sufficient level of fragmentation of the remaining materials will be achieved, enabling them to be directed to further recovery processes.

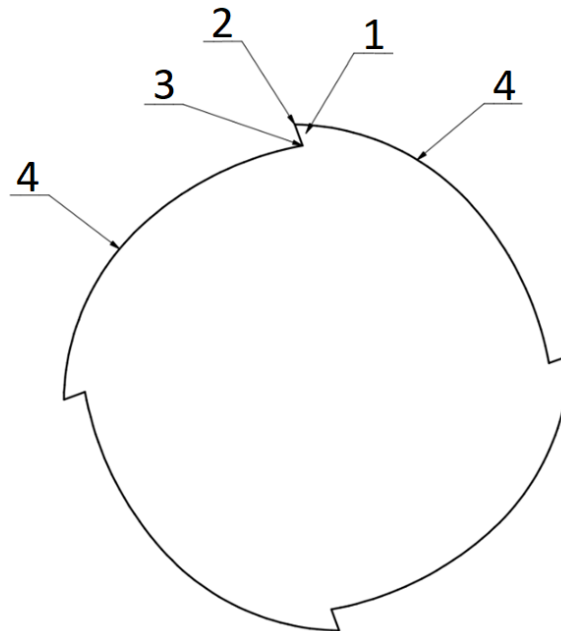


**Fig. 3.** Drawing of the cutting blade featuring the preferred cutting blade shape

Based on the developed sketch, a cutting blade was designed that corresponds to the intended shape. It consists of an inner part and interchangeable blades that are secured with screws. In conventional designs without detachable blades, any damage to the blade requires time-consuming replacement. By using interchangeable blade tips, the device maintenance is significantly accelerated as it eliminates

the need to dismantle the cutting shafts along with the rolling and securing elements. Taking into account the previously established assumptions presented in Table 1 and the considerations provided in the patent application P.442603, a 3D model of the cutting blade was developed (Fig. 4).



Fig. 4. 3D model of the cutting blade

### 3.5. Disintegrator prototype

The components presented above were used to construct the prototype of the disintegrator. This device is also comprised of supporting components, components enabling the loading and collection of the disintegrated material, including covers. The 3D models of the components were created using Autodesk Inventor 2020 software and are presented in the side view (Fig. 5) and top view (Fig. 6) of the disintegrator prototype. The components include the casing (1), cutting shaft no. 1 (2), cutting shaft no. 2 (3), feeding structure (4), flap (5), support structure (6), base (7), gear cover (8), drawer (9), comb assembly (10), clutch cover (11), gear wheel (12), gearbox (13), motor (14), and clutch (15).

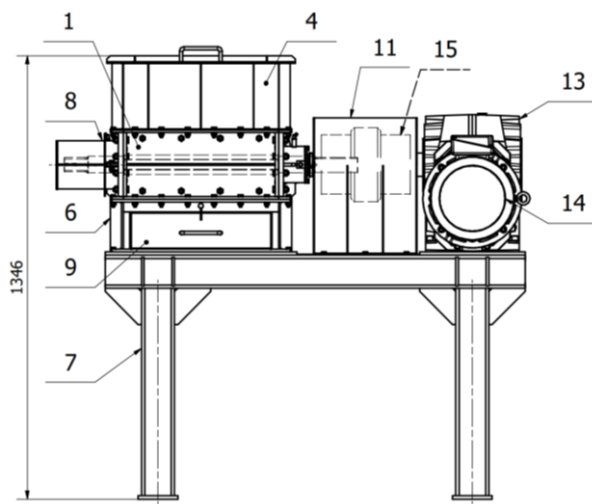


Fig. 5. Side view of the disintegrator prototype.

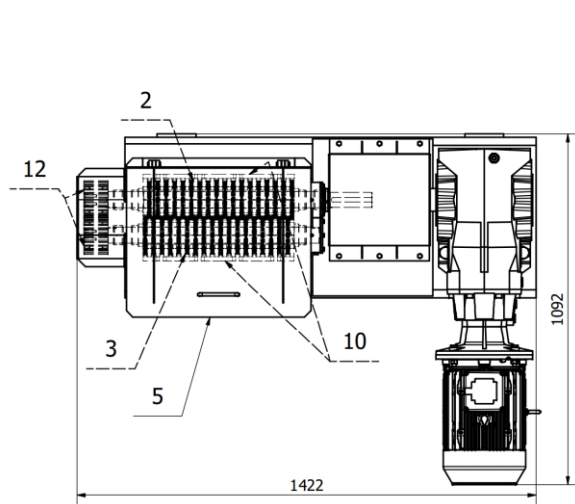


Fig. 6. Top view of the disintegrator prototype.

In the following Table 13, technical data of the designed disintegrator prototype for shredding used equipment equipped with NdFeB magnets are presented [26]. The efficiency of the device at this stage of work is unknown. Currently, detailed technical documentation is being developed.

**Table 13.** Technical data of the disintegrator prototype for shredding used equipment equipped with NdFeB magnets

No.	Parameter	Value
1.	diameter of cutting blades [mm]	129
2.	width of cutting blade [mm]	12
3.	rotation speed of shafts with cutting blades [ $\text{min}^{-1}$ ]	15,8
4.	gear ratio of gear transmission [1]	92,53
5.	power of the motor [kW]	7,5
6.	motor speed, [ $\text{min}^{-1}$ ]	1460
7.	weight of the shredder [kg]	590,0
8.	maximum weight of the installed component [kg]	118,0

#### 4. Discussion

Based on the above calculations and assumptions, a gearbox with a gear ratio of 92.53 was selected, which ensures the appropriate rotational torque. According to the table, in the variant with the chosen gear ratio, there is a motor with parameters of 7.5 kW, 1400 RPM. However, due to local component availability, a motor with parameters of 7.5 kW, 1460 RPM was ultimately used.

The requirement of a minimum bearing life of 5 years has been achieved for the 22207-E1-XL bearing. This bearing has a bore diameter of  $\text{Ø}35$  mm. However, since the shaft that will be supported by the bearing has a diameter of  $\text{Ø}50$  mm, it was necessary to use the 22210-E1-XL bearing, which has the appropriate bore size and also exceeds the specified durability requirement. These bearings allow for angular deviation correction and are lubricated with solid grease, periodically replenished using manual lubricators

The parameters of the gear wheel for power transmission were determined, with a pitch diameter of  $\text{Ø}120$  mm and 22 teeth. Additionally, a cutting blade, which is a component of the cutting shafts, was developed. The width of the cutting edge was determined to be 12 mm, and its diameter was  $\text{Ø}129$  mm.

Considering the strength parameters of the components intended for shredding (WEEE, using HDD as an example), the material for the cutting blade and the manufacturing technology using PowderRange 718 powder for SLM were selected. Details made from this material exhibit higher strength properties than the materials being shredded.

#### 5. Conclusions

The article analyzed the value of metals contained in WEEE, using HDDs as an example. The value of metals contained in 1 Mg of used HDDs was estimated and converted to 100 g of WEEE (HDD), amounting to 3.26 PLN. In southern Poland, 1 million residents discard 13.6 Mg of hard drives per year, resulting in a value of 440,000 PLN for the metals they contain. These estimates illustrate the quantities of valuable elements (including REEs and noble metals) present in WEEE. The Magnet-to-Magnet method allows for the recovery of REEs from WEEE and their reuse in new products - new NdFeB magnets. The first step in processing WEEE using this method is the shredding process, which requires a device with both strong and non-magnetic components.

The publication includes the key elements of the disintegrator prototype project, including calculations and design work using Autodesk Inventor 2022 software. The work involved calculations that resulted in the selection of a gear transmission with a ratio of  $I=92.53$  and an electric motor with specifications of 7.5 kW power and  $1460 \text{ min}^{-1}$  speed. Baryllium roller bearings - 22210-E1-XL were also selected to support the cutting shafts.

The proposed solution is dedicated not only to HDDs but also to the processing of other small WEEE containing NdFeB magnets, such as small motors, power generators, headphones, speakers, mobile



phones, etc. The disintegrator can also be used for the preliminary shredding of other components of computer and telecommunications electronics, such as lithium-ion batteries and printed circuit boards. The approach focused on the recovery and reuse of valuable substances from WEEE aligns with the concept of a circular economy. Due to the low emissions of the proposed Magnet-to-Magnet method, it complies with the principle of "do no significant harm" outlined in Article 11 of Regulation (EU) 2020/852 of the European Parliament and of the Council of 18 June 2020 on the establishment of a framework to facilitate sustainable investment and amending Regulation (EU) 2019/2088. Therefore, it can be considered conducive to sustainable development. Negotiations with manufacturers are underway to produce the device prototype.

## 6. Patents

A project of the disintegrator - was developed based on patent application P.442603 "The method of disintegrating wasted electrical and electronic equipment containing neodymium magnets in order to obtain particles of appropriate sizes for the recovery of neodymium-iron alloy, dysprosium, or other rare earth elements".

## References

- [1] Binnemans K., McGuinness P., Jones P.: Rare-earth recycling needs market intervention. *Nature Reviews Materials*. 6, 2021
- [2] Vishwanath G., Deshmane, Syed Z. Islam, Ramesh R. Bhawe: Selective Recovery of Rare Earth Elements from a Wide Range of E-Waste and Process Scalability of Membrane Solvent Extraction, *Environmental Science & Technology*, 2019
- [3] Schönfeldt M., Brouwer E., Dirks A., Rachut K., Gassmann J., Güth K., Buckow A., Gauß R., Stauber R., Gutfleisch O.: Towards an alloy recycling of Nd–Fe–B permanent magnets in a circular economy. *J. Sustain. Metall.* 4(2), 163–175, 2018
- [4] Diehl O., Schönfeldt M., Brouwer E., Dirks A., Rachut K., Gassmann J., Güth K., Buckow A., Gauß R., Stauber R., Gutfleisch O.: Towards an alloy recycling of Nd–Fe–B permanent magnets in a circular economy. *J. Sustain. Metall.* 4(2), 163–175, 2018
- [5] München D.D., Veit H.: Neodymium as the main feature of permanent magnets from hard disk drives (HDDs). *Waste Manage.* 61, 372–376, 2017
- [6] Yang Y., Walton A., Sheridan R., Güth K., Gauß R., Gutfleisch O., Buchert M., Steenari B. M., Van Gerven T., Jones P. T., Binnemans K.: REE Recovery from End-of-Life NdFeB Permanent Magnet Scrap: A Critical Review. *Journal of Sustainable Metallurgy*, 3(1), 122–149, 2016
- [7] Yue M., Yin X., Liu W., Lu Q.: Progress in recycling of Nd–Fe–B sintered magnet wastes. *Chin. Phys. B* 28(7), 077506, 2019
- [8] Zakotnik M., Tudor C.O., Peiró L. T., Afiuny P., Skomski R., Hatch G., P.: Analysis of energy usage in Nd–Fe–B magnet to magnet recycling. *Environmental Technology & Innovation*, 5, 117-126, 2016
- [9] München, D.D., Stein, R.T., Veit, H.: Rare earth elements recycling potential estimate based on end-of-life NdFeB permanent magnets from mobile phones and hard disk drives in Brazil. *Minerals* 11(11), 1190, 2021
- [10] Prospero D., Bevan A., Rosillo G.U., Tudor C.O., Furlan G., Dove S., Lucia P., Zakotnik M.: Performance comparison of motors fitted with magnet-to-magnet recycled or conventionally manufactured sintered NdFeB. *Journal of Magnetism and Magnetic Materials*, 2018
- [11] Jin H., Afiuny P., McIntyre T., Yih Y., Sutherland J.: Comparative Life Cycle Assessment of NdFeB Magnets: Virgin Production versus Magnet-to-Magnet Recycling. *Procedia CIRP*, 2016
- [12] Tanvar H., Barnwal A., Dhawan N.: Characterization and evaluation of discarded hard disc drives for recovery of copper and rare earth values. *Journal of Cleaner Production*, 249, 119377, 2020 <https://doi.org/10.1016/j.jclepro.2019.119377>
- [13] Abrahamsi S. T., Xiao Y., Yang, Y.: Rare-earth elements recovery from post-consumer hard-disc drives. *Mineral Processing and Extractive Metallurgy*. 124. 2014



- [14] Suponik T., Friebe P., Nuckowski P., Król M.: Dezintegrator do rozdrabniania zużytych sprzętów elektrycznych i elektronicznych zawierających magnesy neodymowe w celu odzysku stopu żelaza, zwłaszcza z neodymem, P.442603, Urząd Patentowy RP, zgłoszenie dnia 24.10.2022
- [15] Zwolak J.: Wytrzymałość materiałów w zadaniach, Uczelnia Państwowa im. Jana Grodka w Sanoku, Sanok, 2020, ISBN 978-83-61802-45-7
- [16] Niezgodziński T.: Wzory wykresy i tablice wytrzymałościowe, Wydawnictwo Naukowo-Techniczne, Warszawa, 2013, ISBN 978-83-79260-07-2
- [17] Pater Z., Samołyk G.: Podstawy technologii obróbki plastycznej metali, Politechnika Lubelska, Lublin, 2013, ISBN 978-83-63569-89-1
- [18] Rutkowski A.: Części maszyn, Wydawnictwo szkolne i pedagogiczne, Warszawa, 2011, ISBN 978-83-02-09886-4
- [19] <https://kacperek.com/wp-content/uploads/2018/02/HS-703-HS-704.pdf> [accessed: 28.12.22]
- [20] <https://medias.schaeffler.pl/pl/plp/SphericalRollerBearings1> [accessed: 18.02.2023]
- [21] Żółtowski J.: Podstawy konstrukcji maszyn przekładnie, Oficyna wydawnicza Politechniki Warszawskiej, 2011, ISBN 83-7207-488-7
- [22] <http://lenaal.com.pl/wp-content/uploads/2017/03/Wlasnosc-stopow-1.pdf> [accessed: 16.09.2022]
- [23] [https://www.matweb.com/search/datasheet\\_print.aspx?mat-guid=e7eda0f5b11243a6a9ea46f21d667dc1](https://www.matweb.com/search/datasheet_print.aspx?mat-guid=e7eda0f5b11243a6a9ea46f21d667dc1) [accessed: 6.09.2022]
- [24] Friebe P., Suponik T., Nuckowski P.M.: Research on Hard Drives in the Context of the Construction of Shredding Knives in the Recovery of Rare Earth Elements. In: Benítez-Andrades, J.A., García-Llamas, P., Taboada, Á., Estévez-Mauriz, L., Baelo, R. (eds) Global Challenges for a Sustainable Society. EURECA-PRO 2022. Springer Proceedings in Earth and Environmental Sciences. Springer, Cham, 2023 [https://doi.org/10.1007/978-3-031-25840-4\\_12](https://doi.org/10.1007/978-3-031-25840-4_12)
- [25] [https://www.carpenteradditive.com/hubfs/Resources/Data%20Sheets/PowderRange\\_718\\_Datasheet.pdf](https://www.carpenteradditive.com/hubfs/Resources/Data%20Sheets/PowderRange_718_Datasheet.pdf) [accessed: 18.02.2023]
- [26] Friebe P.: Instrukcja Użytkownika Dezintegrator do zużytych sprzętów elektrycznych i elektronicznych zawierających magnesy neodymowe, W73.216IU (unpublished materials of KOMAG)

